PHYSICAL SCIENCES INC.

PSI-2873/
TR-2449

UV Ozone Photometer for the HIAPER GV Aircraft: Test Results and Final Report

Purchase Order S05-39689

Prepared by:

W.T. Rawlins, R.H. Krech, P.A. Mulhall, J.A. Polex, D.C. Rossi, and D.M. Sonnenfroh
Physical Sciences Inc.
20 New England Business Center
Andover, MA 01810-1077

Submitted to:

University Corporation for Atmospheric Research
P.O. Box 3000
1850 Table Mesa Drive
Boulder, CO 80307-3000

September 2009

20 New England Business Center Andover, MA 01810-1077 *t* 978.689.0003 *f* 978.689.3232
www.psicorp.com

TABLE OF CONTENTS

20 New England Business Center □ Andover, MA 01810-1077 □ *t* 978.689.0003 *f* 978.689.3232
www.psicorp.com

TABLE OF CONTENTS (Continued)

20 New England Business Center Andover, MA 01810-1077 t 978.689.0003 f 978.689.3232
www.psicorp.com

LIST OF FIGURES

20 New England Business Center □ Andover, MA 01810-1077 □ *t* 978.689.0003 *f* 978.689.3232
www.psicorp.com

LIST OF FIGURES (Continued)

20 New England Business Center □ Andover, MA 01810-1077 □ t 978.689.0003 f 978.689.3232
www.psicorp.com

LIST OF FIGURES (Continued)

20 New England Business Center Andover, MA 01810-1077 *t* 978.689.0003 *f* 978.689.3232
www.psicorp.com

20 New England Business Center Andover, MA 01810-1077 *t* 978.689.0003 *f* 978.689.3232
www.psicorp.com

Abstract

This report describes the design, testing, and operation of the HIAPER GV dual-beam, ultraviolet absorption ozone photometer. The instrument is designed to measure atmospheric ozone mixing ratios in flight by ultraviolet absorption of a flowing air sample in a dual-beam, temperature-controlled sample cell. It is configured for either autonomous or interactive operation within the cabin of the HIAPER GV aircraft. Graphical user interface software provides real-time and post-flight data processing and analysis capabilities for rapid data evaluation and archival. The instrument has been fully integrated on the GV aircraft and operated in preliminary flight tests. The accuracy of its ozone measurements has been extensively characterized and validated through laboratory intercomparisons with an earlier-generation, previously validated flight instrument. This document describes the instrument, its operation, results from initial bench and flight tests, subsequent instrument modifications to improve its measurement accuracy, and final laboratory validation testing.

1. Introduction

The PSI/PI UV Ozone Photometer, built by Physical Sciences Inc. and Proffitt Instruments, is designed to measure atmospheric ozone mixing ratios by ultraviolet absorption of a flowing air sample in a dual-beam, temperature-controlled sample cell. This document describes the instrument, its operation, results from initial bench and flight tests, modifications, and final bench test. A mechanical stress analysis is included in Appendix A. A parts list is given in Appendix B. An operator's manual from Proffitt Instruments is provided in Appendix C. Note that some of the descriptions and conclusions in Appendix C have been superceded by work described in Sections 8 – 10 of this report. Appendices D through G provide documentation of the data formats and data analysis routines. Recommended flight operation procedures are given in Appendix H.

Figure 1 illustrates the basic interface of the instrument to the aircraft platform. The instrument is housed within a Zero Manufacturing aluminum enclosure measuring 12 inches x 18 inches x 10 inches, weighs approximately 29 lbs, and consumes <80 W at 28 VDC. Incoming power is converted from aircraft 115 VAC to 28 VDC by a power supply mounted inside the enclosure. Ambient air is sampled through an externally mounted inlet, passes through a length of 3/8-inch or ½-inch Teflon tubing into the instrument, and is exhausted through Teflon tubing to an aircraft exhaust duct. Instrument operation can be initiated by a remote soft-key signal, and an RS232 data stream is passed from the instrument to an external computer for analysis. In addition to the mechanical mounting of the instrument to the rack, the interface connections are: incoming power, incoming sample air flow, outgoing sample exhaust flow, remote startup, RS232 data stream, and input for an external time stamp (IRIG-B).

20 New England Business Center Andover, MA 01810-1077 t 978.689.0003 f 978.689.3232
www.psicorp.com

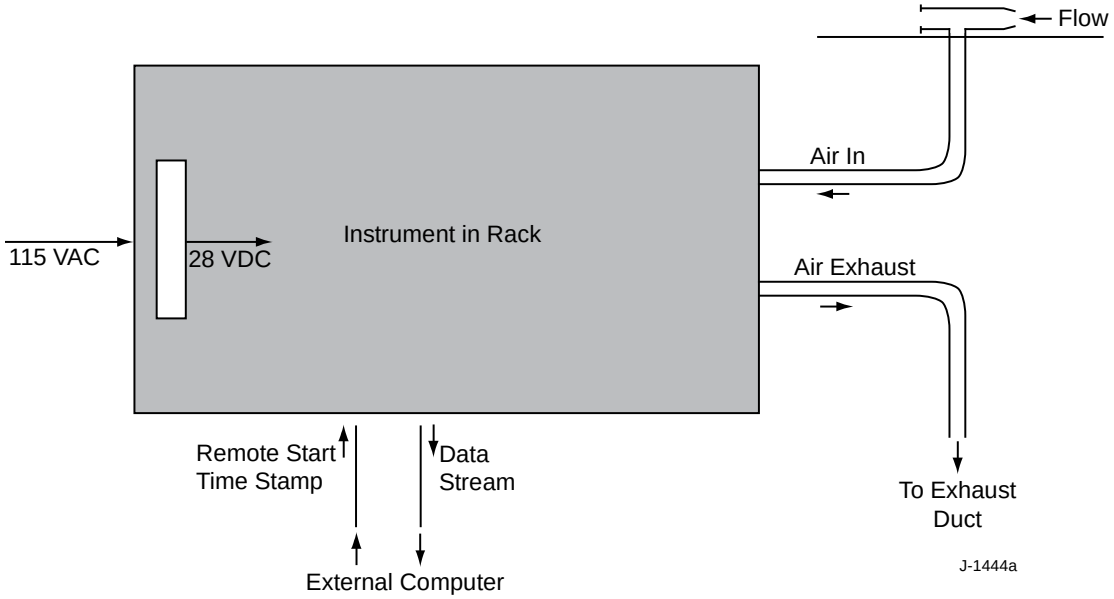

Figure 1. Schematic of aircraft installation and interface.

Figure 2 illustrates an overall schematic of the major instrument components within the enclosure. The incoming power is distributed and controlled via a set of Wall Industries DC-DC converters. The air sample passes through a temperature-controlled dual-beam aluminum absorption cell, where ozone concentrations are measured by absorption of 254 nm light from a BHK light source. The signal from each of the two photodiodes is processed by an electrometer circuit which amplifies the signal and converts it into a frequency signal. The frequency signals are read by a Diamond Systems counter-timer board which is part of the PC104 computer stack. The sample air temperatures and pressure, as well as several housekeeping component temperatures and voltage levels, are read by an A/D board in the PC104 system. The data are archived on a removable hard drive, and are also streamed to an external computer connection via an RS232 interface. The instrument can be described as an assembly of five primary modules, with associated components as shown below:

I. Photometer
   - A. Absorption cell
   - B. Optical
     1. Beamsplitter
     2. UV mirror
     3. Quartz windows
     4. UV filter
     5. Mercury lamp
     6. Lamp power supply
   - C. Detection
     1. Detector PC boards
     2. Photodiode detectors

20 New England Business Center □ Andover, MA 01810-1077 □ *t* 978.689.0003 *f* 978.689.3232
www.psicorp.com

D. Flow components
    1. Scrubber
    2. Brass fittings
    3. Teflon tubing
    4. Teflon fittings

II. Valve
- A. Controller PC board
- B. DC gear motor
- C. Drive train
    1. Spider coupling
    2. Valve shaft
- D. Glass filled Teflon parts
    1. Sleeve
    2. Rotating insert
- E. Position sensor
    1. Modulator
    2. Reflective object sensors
- F. Pressure can

III. Pressure and temperature
- A. Pressure sensors
    1. Absolute
    2. Differential
- B. Thermistors
    1. Sample chambers
    2. Housekeeping
- C. Temperature control
    1. Controller unit
    2. Control thermistor
    3. Heaters

IV. Data system
- A. CPU
- B. VGA
- C. A/D converters
- D. Counter/timers
- E. Front panel
- F. Hard drive

V. Interface
- A. Vector board
- B. Circulating fan
- C. PS Panel
    1. +12volt 1.25A
    2. ±12volt Triple supply with 5V 4 amp
    3. ±15volt 1 amp PS (reserved for use with Baratron if needed)

We will address each of these modules in the descriptions below.

20 New England Business Center Andover, MA 01810-1077 t 978.689.0003 f 978.689.3232
www.psicorp.com

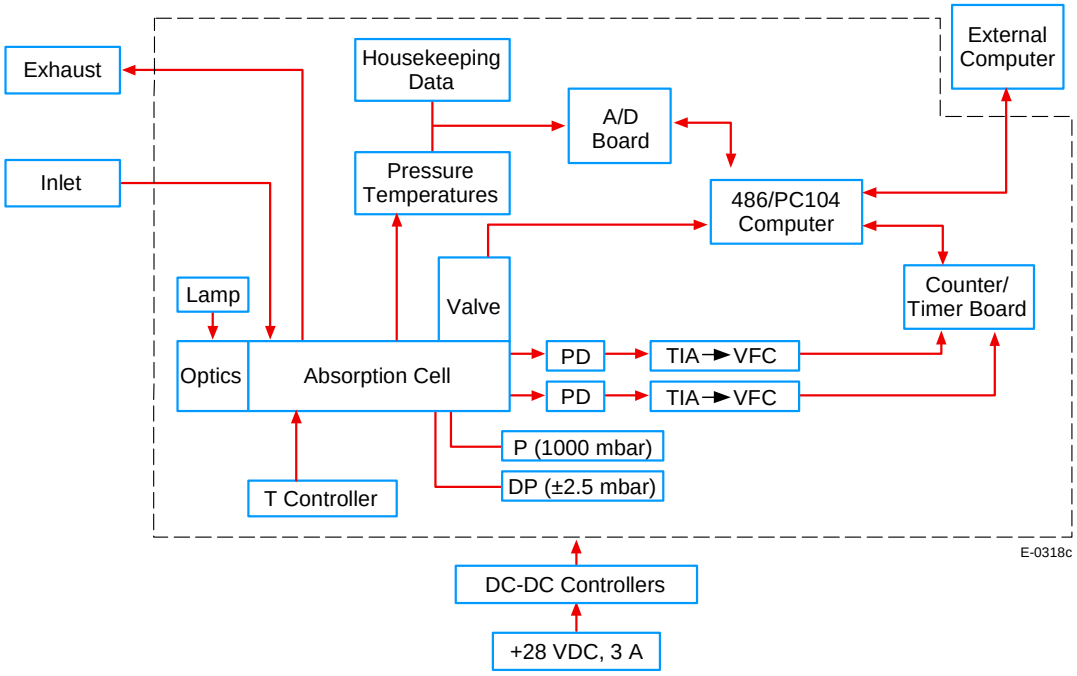

Figure 2. Schematic of instrument components.

2. Photometer

2.1 Absorption Cell

Figure 3 illustrates the functionality of the absorption cell. The cell is a machined aluminum block, 10.5 inches long x 3.5 inches wide x 1.5 inches thick, with three ¼-inch diameter flow channels drilled out by the EDM process. The internal surfaces of the flow channels are coated with Teflon. The sample air enters the cell through the center channel. Half the flow passes through the scrubber, where ozone in the sample is removed by a MnO_2 catalyst (Tanabyte SCN001), and then to one inlet port of the four-way valve. The other half of the flow bypasses the scrubber and goes to the other inlet port of the valve. Each outlet port of the valve connects to one of the two optical flow channels. Periodic 90º rotation of the valve alternates the scrubbed flow from one channel to the other, interchanging the ozone-free and ozone-laden flows. The exhaust flow from each channel is combined into a common exhaust flow after leaving the cell. Emission from the light source lamp passes through a beamsplitter-mirror optical arrangement which directs the light down each of the optical flow channels. Quartz windows are mounted on o-ring seals on each end of each channel. The light from each channel passes through a 254-nm interference filter and onto a photodiode detector. The signal output from the detectors is processed by electrometer circuits on a pair of printed circuit boards mounted in the base of the cell block. The cell temperature is controlled to ~35ºC by a Wavelength Electronics MPT-5000 temperature controller connected to strip heaters (Minco HK5164R78.4L12B and HK5165R52.3L12B) on the sides of the cell block and a thermistor imbedded in the cell body. The four-way valve is constructed of Teflon-like ceramic material, and is driven by an automated gear motor mechanism as described below.

20 New England Business Center □ Andover, MA 01810-1077 □ t 978.689.0003 f 978.689.3232
www.psicorp.com

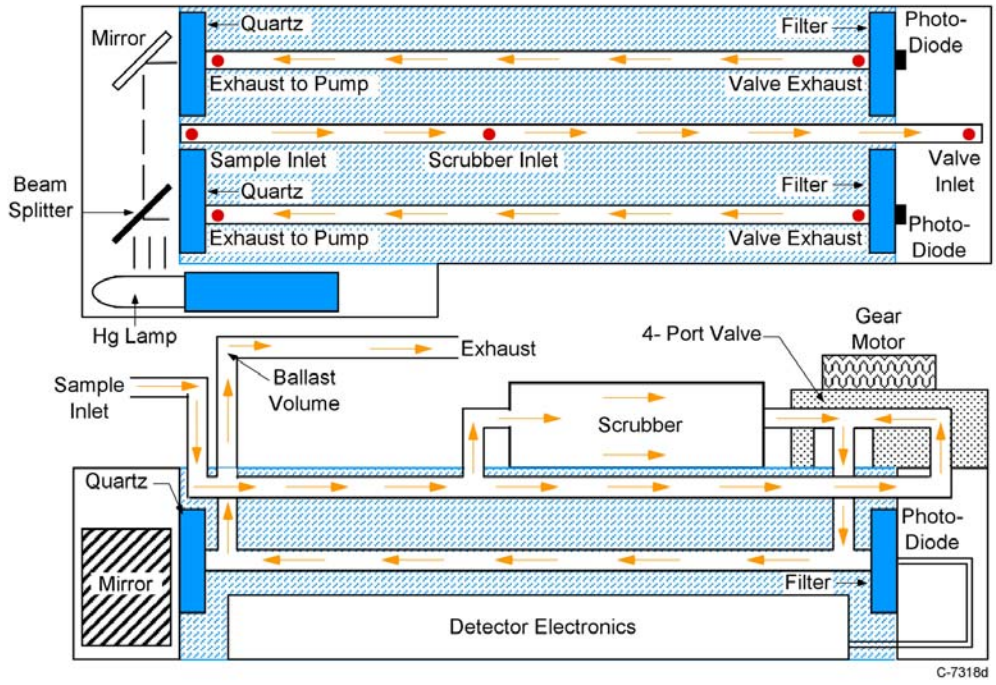

Figure 3. Dual Beam Absorption Cell.

2.2 Optical Components

The optical components are all COTS parts. The lamp and its power supply are BHK 80-1025-33 and BHK 68-0020-04, respectively. The lamp is mounted in a glass-filled Teflon housing. The UV beamsplitter is Esco PLT-UV-25.4x25.4. The mirror is Thorlabs PF10-03-F01. The quartz windows, ½-inch diameter x 1/8-inch thick, are Esco WD-CQF-S1-AS.7DIA2.18TH. The 254 nm filters are from Barr Associates. The silicon photodiodes are Hamamatsu S1336-8BQ.

2.3 Electrometer Boards

Figure 4 shows a general schematic illustrating the electrometer circuit functionality. Each printed circuit board measures 5 inches long x 1.375 inches wide; two boards are mounted in the base of the cell block (one board for each photodiode). The photocurrent from the photodiode is amplified and converted into a voltage by a high-gain transimpedance amplifier circuit. The resistor values R_1, R_2, and R_3 are chosen to give a high fixed gain, typically on the order of 10^8 V/A. The amplified voltage signal is fed to a voltage-to-frequency conversion circuit, where it is transformed into a frequency signal on the order of 1-2 MHz. Ancillary circuitry on the board deals with optical isolation of the clock signal, voltage regulation, and isolation from EMI effects. The frequency signals are passed through SMA cables to a counter-timer board in the PC104 stack (see below).

20 New England Business Center □ Andover, MA 01810-1077 □ t 978.689.0003 f 978.689.3232
www.psicorp.com

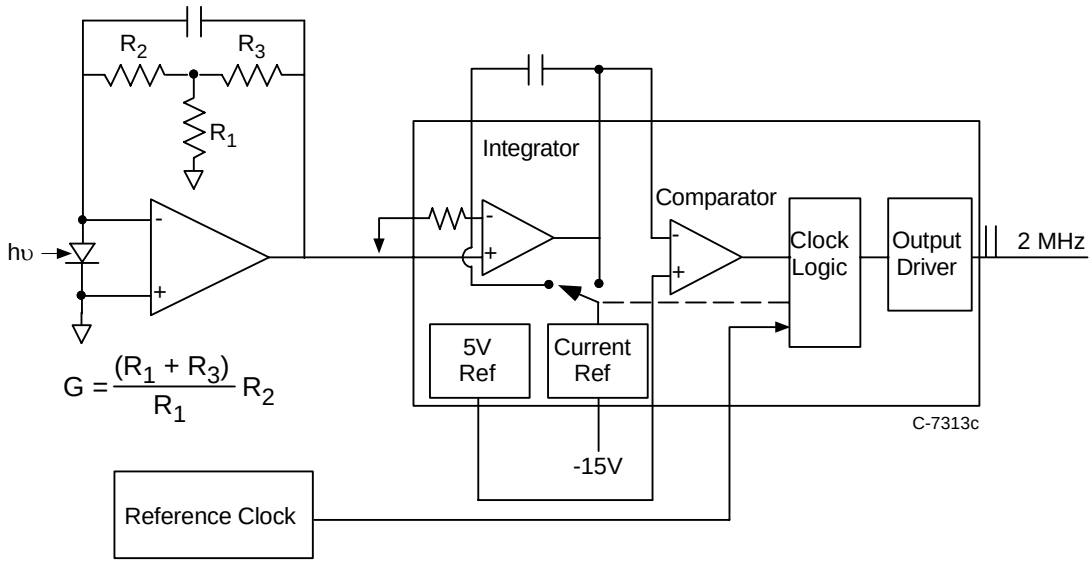

Figure 4. General schematic of electrometer circuit.

2.4 Four-way Flow Switching Valve

The design of the four-way flow switching valve is proprietary to Proffitt Instruments. A general schematic illustrating the functionality of the valve is shown in Figure 5. The valve sleeve is made of Tefzel HT2004, 25% glass, and is inserted into the aluminum body of the cell. The valve core is made of Ultraflon CFX, and rotates within the sleeve. Channels within the valve core connect the inlets and outlets of the valve. The valve core is rotated by a gear motor (Faulhaber 1727U012CL 86:1+X0814C) connected through a flexible coupling assembly. Reflective object sensors monitor the valve position. A small circuit board inside the valve motor housing contains the circuitry which controls the valve position and rotation. Connections of this circuit to the data system permit recording of the valve position data, and switching of the functional mode from manual to automatic. The entire motor and valve assembly are housed within a pressure-tight enclosure. Following the initial bench and flight tests of the instruments, the original interface between the gear motor shaft and the valve core was substantially modified by PSI to allow installation of an O-ring seal on the shaft, which was omitted by PI. These modifications are described in Section 9.

20 New England Business Center □ Andover, MA 01810-1077 □ t 978.689.0003 f 978.689.3232
www.psicorp.com

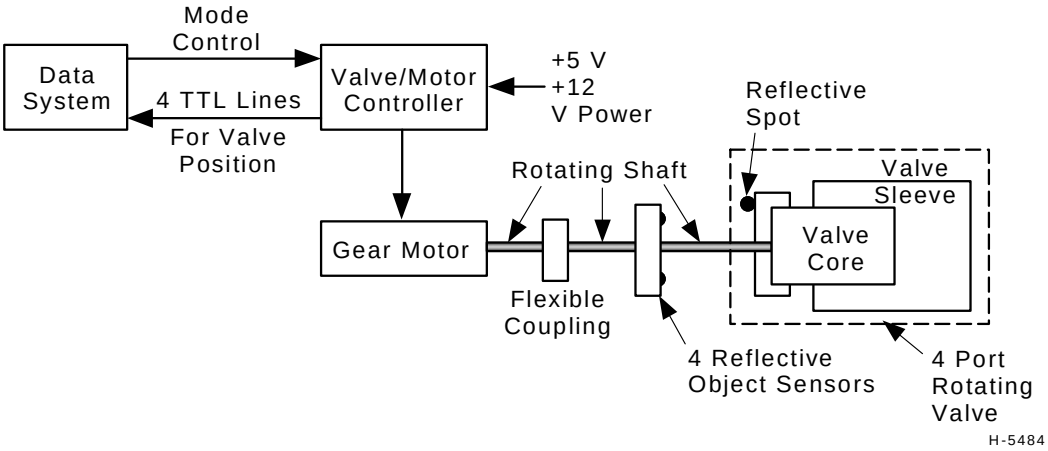

Figure 5. Design of four-way flow switching valve.

2.5 Pressure and Temperature Sensors

Pressure in each optical flow channel is monitored through ports at the midpoint of the channel. Absolute pressure in one of the channels is monitored by an All Sensors 683-15PSIA4V sensor. Differential pressure in the other channel (relative to the exhaust pressure) is monitored by an All Sensors 683-1INCHD4V sensor. The sensors are mounted directly on the ports via Teflon fittings, and are connected to the data system by a 9-pin cable.

Temperatures are monitored in several locations by Fenwal Unicurve thermistors. Gas flow temperatures are monitored at the inlets and outlets of the optical channels by thermistors suspended in the flow via small MicroCom feedthrough connectors. Hardware temperatures are monitored in several locations, including the cell body, the CPU, and other locations around the instrument for housekeeping purposes. The resistance of the thermistor is determined by measuring the voltage drop across the thermistor for a 5 V input and a load resistor, as illustrated in Figure 6. The circuitry for these measurements is mounted on the central interface board as described below.

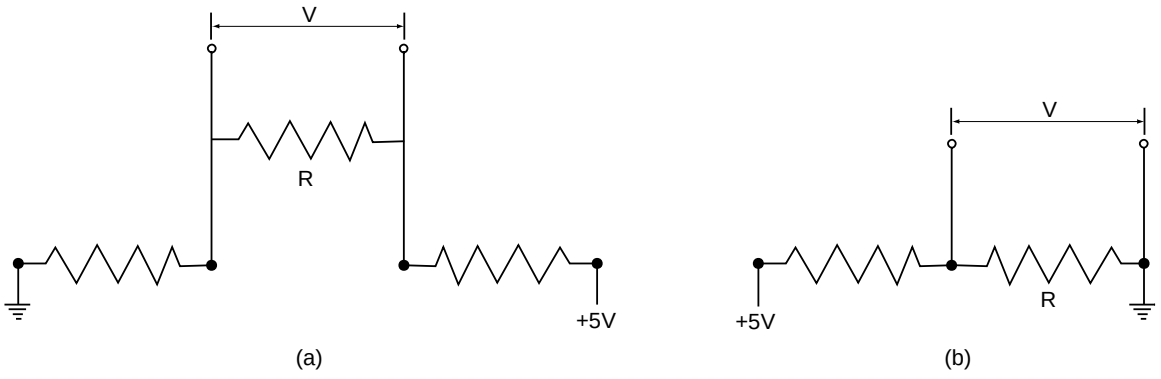

Figure 6. Circuit for temperature measurements: (a) gas flow temperatures; (b) housekeeping temperatures. "R" signifies the probe thermistor.

20 New England Business Center □ Andover, MA 01810-1077 □ *t* 978.689.0003 *f* 978.689.3232
www.psicorp.com

3. PC104 Data System

The data system is a PC104 stack consisting of the following:

- Diamond Systems Prometheus CPU, PR-Z32-EA-ST
- Diamond Systems VGA board, ACC-VGA-02
- Diamond Systems panel I/O board, PNL-Z32-EA
- Diamond Systems counter-timer board, QMM-5
- Diamond Systems 16 channel 12-bit A/D, DMM-NA-XT
- Diamond Systems front panel, PBEC-05-K
- Brandywine PC104-SG board (IRIG-B time stamp)
- 20 GB removable hard drive, Seagate ST92011A

4. Overall Instrument Assembly and Layout

Assembly views of the absorption cell design are shown in Figure 7. A cutaway view along the cell midline is shown in Figure 8. An exploded view is shown in Figure 9, illustrating the components discussed above. Not shown are short ¼-inch Teflon tubing connections for air input and exhaust and for connection of the scrubber output to the valve, and the pressure sensor connections.

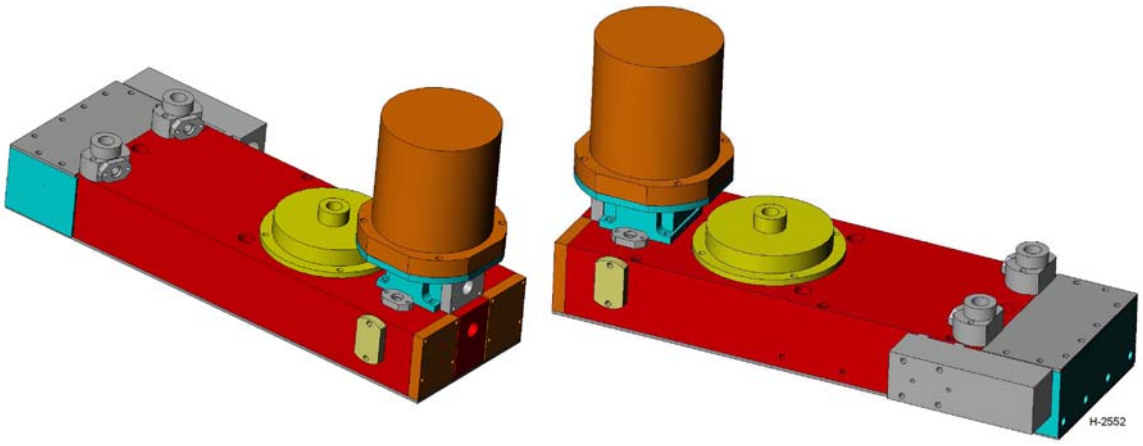

Figure 7. Assembly view of absorption cell.

20 New England Business Center Andover, MA 01810-1077 t 978.689.0003 f 978.689.3232
www.psicorp.com

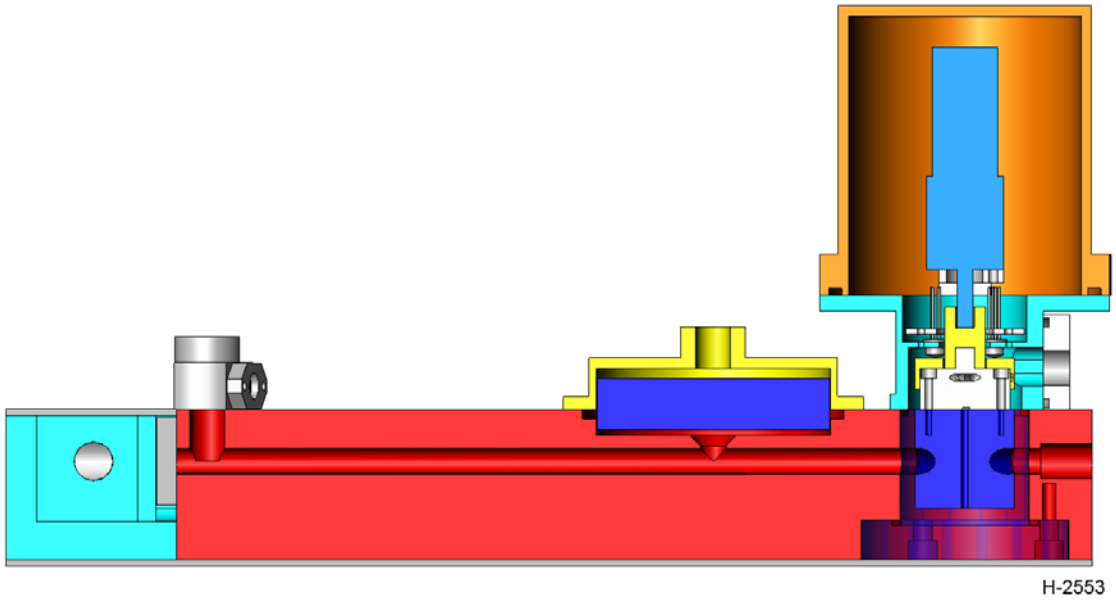

Figure 8. Cutaway view of absorption cell assembly.

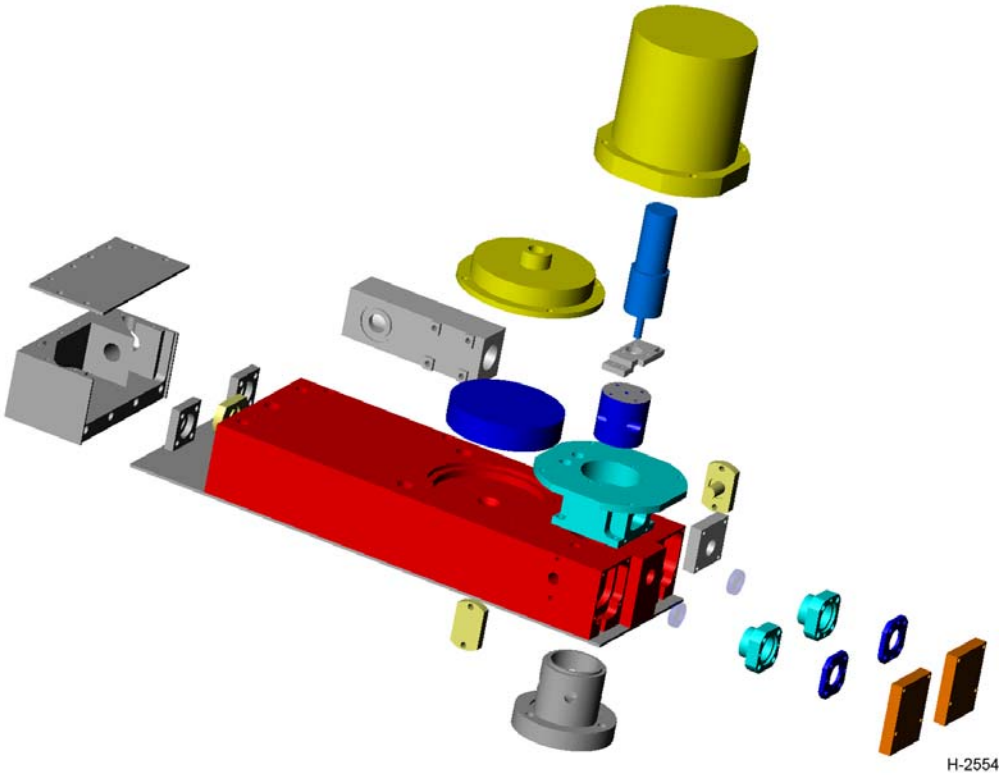

Figure 9. Exploded view of absorption cell assembly.

20 New England Business Center Andover, MA 01810-1077 *t* 978.689.0003 *f* 978.689.3232
www.psicorp.com

Figure 10 shows a diagram of the overall instrument assembly. The components are mounted on a base plate which is installed in the housing as described below. A top view of the layout is shown in Figure 11. The absorption cell is mounted on one edge, with the lamp housing on the bottom. The cell is supported on stainless steel standoffs screwed to the base plate. The interface board contains the power distribution network, signal conditioning electronics and A/D connections for the temperature sensors and housekeeping monitors, and valve mode control circuitry. A schematic of the interface panel is shown in Figure 12, as provided by Proffitt Instruments. This board is further described in the PI Operator's Manual. The PC104 data system is located on the back side of the interface panel. The fan (Rotron FE12H3) provides air circulation within the instrument housing. Photographs of the instrument with the housing cover removed are shown in Figures 13 and 14.

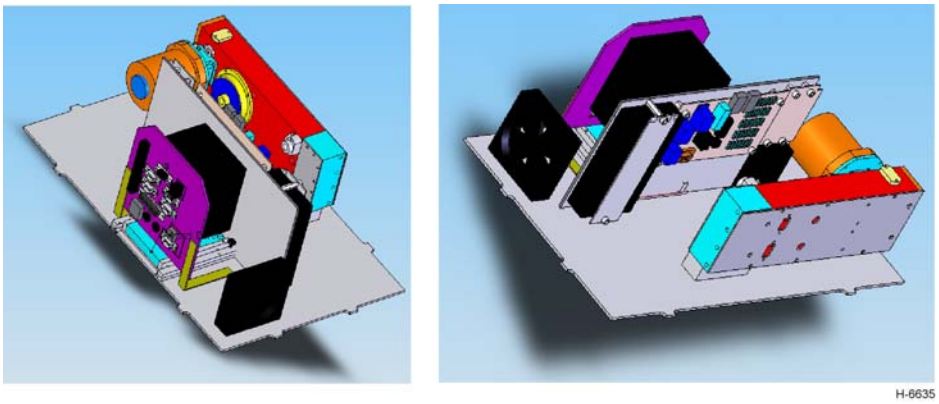

Figure 10. Diagram of instrument assembly.

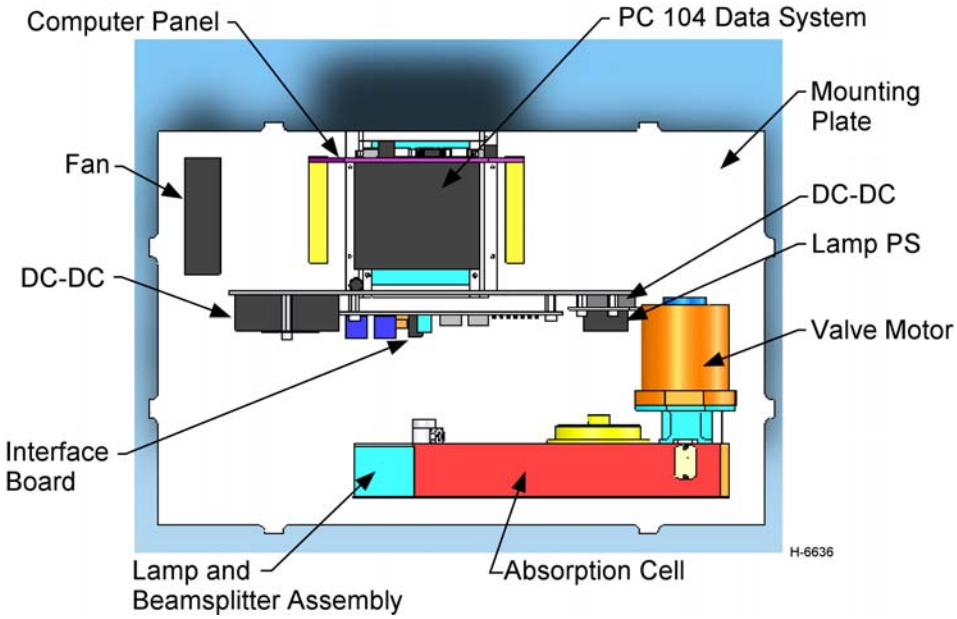

Figure 11. Top view, layout of instrument components on base plate.

20 New England Business Center □ Andover, MA 01810-1077 □ *t* 978.689.0003 *f* 978.689.3232
www.psicorp.com

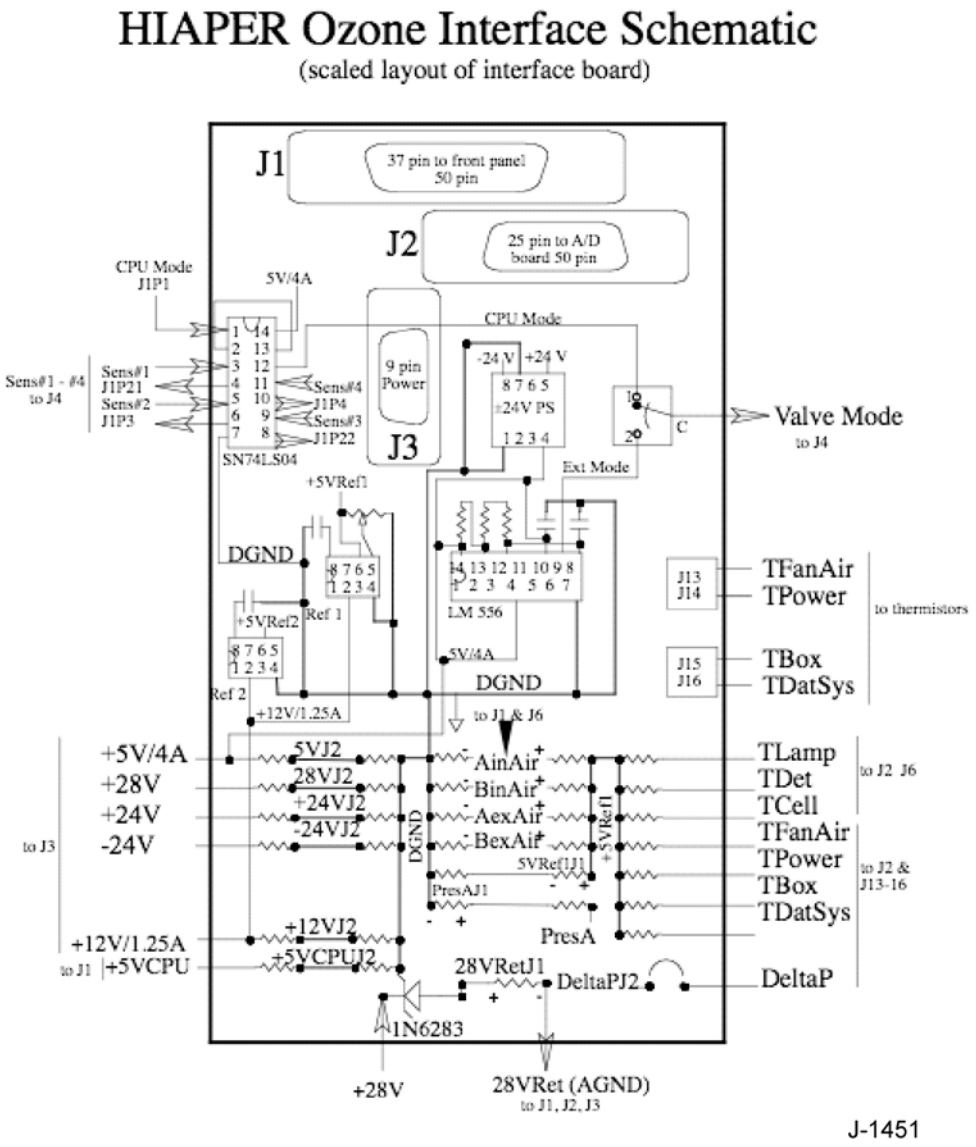

Figure 12. Proffitt Instruments schematic of interface panel (see Appendix C).

20 New England Business Center □ Andover, MA 01810-1077 □ *t* 978.689.0003 *f* 978.689.3232
www.psicorp.com

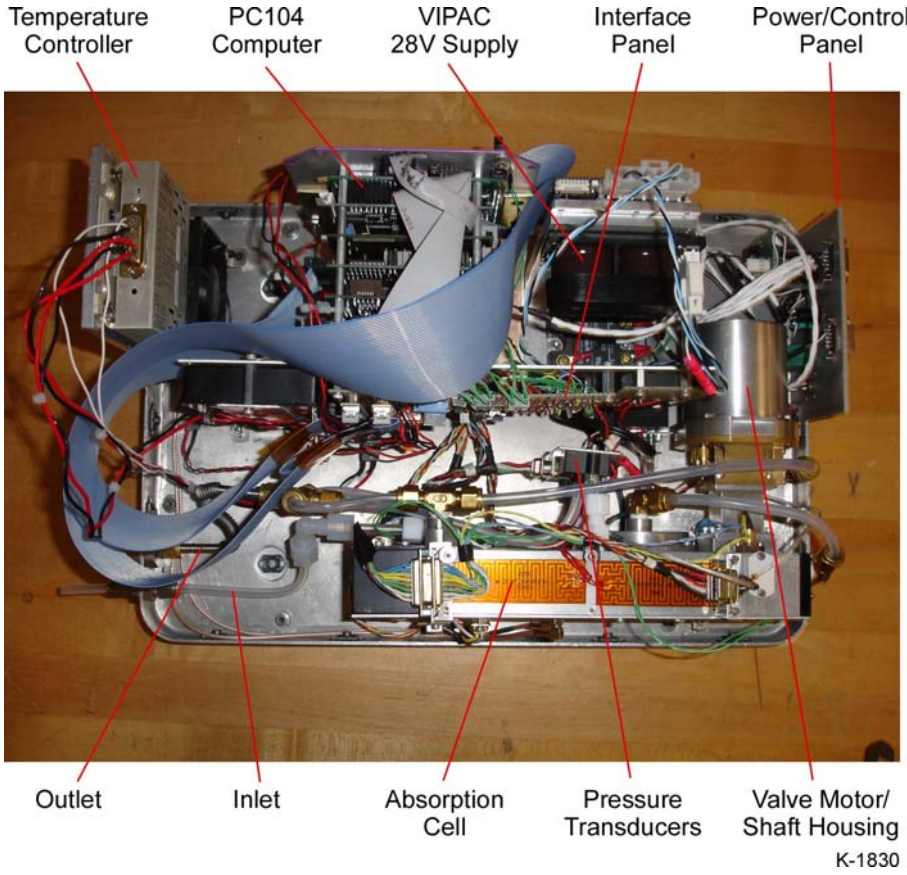

Figure 13. Photograph of instrument assembly: top view.

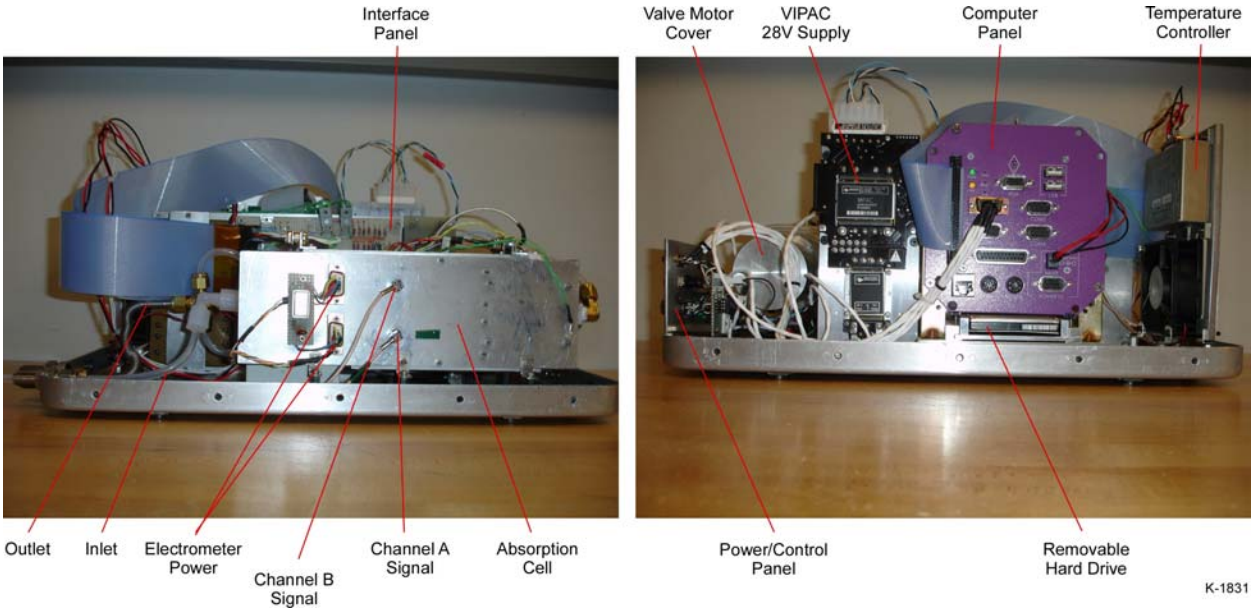

Figure 14. Photograph of instrument assembly: side view.

20 New England Business Center □ Andover, MA 01810-1077 □ *t* 978.689.0003 *f* 978.689.3232
www.psicorp.com

The instrument assembly is housed in a Zero Manufacturing box and cover (Z192-288A, Z192-288A-CI). The housing is made of deep-drawn 6061-0 aluminum. The instrument assembly and base plate are screwed into the housing base, which is ~1 inch deep, and the housing cover fits over the top, as illustrated in Figure 15. The fasteners are MS21059 floating nut plates. External connections for the inlet and exhaust air, power, and computer panel are installed in the housing base.

Figure 15. Instrument with housing cover installed (PC-104 access panel removed).

To install the instrument in the rack, the housing base is first screwed to a rack mounting plate by 4 ¼-28 bolts. The instrument assembly on its base plate is then screwed into the housing base by 8 10-32 screws, and the connections to the external connectors are completed. The housing cover is then fit over the top of the instrument assembly and is screwed to the housing base. A mechanical stress analysis of this assembly is given in Appendix A.

5. Power Distribution

Figure 16 shows the 28 VDC power distribution within the instrument. Measured current usages for the different subcircuits are also shown in the figure. The total 28 VDC current ranges from 0.6 A when the cell heaters are off to 2.5 A when the cell heaters are fully on. The incoming 28 VDC power is split into four subsystems: (1) the cell temperature control system, which operates the Minco strip heaters at 28 VDC and 0 to 1.6 A; (2) a Wall LCSW 2412-15 DC-DC converter, which provides 12 VDC at 0.4 A to the BHK lamp power supply; (3) a Wall SIW24D 15-30 DC-DC converter, which provides connections for ±15 VDC that are not presently used; and (4) a Wall SIW24T 12-30 DC-DC converter which provides 12 VDC and 5 VDC power to other subsystems. The 12 VDC power goes to the circulation fan and to the Faulhaber gear motor for the four-way flow switching valve. The combined current draw for these is 0.3 A. The 5 VDC power drives the PC104 data system (1.9 to 2.5 A), the valve logic board (0.1 A), and components on the electrometer boards (0.4 A). The 5 VDC power (0.04 A) also is converted to ±24 VDC by a Wall LANH524ND DC-DC converter; this voltage is passed

20 New England Business Center □ Andover, MA 01810-1077 □ t 978.689.0003 f 978.689.3232
www.psicorp.com

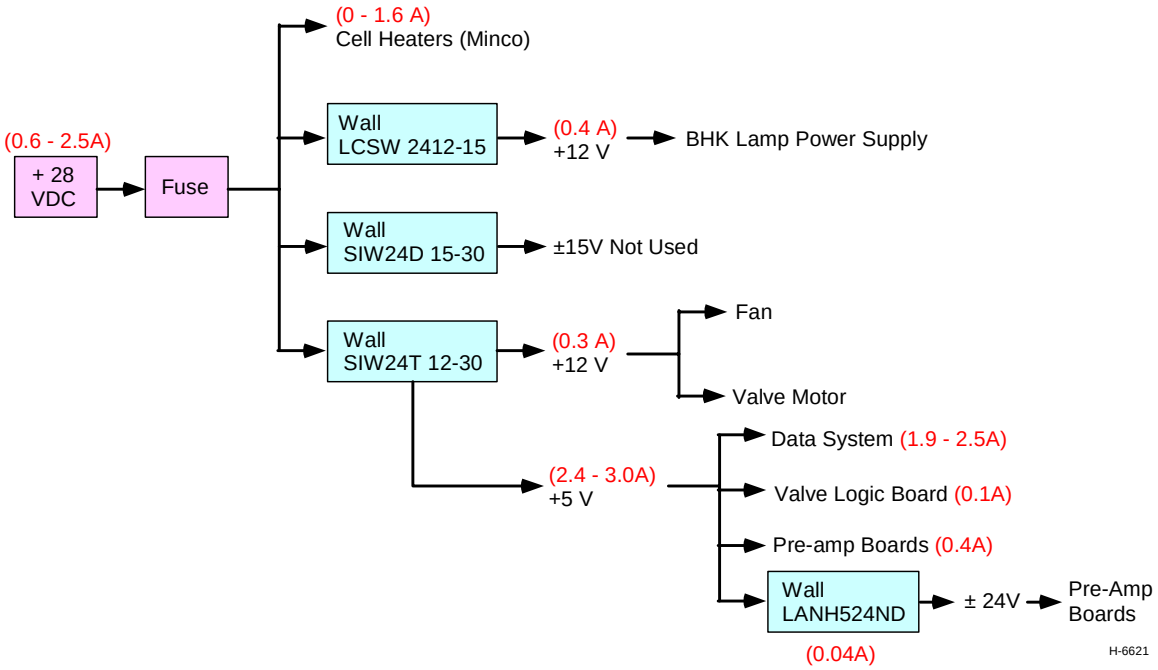

Figure 16. Power distribution network.

to the electrometer boards, where it is converted to ±15 VDC on each board and used to power several components. This power distribution network is mounted on the interface board as described above.

The source of the 28 VDC power is a Vicor 150 W power supply, VP-G1148441, as recommended by NCAR/RAF. This unit is connected to the aircraft 115 VAC power. A schematic of this setup is shown in Figure 17, as provided to us by NCAR/RAF. The instrument operation is switched either manually or remotely via a relay circuit, also recommended by NCAR/RAF. A schematic of this circuit is shown in Figure 18, as provided to us by NCAR/RAF.

For housekeeping purposes, the voltage levels of the +28, +5, +12, and ±24 VDC circuits are monitored by voltage divider circuitry as shown in the bottom left-hand side of the interface panel schematic in Figure 12. The total current draw at 28 VDC is also monitored by measuring the voltage drop across a 0.2 Ω resistor (bottom center of Figure 12). These values are read into the data file via the A/D converter, and are stored and streamed to the RS232 port.

20 New England Business Center □ Andover, MA 01810-1077 □ t 978.689.0003 f 978.689.3232
www.psicorp.com

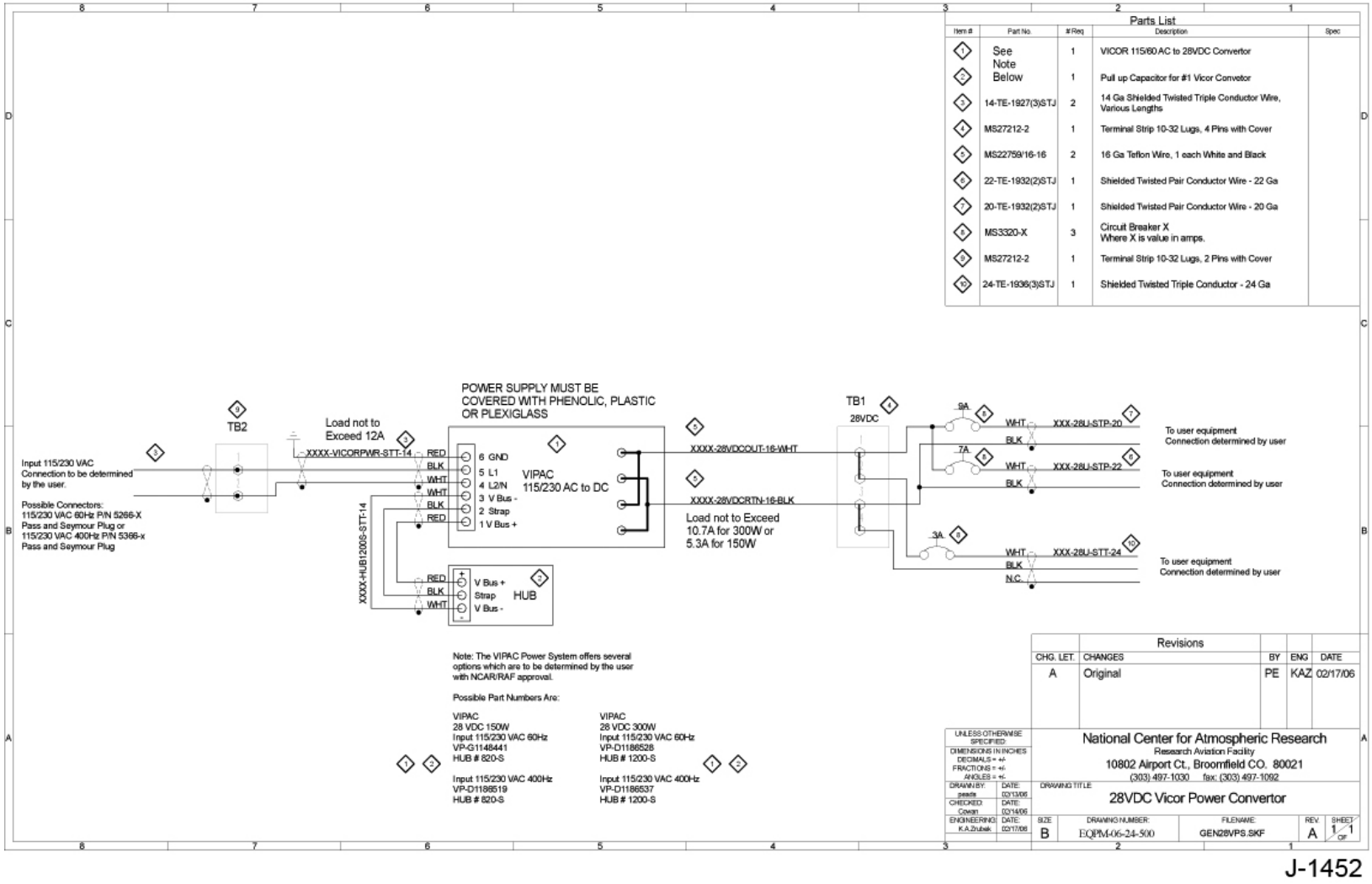

Figure 17. NCAR schematic of 28 VDC power converter circuit.

20 New England Business Center □ Andover, MA 01810-1077 □ *t* 978.689.0003 *f* 978.689.3232
www.psicorp.com

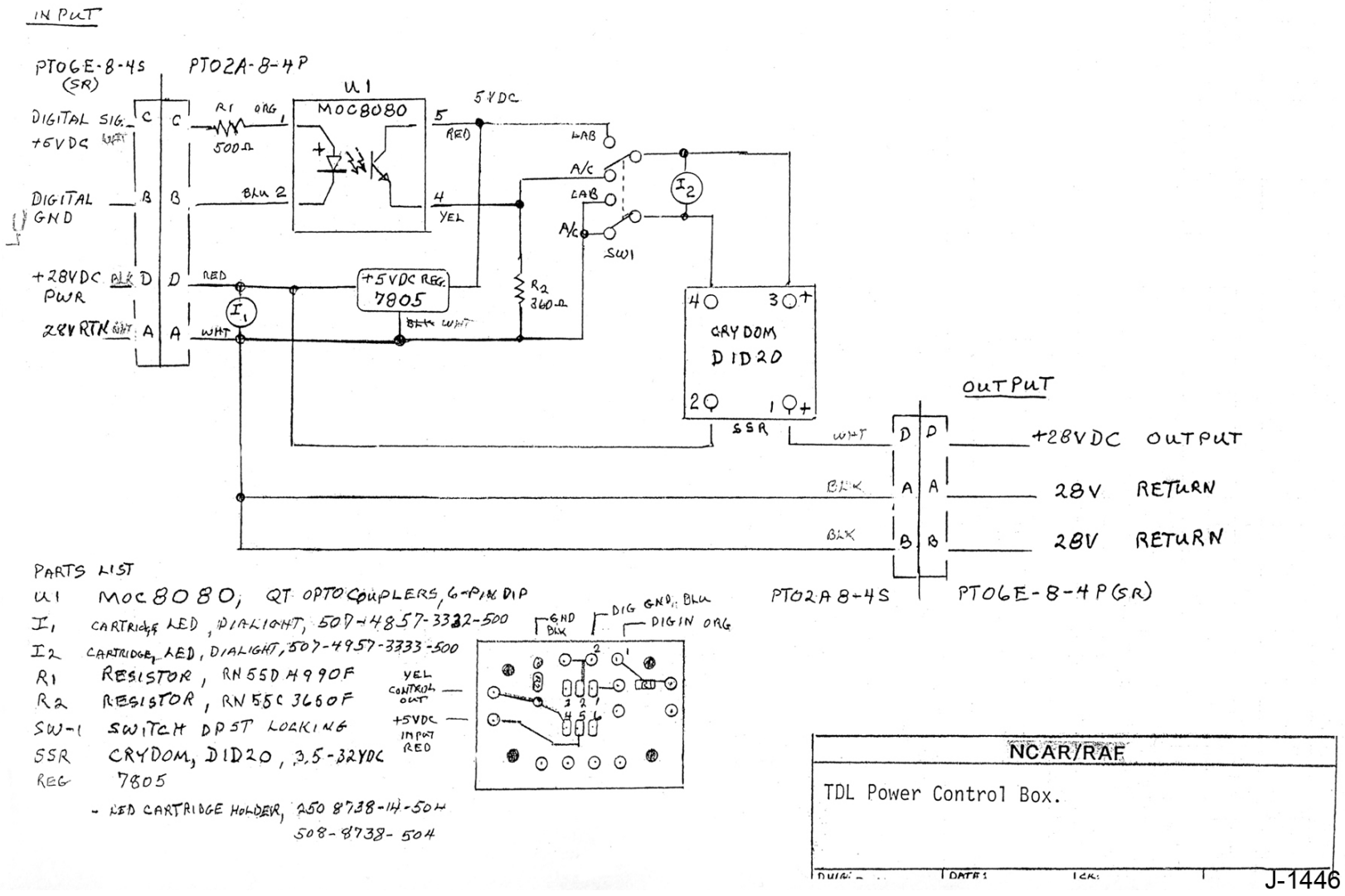

Figure 18. NCAR schematic of remote power control circuit.

20 New England Business Center □ Andover, MA 01810-1077 □ t 978.689.0003 f 978.689.3232
www.psicorp.com

6. Inlet and Exhaust Requirements

We have carried out an analysis of the flow in the air sampling system in order to evaluate the desirable range of flow rates for the flight measurements. The flow rates must be slow enough to allow good thermal accommodation in the inlet tubing, and fast enough to give short residence times in the absorption cell for 1 Hz ozone measurements. In addition, it is important to have small Reynolds numbers in the cell's flow channels so that boundary layer separation and recirculation effects do not introduce noise into the measurements. From a simple heat transfer analysis, the sample mass flow rate must be no greater than ~0.1 g/s to ensure adequate thermal accommodation within the inlet transfer tubing.

A simplified schematic of the flow sampling system is shown in Figure 19. The ram air flow enters the forward-facing external inlet and passes straight through to exit through an orifice at the rear of the inlet. A very small fraction of the total ram air flow is diverted into the ozone instrument, and exits through a small orifice in the instrument exhaust line. The larger orifice in the external inlet basically generates a pressure drop such that the pressure in the sampling line and instrument is ~10 to 30 mbar higher than in the ambient atmosphere. The pressure drop from the external inlet to the instrument absorption cell is relatively small and can be neglected to first order. Almost all of the pressure drop occurs at the instrument exhaust orifice, and this orifice restricts the flow rate through the instrument. The choice of the combination of inlet and exhaust orifice sizes dictates the sample flow rate for a given ambient pressure, temperature, and airplane speed. For example, in our previous WB-57F flights of the PSI UV Ozone Photometer, we used a forward-facing inlet with in inner diameter of ½-inch and a rear exit orifice of 1/8-inch I.D. x 3/8-inch long, together with instrument exhaust orifices 0.03 long x 0.020 to 0.035 inch I.D. for various altitude ranges.

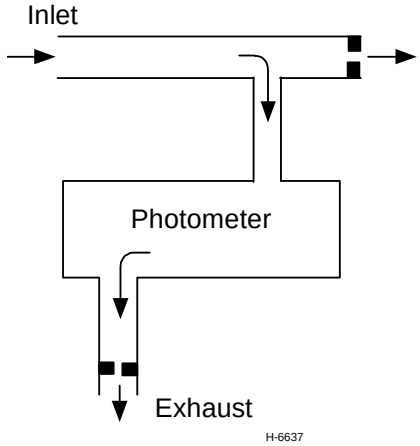

Figure 19. Schematic of inlet and flow sampling system.

For the HIAPER GV application, the inlet should be forward facing, with all internal surfaces lined or coated with Teflon to prevent catalytic ozone loss. Provision should be made for a variable or interchangeable exit orifice at the rear of the inlet so that the flow rates can be optimized. The I.D. of the inlet should be nominally ½-inch. The sample line should be several L/D downstream of the leading edge of the inlet to allow flow development. The sample line

20 New England Business Center Andover, MA 01810-1077 t 978.689.0003 f 978.689.3232
www.psicorp.com

should connect to Teflon tubing inside the cabin for transport of the sample flow to the instrument. This tubing should be nominally ½-inch O.D. We recommend a small amount of active pre-warming of the incoming air sample prior to the instrument inlet, to maintain a temperature difference < 1° C between the inlets and outlets of the absorption cell channels. For best measurement results, the inlet should be mounted on the fuselage as far forward as practicable, so that it extends beyond the boundary layer, and is not obstructed by protuberances or other inlets.

The exhaust air flow should go into a common exhaust duct which is not contaminated by non-ambient chemicals or back pressure from other instrument exhausts. The transfer tubing to the exhaust duct, nominally ½-inch O.D., can be any material, although Teflon is convenient for flexibility. The composition of the instrument exhaust flow is the same as that of the ambient atmosphere, except that half of the ozone has been removed by the catalytic scrubber.

7. Data Acquisition, Processing, and Analysis

7.1 Data Acquisition

The instrument data is acquired, processed, and stored by a QBASIC code, "**psi-irig.exe**", which is resident on the instrument computer as an executable file. The computer has two drives: "**A:**" is the on-board flash memory (~1.3 Mb) and contains the operating system and essential boot files; "**C:**" is the removable hard drive (~2.1 Gb) and contains the data acquisition code and the stored data files. Note that the data files should occasionally be removed from the **C:** drive. The data acquisition code can be initiated on the **C:** drive through the "**RUN**" command within QBASIC, or by simply entering the line "**psi-irig**" following the DOS prompt. For flight measurements, this command is built into the **AUTOEXEC.BAT** file so that the code is initiated automatically during the boot sequence following power-up. To terminate the code and return to the DOS prompt, press the "**ESC**" key. Since the output file is opened and closed each time a 1-second line of data is written, the code can also be safely terminated by simply turning off the power. Every initiation of the code results in the creation of an output file in the **C:/DATA/** directory. The name of each file is automatically chosen from the date and hour of the start-up: **yymmddhh.nnn**. The three-digit file extension "**nnn**" comes from the milliseconds value of the start time, and is thus very unlikely to result in duplicate file names.

The data acquisition code controls the valve operation, reads the IRIG time, reads the counter signals and converts them to counts/s, reads the pressure signals and converts them to millibars, reads the gas flow and hardware temperatures and converts them to degrees Celsius, and monitors the supply voltage levels, total current, and valve position. At 1-second intervals, the data required for ozone determinations (counter signals, pressures, gas flow temperatures) are recorded in the data file. Every 5 seconds, additional "housekeeping" data (hardware temperatures, voltages, current, valve position) are also recorded. If a video monitor is attached, the entire data block is shown on the screen and is refreshed every second. The data are also streamed via RS232 to an external computer for real-time graphical display, analysis for ozone mixing ratio, and storage. The QBASIC subroutines for writing to the disc, screen, and serial port are given in Appendix D to show the output formats.

20 New England Business Center Andover, MA 01810-1077 t 978.689.0003 f 978.689.3232
www.psicorp.com

The on-board data acquisition code does not determine ozone mixing ratios. These must be determined by analysis on an external computer, either by batch analysis after the flight or in real time by analysis of the RS232 data stream as described in the next subsection.

7.2 Off-Board Data Processing and Analysis

The instrument's QBASIC software stores the housekeeping and photometric data in engineering units on the hard drive, and also transmits the data in real time in a data stream through the "COM1" serial port of the PC104 computer. The data can be processed and inspected graphically in both batch form and real-time display using PSI's LabWindows based "**BATCH**" and "**TELEMETRY**" graphical user interfaces (GUI). The "**TELEMETRY**" GUI provides readouts and graphical displays of the housekeeping and raw photometry parameters in real time, and plots the 1-Hz ozone mixing ratio determinations with a 20-s delay. (This delay is necessitated by the forward and backward extrapolation requirements of the linear segment fitting algorithm for determining ozone mixing ratios, see below.) The routine also writes a spreadsheet-compatible data file containing the key sample temperatures, pressures, and photometric data and the 1-Hz ozone mixing ratios. The "**BATCH**" routine reads the data files written by the QBASIC code, displays plots of the housekeeping and photometric data, and calculates and displays the 1-Hz ozone mixing ratios, all as functions of instrument time. This code also provides the capability to average the data and remove noise spikes if desired. Written file output includes an extended data file containing the full data set as well as an archival file of the fully processed ozone mixing ratios.

7.2.1 Algorithm for Ozone Mixing Ratios

The ozone mixing ratio is determined from a ratiometric absorbance analysis, using the A/B lamp signal ratio for the primary determination. As a backup, the "**BATCH**" code also performs single-channel analyses of the individual A and B channel data; these results are useful for determining confidence in the validity of the dual-channel data in certain situations. The UV absorbance is related to the ozone concentration in the cell by the Beer-Lambert law:

$$\ln (I_o/I) = \sigma[O_3]\ell$$

where I_o and I are the detected intensities in the absence and presence of ozone, respectively, σ is the absorption cross section of ozone at 253.7 nm ($\sigma = 1.147 \times 10^{-17}$ cm^2), and ℓ is the path length (20 cm). However, the photometer measures the ozone concentration in the cell, not in the ambient air, so it is necessary to convert the concentration measurements to mixing ratios (MR) in order to represent the ambient ozone abundance:

$$MR = 1.3802 \times 10^{-10} [O_3] T_{cell}/P_{cell}$$

where T_{cell} and P_{cell} are the temperature in K and the pressure in mbar of the air flow inside the cell, and MR is expressed in ppbv (parts per billion by volume). The constant is a collection of

20 New England Business Center □ Andover, MA 01810-1077 □ t 978.689.0003 f 978.689.3232
www.psicorp.com

conversion factors including the ideal gas constant and the factor 10^9. The two equations combined together give the working equation for the ambient ozone mixing ratio:

$$MR = 6.0166 \times 10^5 \, (T_{cell}/P_{cell}) \ln(I_o/I)$$

The quantities T_{cell}, P_{cell}, and I_o/I must be determined from the data.

The ozone measurement has two modes, governed by the position of the flow switching valve. These are illustrated by the alternately oscillating single-channel signal intensities shown in Figure 20. In one mode, the sample (ozone-laden) air flows through Channel A and the scrubbed (ozone-free) air flows through Channel B. The intensities observed in this case are I_A and I_{oB}. This mode occurs for the first and third valve positions. For the second and fourth valve positions, the situation is reversed, and the measured intensities are I_{oA} and I_B. The ratio of the A and B signals cancels out common-mode variations in the lamp intensity, and gives a square-wave signal that oscillates between I_A/I_{oB} and I_{oA}/I_B. This is illustrated by the ratio waveform plotted in Figure 21, computed from the signals in Figure 20. The smaller of the two ratios occurs when A is in sample mode. Let us define the signal ratios as follows:

$$\text{A in sample mode: } r_A = I_A/I_{oB}$$

$$\text{B in sample mode: } r_B = I_{oA}/I_B$$

These values are determined rigorously in the code, however there is a convenient analytical approximation that can be made by realizing $r_A \approx r_B$:

$$r_B/r_A = I_{oA}I_{oB}/(I_AI_B) \approx (I_o/I)^2$$

$$\ln(I_o/I) = \tfrac{1}{2} \ln(r_B/r_A) \approx \tfrac{1}{2} (r_B/r_A - 1)$$

This approximation provides an easy way to estimate the absorbance from digital readouts of the ratio values on the QBASIC display screen. In addition, the absorbance noise levels can also be estimated from $\tfrac{1}{2} \Delta r/r$ using the displayed Δr values.

The magnitudes of the ratios drift with time due to slight changes in the flow characteristics and in the lamp plasma distributions and viewing factors with changing temperatures, pressures, and mass flow rates. However, when these variations are detrended from the ratio waveform, the amplitude of the square wave envelope is directly related to the absorbance and hence to the ozone mixing ratio.

20 New England Business Center □ Andover, MA 01810-1077 □ t 978.689.0003 f 978.689.3232
www.psicorp.com

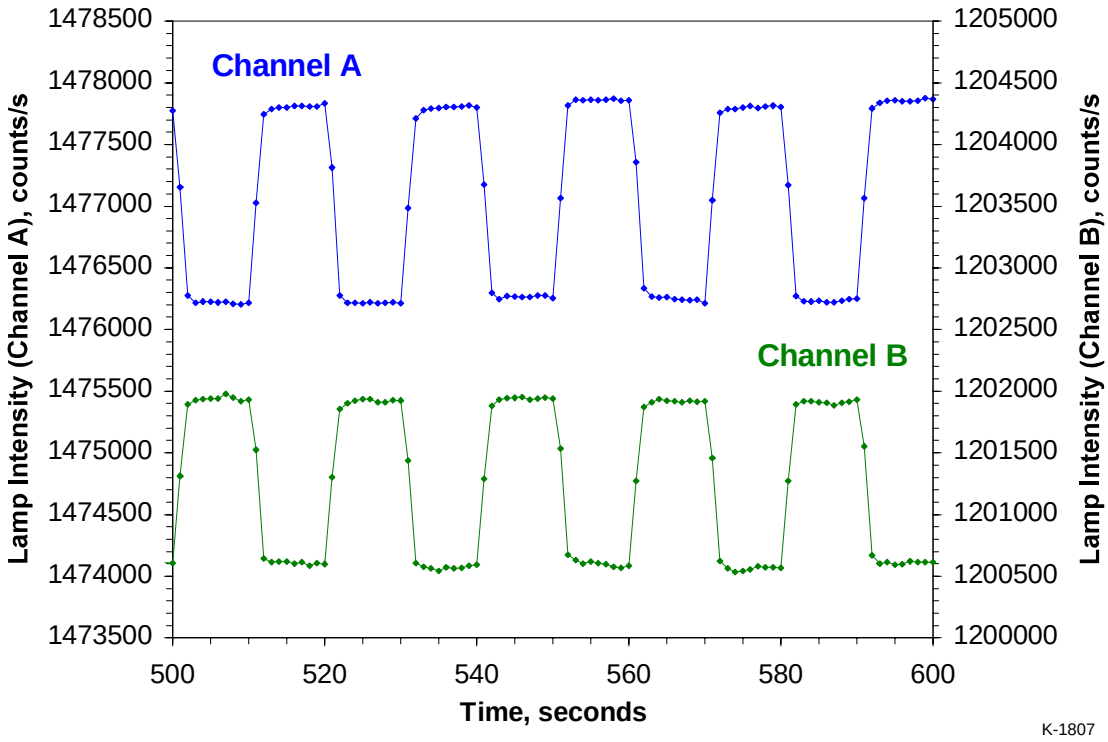

Figure 20. Single-channel ozone absorption signals.

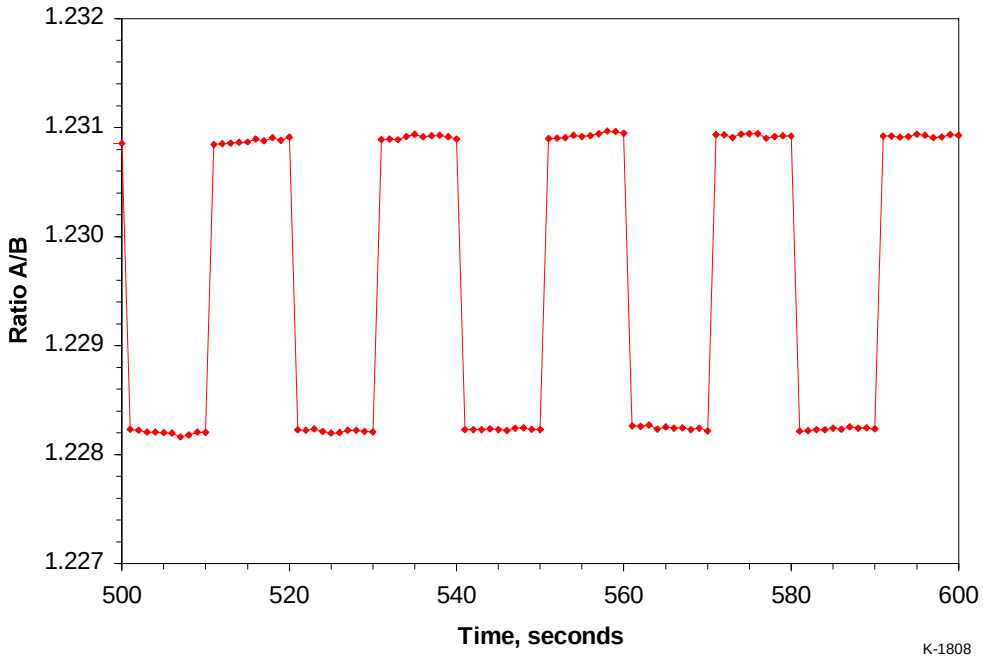

Figure 21. Ratio of Channel A and Channel B signals.

20 New England Business Center Andover, MA 01810-1077 t 978.689.0003 f 978.689.3232
www.psicorp.com

To perform the detrending, we use a linear segment fitting approach. First, we must determine an instrument response function. The values of this function can be determined rigorously only at the valve switching points (every 10 s), where simultaneous values of r_A and r_B can be determined by short extrapolations of the data. For the HIAPER instrument, we have determined that (1) the first two data points for each valve position must be ignored because of the combined time response of the detection and flow systems, and (2) an extrapolation of a five-point linear least squares fit from each side of the valve switching time gives acceptably accurate determinations of the ratio values for the first 2 s of each valve position. We can then determine an instrument calibration factor F_{CAL} for the first time point of each valve position:

$$F_{CAL} = (r_A r_B)^{1/2} = (I_{oA} I_A / I_{oB} I_B)^{1/2}$$

(Note that F_{CAL} is approximately the same as the average of r_A and r_B, i.e. $F_{CAL} \approx (r_A + r_B)/2$.) Since $I_A/I_{oA} = I_B/I_{oB}$ at each point of simultaneity, F_{CAL} is essentially a measure of the relative optical response of the two channels, I_{oA}/I_{oB}, at times every 10 s when all four of the absorbed and unabsorbed intensities can be determined with high accuracy.

For normal flight measurement conditions, this relative response changes very slowly compared to the 10-s flow switching time. As long as this is the case, additional values of F_{CAL} can be accurately interpolated linearly between adjacent flow switching points to give determinations for each sample time, i.e. every 1 s. The ratio of I_o and I for each sample time is then given by

$$I_o(t)/I(t) = F_{CAL}(t) / r_A(t), \text{ A in sample mode}$$

$$= r_B(t) / F_{CAL}(t), \text{ B in sample mode}$$

The r values for the first two time samples of each valve position are determined by the five-point linear fitting extrapolation described above. In this way, we determine the absorbances and hence the ozone number densities in the cell at 1-s time resolution.

It is also necessary to determine T_{cell} and P_{cell} in order to calculate the ozone mixing ratios in the sampled air flow. T_{cell} is determined from the average of the inlet and outlet temperatures for the channel that is in sample mode. If the instrument is working correctly, i.e. with a cell temperature gradient <1 °C, the value of T_{cell} can be determined with an uncertainty well below 1% by this method.

The value of P_{cell} is simply given by the absolute pressure transducer mounted at the midpoint of Channel A. Although this value decreases slightly when Channel A is in scrubbed mode (due to the pressure drop across the scrubber), the change is negligibly small. For the flow rates of interest, the pressure drop is <0.5 mbar at atmospheric pressure, and we expect it to remain <1 mbar over the altitude range of interest to HIAPER.

20 New England Business Center □ Andover, MA 01810-1077 □ t 978.689.0003 f 978.689.3232
www.psicorp.com

As a crosscheck of the ratiometric data, the "**BATCH**" routine also determines ozone mixing ratios using each of the individual single-channel data sets independently. This analysis provides ozone values only for each 10-s period when that channel is in sample mode. In this case the intensity in scrubbed mode represents I_o and the intensity in sample mode represents I. The values of I_o during the sample mode period are constructed by linear fitting and interpolation from five-point samples of the scrubbed modes prior to and following the sample-mode period. The ozone mixing ratios estimated in this way are not corrected for the relative optical response of the two channels, and do not have the noise cancellation advantage of the ratiometric values. However, the single-channel determinations provide a useful characterization of the upper and lower bounds on the measurements, as well as indications of noise spikes and rapidly changing measurement conditions for which the dual-channel analysis method is more uncertain. Significant divergence of the single-channel and dual-channel results is usually a flag for highly uncertain ozone determinations.

A section of the LabWindows code which determines the ozone mixing ratios is reproduced in Appendix E.

7.2.2 "**TELEMETRY**" Graphical User Interface

To use the "**TELEMETRY**" data processing capability, connect the COM1 output of the instrument computer to the serial port of an external PC computer using a null-modem RS232 cable, and initiate the "**psi-irig**" data acquisition program on the instrument computer. Use the installation package to install the executable program on the computer in a WINDOWS environment, and run the executable. The opening page offers the option of changing the automatically selected folder and file name for storage of the processed data. The program saves the processed data in a spreadsheet-compatible output file in the designated folder. This output file contains ozone mixing ratios, and serves as a backup to the archival data that is written on the instrument's hard drive and analyzed by the "**BATCH**" software described below. Click the cursor on "**START**" and the program is initiated. If there is no data stream, the program will stop at this point. The next page to appear is the "**Diagnostics**" page, which displays the numerical values of all of the data parameters being transmitted. There is a brief pause while the program synchronizes its internal counters with the rotations of the valve. Sometimes this step is unsuccessful, and the program must be restarted. Once the synchronization is successful, the page selection tabs at the bottom of the page become operative.

The remaining pages display graphical results. For each graph, the scales of the x and y axes can be changed by right-clicking on the axis and changing the numerical values in the displayed boxes. The "**Temps**" page displays real-time plots for each of the four air flow temperatures: A-in, A-out, B-in, and B-out. The instrument's accuracy for ozone determinations is within specifications when these temperatures are at or above their set points and when the differences between the inlet and outlet temperatures are <1 °C. Lower temperatures and/or larger inlet-to-outlet temperature gradients, as during the initial warm-up period or rapidly changing altitudes, are likely to result in significant noise levels in the ozone determinations.

20 New England Business Center □ Andover, MA 01810-1077 □ *t* 978.689.0003 *f* 978.689.3232
www.psicorp.com

The "**Motor**" page displays the real-time valve position data. Every ten seconds, the motor turns the valve 90 degrees counter-clockwise (viewed from the top). This defines four quadrants, of which two are redundant. Positions 1 and 3 direct the sample flow to Channel A and the scrubbed flow to Channel B. Positions 2 and 4 direct the sample flow to Channel B and the scrubbed flow to Channel A. The quantity "**EXPECT QUAD**" is the expected valve position based on the PC-104 generated valve commands. "**VALVE QUAD**" is the actual position as reported by the valve position sensors. The valve control logic does not select between the two redundant positions for each flow sampling configuration, so sometimes the actual and expected positions can be 180 degrees different but still working correctly. As long as the two values are either both odd or both even, the valve operation is correct. The uppermost plot displays the state of the valve position: "0" denotes A in sample mode (odd valve position) and "1" denotes B in sample mode (even valve position). The valve state is then used in the analysis of the data for ozone mixing ratio.

The "**Ratios**" page displays the real-time photometric data. The upper plot displays the optical signal levels in counts/s. The middle plot displays the A/B ratios. The lower plot displays the running derivative of the ratios as a measure of the noise level.

The "**Ozone**" page displays the ozone mixing ratios and pressure data, 20 seconds behind real time. The pressure graph plots both the cell pressure (Channel A) and the differential pressure (Channel B) between the cell and the exhaust. Note that the differential pressure is set up within the instrument to read negative: the larger the differential pressure, the more negative the displayed value. The cell and differential pressures are on very different scale settings, since the cell pressures range from 100 to 1000 mbar depending on altitude and the differential pressures are small (<1 mbar) and negative. To see the plot of the differential pressure (an indicator of flow rate and flow noise), set the y-axis scale to read from 0 to -1 mbar.

Examples of the "**TELEMETRY**" GUI pages are shown in Appendix F.

7.2.3 "**BATCH**" Graphical User Interface

The "**BATCH**" processing code is designed for rapid post-flight data analysis, evaluation, plotting, printing, and archival storage. It provides more capability for evaluation of the instrument performance and data quality than the "**TELEMETRY**" code, and is the preferred method of final data processing and archival. This program reads the data files written by the "**psi-irig**" data acquisition program. These data files must be downloaded from the instrument computer to the off-board data analysis computer as described in the following subsection. At the end of the analysis sequence, the program produces a print-compatible plot of the ozone mixing ratio and cell pressure vs. instrument or IRIG time, writes an archival spreadsheet-compatible text file of ozone mixing ratios in a ***.PRN** format, and writes an optional expanded, spreadsheet-compatible text file containing all of the processed, photometric, and housekeeping data in a ***.TXT** format.

20 New England Business Center Andover, MA 01810-1077 *t* 978.689.0003 *f* 978.689.3232
www.psicorp.com

When the "**BATCH**" software is executed, the entry screen allows setup of the input and output folders. First, change the data directory and output directory as desired by right-clicking on each window and following the menus. Then click on "**Batch File**" and select the data file to be processed. To save an expanded ***.TXT** batch file, click on the box and change the name of the file if desired. (Note that existing ***.PRN** and ***.TXT** data files will be overwritten in the unlikely event that they have the same year, date and hour as the one being processed.) When all the selections are completed, click on "**Start**". The program will rapidly run its course and then display the "**Ozone-Press**" page containing plots of ozone mixing ratio and pressure data for the entire data set. Additional pages include the "**Temps**", "**Motor**", and "**Ratios**" pages which are the same as those discussed above for the "**TELEMETRY**" software, and additional graphical display pages named "**Diagnostics**", "**Post-Process**", and "**Print**".

The "**Ozone-Press**" page displays ozone mixing ratios calculated for both the dual-channel ratiometric analysis and the single-channel analysis. As discussed above, the single-channel results are somewhat less accurate but have faster response to rapidly changing conditions, and provide a crosscheck of the dual-channel results. The lower graph provides the cell and differential pressures on separate right and left y-axes so that both can be viewed together. As with all the graphs, the axis scales can be changed by right-clicking on the axis and entering the range values in the input boxes. This page provides for detailed inspection and qualification of the ozone mixing ratio data and the effects of changes in altitude and sample flow rate.

The "**Post-Process**" page provides options for data smoothing and deletion of noise perturbations. The upper plot displays the 1-Hz dual-channel and single-channel ozone data, and the lower plot displays smoothed and noise-scrubbed data. The data are smoothed by a running average of N points, where N is entered into the window at the left. Each 1-Hz data point is averaged with the preceding and following points according to the value of N. For example, a 9-point running average gives the average of each 1-Hz point with four points before and four points after. For most flight data requiring the highest possible spatial resolution, N=1 is the desired option, resulting in no averaging. The "Revert" button cancels the results of the smoothing. To remove noise spikes or bad sections of data, click "**Remove Spikes**" to "**On**". This activates two cursors, which can be positioned to bracket the segment of data to be removed. The "**Undo**" button reverses the process. "**O3 vs. Time**" displays the final processed ozone and pressure data vs. either instrument time or IRIG time, in a printable graph. "**Store**" saves the output files with the final processed ozone data. Note that the original data is always preserved and is not altered by the smoothing and scrubbing process.

Examples of the "**BATCH**" GUI pages are shown in Appendix G.

7.2.4 Data Download for "**BATCH**" Analysis

The data files written by the instrument computer can be downloaded using the removable hard drive at the base of the PC-104 stack and an appropriate adapter, or by LAPLINK software or the equivalent. PSI has provided a USB capability for convenient data transfer via a portable USB drive.

20 New England Business Center Andover, MA 01810-1077 *t* 978.689.0003 *f* 978.689.3232
www.psicorp.com

By design, DOS 6.22 does not support the USB standard. However, Panasonic developed a set of drivers for their product lines so that the DOS community could connect USB devices to their computers. The driver file is called **USBASPI.SYS**. It must be loaded during the boot sequence from within **CONFIG.SYS**. The syntax is as follows:

devicehigh = usbaspi.sys

This must next be followed by a driver which specifically supports hard drives, CDROMs etc. The syntax to load the driver specifically for an external hard drive is as follows:

devicehigh = di1000dd.SYS

Note that the hard drive must be connected to a USB port on the front panel and powered prior to powering up the sensor. The drive can be hot swapped (disconnected and reconnected) at any time after the boot procedure has loaded the drivers.

After the system has completed booting, the drive is recognized as the **D:** drive. This can be accessed from the DOS prompt by simply typing **D: <cr>**. There will be an incorrect error message the first time claiming that the drive cannot be found. Hit the character **A** to **Abort** the command error and the **D:** drive will become the current drive. This error message only occurs the first time the drive is accessed after booting.

To download the data, connect a video monitor, keyboard, and the USB drive to the instrument computer panel, turn on the USB drive, and turn on the instrument. When the power is turned on, the computer will boot and initiate the data acquisition code. The monitor will display the boot sequence, followed by the information written by the data acquisition code. Press the **ESC** key to terminate the code. The monitor will display the DOS prompt for the **A:** drive. Enter **D:** to get to the USB drive. As noted above, there will be an error message; type "**A**" for "**Abort**" and the **D:** prompt will appear. Enter **C:/DATA <cr>** to access the data directory. Then use the DOS copy command "**COPY <filename> D: <cr>**" to copy the data file from the **C:/DATA** directory to the USB drive. The USB drive can then be disconnected from the instrument computer and connected to the off-board computer for further file transfer.

8. Initial Test Results

The instrument was assembled by Proffitt Instruments, Inc. (PI) and was delivered to PSI, where it was integrated into an aircraft-compatible power and mechanical package including IRIG timing, housing, power supply, external data interface, and certification requirements. PSI performed an initial set of bench tests and a limited series of flight tests in 2007, described in this section. These tests showed that the basic instrument functionality on the bench and in flight was very good, however the ozone measurements on the bench showed a significant negative offset, sufficient to cloud the accuracy of any potential flight measurements. In addition, the Minco temperature controller originally installed by PI generated unacceptable noise spikes in the photometric data. After conclusion of the flight tests, the instrument was returned to PSI to

20 New England Business Center Andover, MA 01810-1077 t 978.689.0003 f 978.689.3232
www.psicorp.com

have these two issues resolved. The PSI modifications and successful bench tests are described in Sections 9 and 10, respectively.

8.1 Initial Bench Tests (May-June 2007)

8.1.1 Flow Rate Calibrations

The HIAPER Ozone photometer was calibrated for internal flow rate at atmospheric pressure by observing the ΔP readings as a function of air flow rate measured by a digital mass flowmeter. Dry air from a high-pressure cylinder (AirGas, Dry Grade) was passed through a mass flowmeter (Aalborg GFM37) and a regulating valve via ¼-inch o.d. teflon tubing, and into the instrument sample inlet. The ΔP pressure sensor, located at the midpoint of the Channel B optical path, measures the pressure difference between the Channel B flow and the combined outlet of the two channels. The sensor is configured to give a negative reading for a positive difference between Channel B and the outlet. As the flow sampling valve periodically interchanges the scrubbed and unscrubbed flow streams between Channels A and B every 10 s, the ΔP signal changes. The amplitude of this 10-s periodic change in the ΔP signal signifies the pressure drop across the scrubber and its outlet tubing. This pressure drop is a function of the flow rate through the instrument. This provides an approach for estimating the flow rate through the instrument in the field: based on the Poiseuille equation, we expect the pressure drop for a given mass flow rate to vary inversely with pressure, so that the 1-atm calibration can be scaled to higher altitudes. We observed δΔP values for periods of nominally ~50 s for each flow rate, and determined averages and standard deviations. The results are plotted vs. mass flow rate in Figure 22. (The mass flow rate for air is 0.0208 x slm (standard liters/min).)

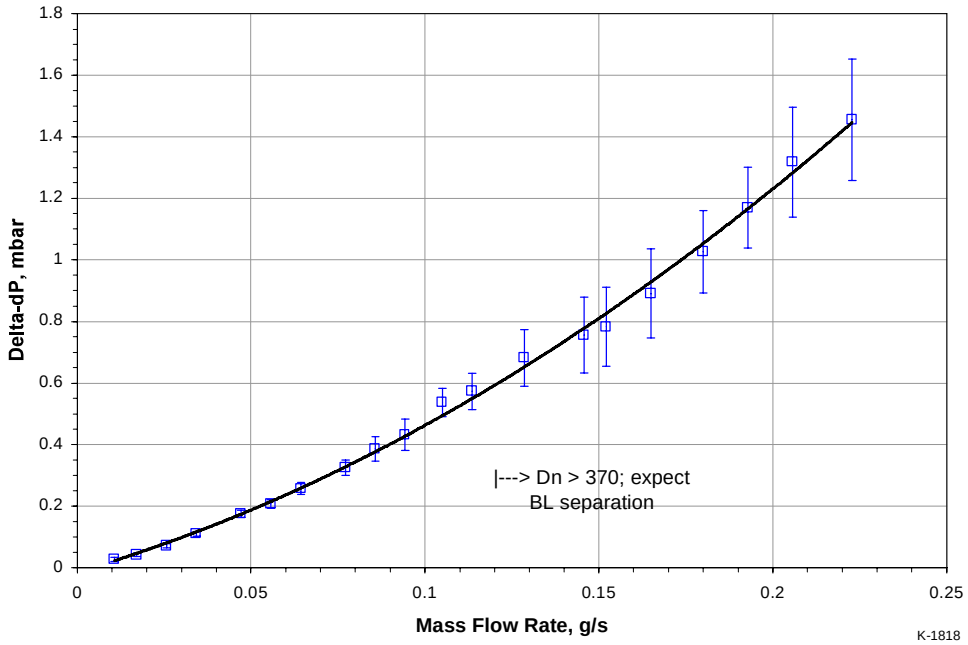

Figure 22. Initial flow rate calibration for HIAPER ozone photometer.

20 New England Business Center □ Andover, MA 01810-1077 □ t 978.689.0003 f 978.689.3232
www.psicorp.com

As indicated by the error bars, we noted a rather sharp onset of extra noise in the ΔP data for total inlet flow rates above ~0.1 g/s (4.8 slm). We believe this noise results from boundary layer separation immediately downstream of the right-angle bends entering the optical measurement channels. We note that the Reynolds numbers for these flows are ~300 (per channel) at 0.1 g/s total flow rate, and are at most ~675 (per channel) for the highest flow rate used, so the flow is never turbulent for any of the flow rates we used. (Flows are generally considered turbulent for Reynolds numbers >2300.[1]) However, we must also consider the Dean number for 90-deg bends. The Dean number (Dn) is the ratio of the Reynolds number (Re) to the square root of the ratio of the radius of curvature of the bend (R) to the channel radius (r):

$$Dn = Re / (R/r)^{1/2}$$

Experimental measurements and computations in the literature show that a Dean number of 370 marks the onset of pronounced vortical motion and boundary layer separation from the inner channel wall immediately downstream of the bend.[2-4] Based on the published results, we estimate that such an onset should occur in the photometer cell channels at ~0.12 g/s (6.7 slm) total inlet flow rate. This is in excellent agreement with our observations of increasing noise in the pressure measurements as shown in Figure 22. Based on these observations, we recommend that the total flow rate admitted to the instrument be kept below ~0.1 g/s (~5 slm), to avoid any possibility of flow-induced photometric noise. The 0.1 g/s level is also a benchmark for good thermal accommodation in the inlet transfer tubing as discussed in Section 6, and corresponds to the maximum recommended flow rate (~0.09 g/s) for accurate ozone measurements as discussed in Sections 9 and 10.

Note that the flow rate calibration results in Figure 22 are amended by the modifications and tests described in Sections 9 and 10.

8.1.2 Negative Offset in Ozone Measurements

During the flow rate calibrations, which used dry air containing no ozone, we observed a substantial negative "ozone signal" amounting to several tens of ppbv which increased with increasing flow rate. We conducted a great many tests which confirmed that this effect is not due to contamination, optics effects, or scrubber malfunction. We have isolated the cause to the flow switching valve and/or its pressure-tight motor housing. The housing volume is connected to the flow exhaust outlet of Channel B, and also communicates with the inlet and Channel A and B sample and scrubbed flows via leakage along the shaft connecting the motor to the valve. While the motor housing volume is isolated from the external environment by o-ring seals, there is no seal on the connecting shaft to isolate the sample air channels from the motor housing volume. For comparison, the PSI Ozone Photometer, designed for operation in ambient pressure conditions, does not have a pressure-tight housing on the valve motor, but does have an o-ring seal on the valve shaft which isolates the sample air inside the photometer from the air outside the photometer. The PSI photometer does not exhibit the negative offset effect observed for the HIAPER photometer.

20 New England Business Center Andover, MA 01810-1077 t 978.689.0003 f 978.689.3232
www.psicorp.com

We have conducted extensive testing to characterize the negative offset in hopes of identifying its cause and eliminating it. The results are summarized as follows:

(1) The absolute value of the offset increases with increasing flow rate. This behavior is consistent and reproducible for a given environmental (temperature) condition.
(2) The offset persists even when the scrubber is removed from the instrument.
(3) The offset is larger with the cell heaters turned off (cell temperature ~25 °C), and is smaller when the instrument cover is installed (i.e. when the cell temperature warms up to >35 °C).
(4) When the cell is at room temperature, the magnitude of the offset is approximately the same in Channels A and B. There is also a dependence on valve position, i.e. a variation in the offset through the four positions of the valve rotation cycle.
(5) When the cell is warm (cover on), the offset is considerably larger in Channel B than in Channel A, see Figure 23. We have noted visually that the valve position is misaligned with the flow channels when the cell is cold, but comes into good alignment as the cell warms up to its set point temperature.
(6) When the volume inside the motor housing is pumped out by a small rotary vane pump, the absolute value of the offset increases substantially.
(7) When the motor housing volume is pressurized by dry nitrogen, the offset approaches zero, but still shows significant dependence on the valve position.

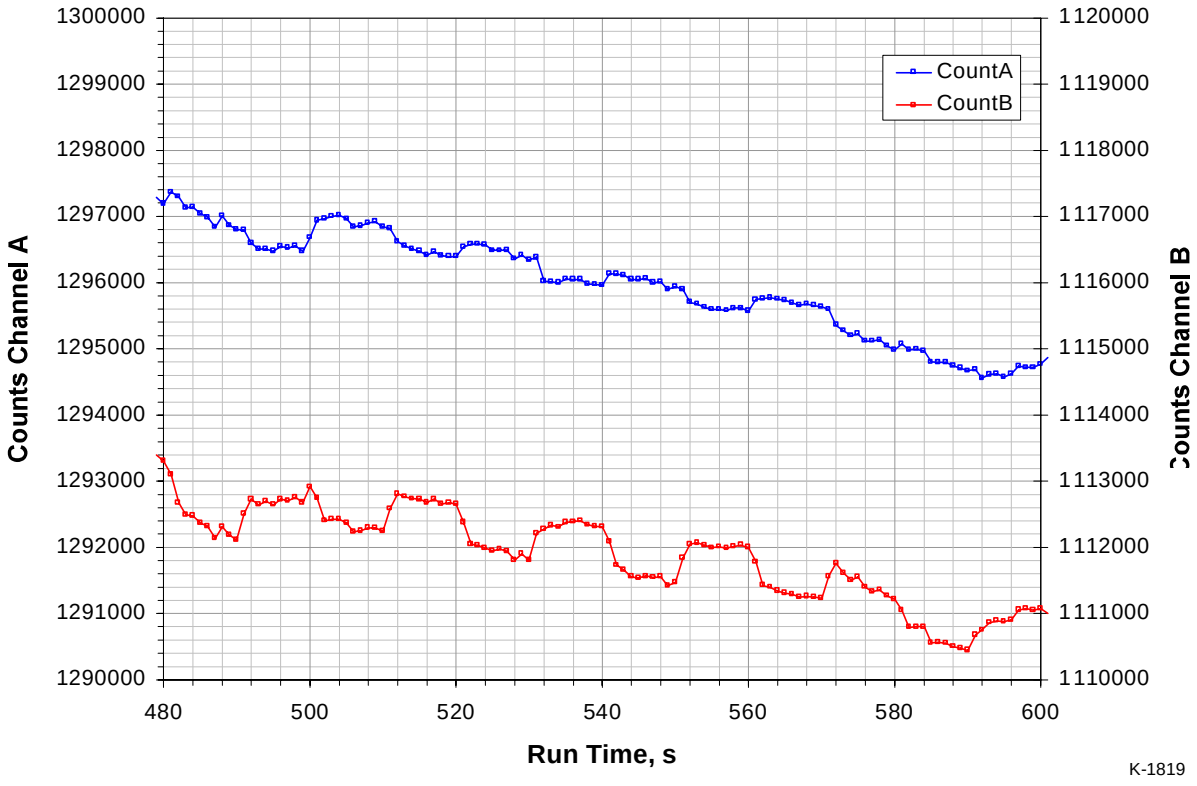

Figure 23. Offset effect: Channel A and B signals for ozone-free air, 4 slm (instrument cover on.)

20 New England Business Center □ Andover, MA 01810-1077 □ t 978.689.0003 f 978.689.3232
www.psicorp.com

A plot summarizing measurements of the negative offset for a variety of conditions is shown in Figure 24. Dry air was passed through a mass flowmeter as described above for the flow rate calibrations. Offset values, determined from the ratio of the Channel A and B signals, were averaged over typically ~100 s. The error bars represent 1σ standard deviations. The blue-square data points were observed with the instrument cover off; the heaters maintained the cell at its set point of 34 °C. The red-triangle points were obtained with the cover on; in this case the cell temperature drifted above its set point to ~38 °C. The grey data points were determined by M. H. Proffitt for a separate but similar photometer cell setup, using room air and no scrubber.

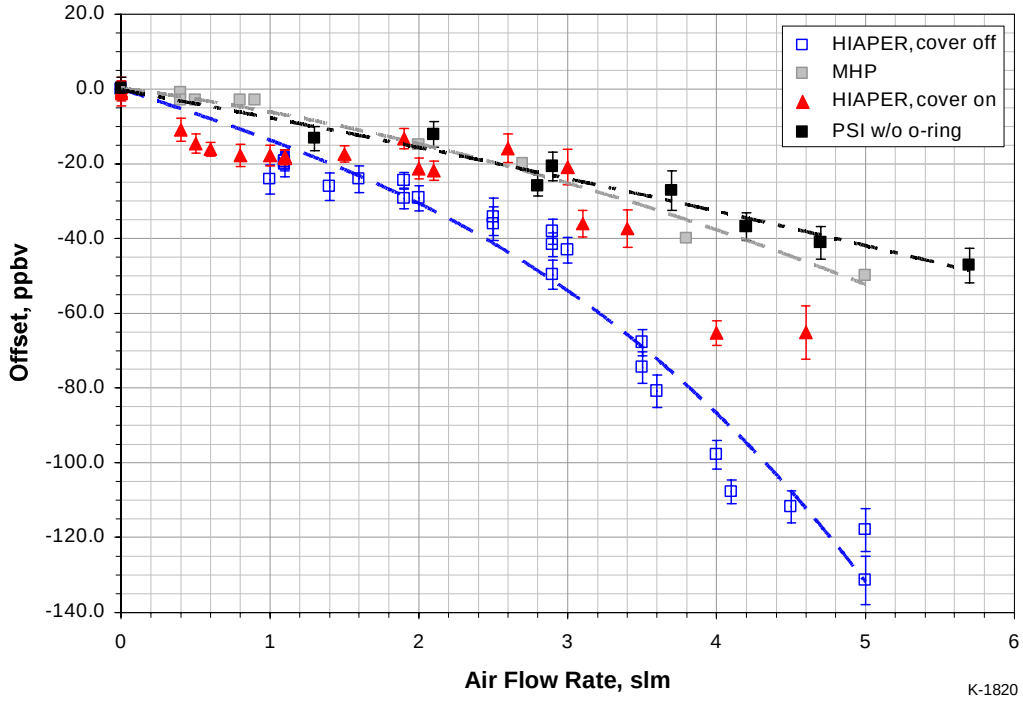

Figure 24. HIAPER ozone photometer zero offset.

The black data points were determined using the PSI photometer with the o-ring removed from the valve shaft. We observed in this case that the offset appeared primarily in Channel A, rather than in Channel B as observed for the HIAPER instrument. The striking similarity of this last data set to the observations for the HIAPER photometer suggests that the HIAPER valve assembly should be modified to include an o-ring seal on the valve shaft. An intercomparison of the HIAPER and PSI photometer measurements for ozone-free air is shown in Figure 25, using the setup described in the next subsection. For the measurements in Figure 25, both instruments were fully assembled with covers on; note that the flow rates indicated in the plot are the totals supplied to both instruments.

20 New England Business Center □ Andover, MA 01810-1077 □ t 978.689.0003 f 978.689.3232
www.psicorp.com

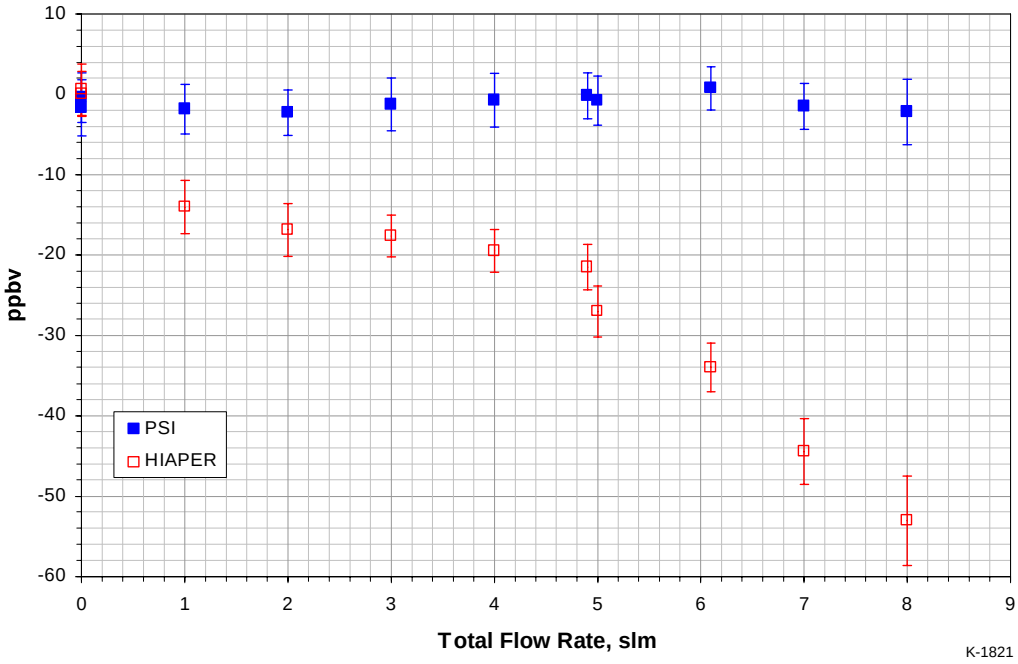

Figure 25. Intercomparison of HIAPER and PSI photometers for ozone-free air.

8.1.3 Intercomparison of Ozone Measurements by the HIAPER and PSI Photometers

The HIAPER and PSI photometers were set up in tandem to measure concentrations of ozone generated by photolysis in a common air stream. A photograph of the setup is shown in Figure 26. Both instruments were fully assembled with covers on. Dry air was passed through the mass flowmeter and regulating valve as above, and then through an ozone generator consisting of a section of quartz tubing and a mercury pen lamp with a quartz envelope. The pen lamp was positioned alongside the tubing so that radiation from the lamp (185 nm) photodissociated a small amount of the O_2 in the air flow, to produce O_3 by three-body recombination:

$$O_2 + h\nu(185\ nm) \rightarrow O + O$$
$$O + O_2 + M \rightarrow O_3 + M.$$

The effluent of the generator passed through some 18 inches of ½-inch (o.d.) Teflon tubing and was split via a ¼-inch tee and tubing into the sampling inlet of each instrument. The lengths of the sampling splits were closely matched to ensure equal flow rates to each instrument; this was confirmed by the δΔP flow rate measurements. The total flow rate was varied from 1 to 8 slm, half to each instrument. In preliminary measurements, we observed, as in previous intercomparisons of this type, that it is important to have sufficient mixing volume downstream of the photolysis source to ensure that equal ozone mixing ratios are sampled by each instrument (hence the length of ½-inch tubing).

20 New England Business Center □ Andover, MA 01810-1077 □ t 978.689.0003 f 978.689.3232
www.psicorp.com

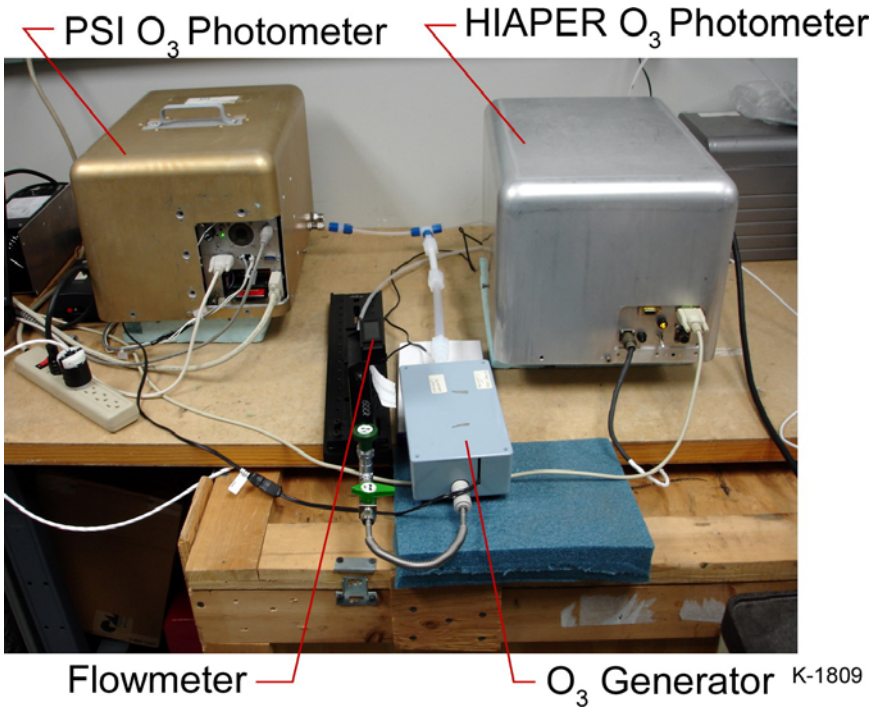

Figure 26. Photograph of setup for the PIS and HIAPER ozone measurement intercomparisons.

During preliminary ozone measurements using only the HIAPER instrument, we noted that the photometer signals exhibited 2-point transitions at each valve change. Normally, when the scrubbed and unscrubbed flows are interchanged between Channels A and B, there is a 1-second transition period when both channels sample an erroneous intermediate absorbance value. For flow rates >1 slm per channel, the air in the measurement cell is completely interchanged within <0.33 s, and the only a single transition data point, occurring during the valve change, needs to be ignored in the analysis. For sufficiently slow flow rates, the transition period becomes 2 1-second data points instead of 1, and the data analysis software has to be modified accordingly. This behavior is exhibited by the PSI instrument, as well as by an instrument built by PSI for Woods Hole Oceanographic Institute (see below). However, for the HIAPER instrument, we observe 2-point transitions for inlet flow rates up to ~5 slm (2.5 slm per channel), even though the flow time through the length of each measurement channel is ~0.13 s. The effect is not due to any normal electronic time response of the electrometer; both the PSI and the HIAPER electrometers contain the exact same circuit boards and components, including the same RC characteristics on the signal input. We have modified the HIAPER data processing algorithm to take the 2-second transition into account, and have used the modified algorithm for all of the HIAPER ozone and offset determinations reported here. However, as noted below, for the slowest flow rates used in the intercomparison measurements, the PSI photometer's 1-second transition period was slightly exceeded, resulting in additional noise in the ozone mixing ratio determinations for those cases.

20 New England Business Center □ Andover, MA 01810-1077 □ *t* 978.689.0003 *f* 978.689.3232
www.psicorp.com

A sample intercomparison data set is shown in Figure 27. The plot shows ozone mixing ratios determined simultaneously by the PSI and HIAPER instruments as a function of laboratory time. The test begins with no flow for ~300 s, then the air flow is turned on, and the ozone generator is turned on at ~600 s. The periods with no ozone in the flow are 300-600 s, 3700-3900 s, and 6400-7700 s. During the last of these periods, the total flow rate was systematically varied, resulting in the data plotted above in Figure 25.

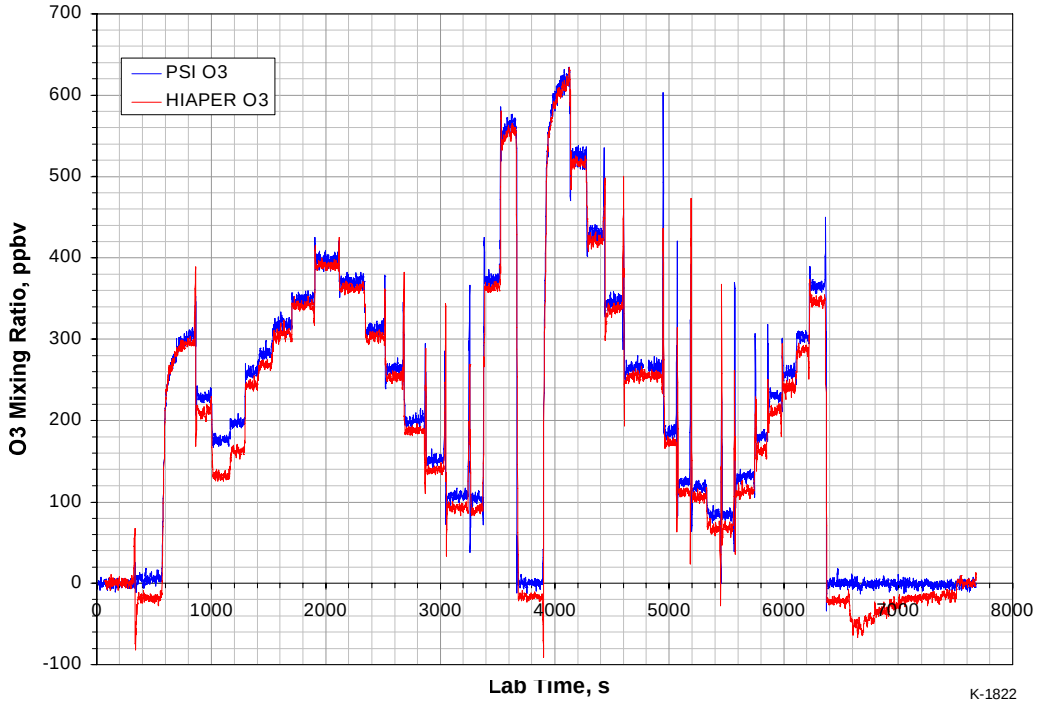

Figure 27. Initial intercomparison data: HIAPER and PSI photometer measurements of photolytically generated ozone.

The ozone mixing ratio was varied in two ways. From 800 to 2200 s, the ozone concentrations were varied by adjusting the total flow rate through the photolysis cell. At lower flow rates (longer reaction times), the generator produced higher ozone concentrations. However, variations in the flow rate can produce a bias in the photometer measurements: low flow rates approach the limit of the PSI photometer for a 1-second flow switching transition as noted above, and the high flow rates approach the regime of flow instability as observed in the $\delta\Delta P$ measurements, as well as larger negative offsets in the HIAPER instrument. For best results, we performed the measurements at each of several constant flow rates using a series of apertures to partially block the radiation between the photolysis lamp and the quartz tube. Figure 27 shows measurements of this type for total photolysis cell flow rates of 3.4 slm (2100-3800 s), 3.1 slm (3800-5300 s), and 4.9 slm (5300-6400 s).

20 New England Business Center □ Andover, MA 01810-1077 □ *t* 978.689.0003 *f* 978.689.3232
www.psicorp.com

The data show systematic differences in the ozone determinations of the two instruments. The instruments tend to agree better at lower flow rates, however the HIAPER result is always lower than the PSI result. The differences become larger at total (combined) flow rates of ~4.9 slm and higher. For comparison, in Figure 28 we show an intercomparison data set from May 2001, for the PSI instrument and the instrument built for the Woods Hole Oceanographic Institute (WHOI).[5] The data in Figure 28 were obtained by varying the flow rate, and illustrate very good agreement between the two instruments.

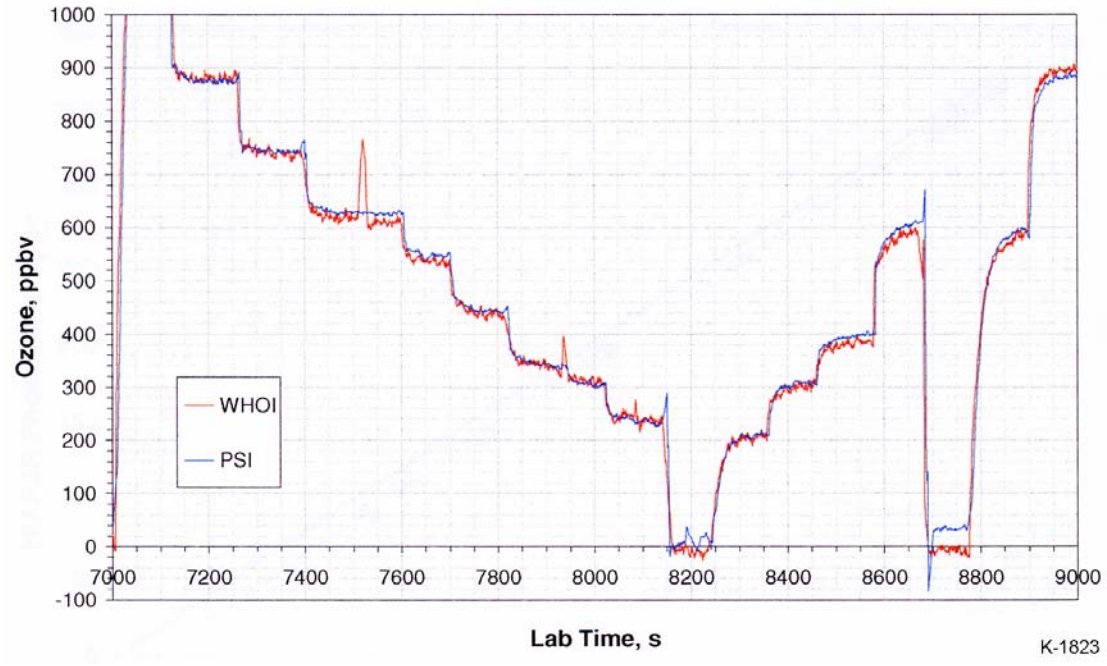

Figure 28. Intercomparison of ozone measurements by the PSI and WHOI ozone photometers, May 2001.

The HIAPER-to-PSI intercomparison results are plotted against each other in Figure 29, for three different total flow rates. Each data point represents an average over ~100 s; the standard deviations in these averages are typically 2-4 ppbv. For the low to moderate total flow rates of 3.1-4.1 slm, the data points all lie on essentially the same straight line fit. These data show a skewing from the 1:1 correlation, with a larger discrepancy at low mixing ratios and better agreement at higher mixing ratios. However, for 4.9 slm, the data lie on a significantly different line, which is parallel to the 1:1 correlation but shifted down by 19 ppbv throughout. This shift is much larger for higher flow rates (cf. Figure 27, 1000-1300 s for 8 and 7 slm), and appears to be consistent with the negative offset effect shown in Figure 25. The data are independent of flow rate for 3.1-4.1 slm, i.e. <2 slm per instrument, as shown in the combined plot in Figure 30, but the ozone mixing ratios are consistently low by about 10-20 ppbv. We have only characterized this effect at sea-level atmospheric pressure. Additional measurement intercomparisons during flight are required to evaluate whether this behavior extends to the lower pressures and higher altitudes of interest.

20 New England Business Center Andover, MA 01810-1077 t 978.689.0003 f 978.689.3232
www.psicorp.com

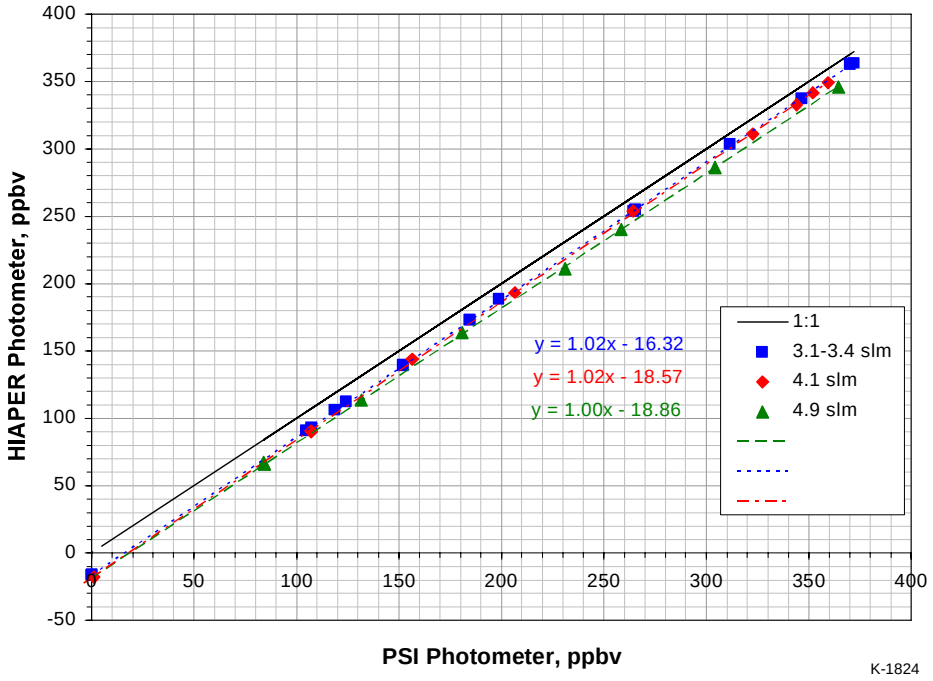

Figure 29. Initial intercomparison data: correlations of HIAPER and PSI ozone measurements for different flow rates.

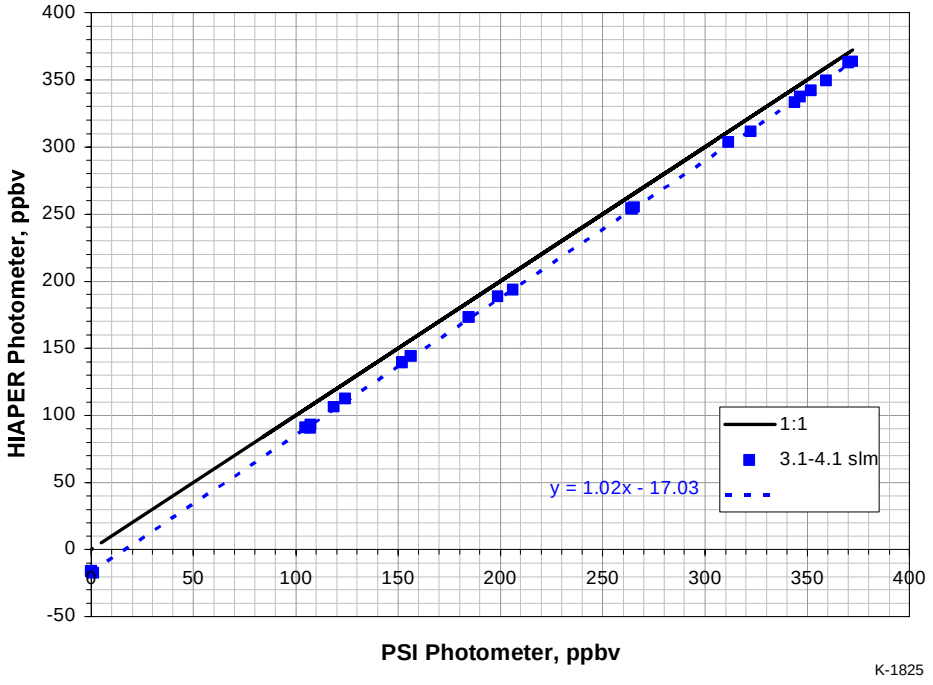

Figure 30. Initial intercomparison: correlations of HIAPER and PSI photometer flow rates, 3.1-4.1 slm

20 New England Business Center □ Andover, MA 01810-1077 □ *t* 978.689.0003 *f* 978.689.3232
www.psicorp.com

The negative offset behavior exhibited by the HIAPER instrument is completely unexpected by both PSI and PI, owing to the excellent and well validated performance of the three previous PSI prototypes on which its design is based. Intercomparison data for the PSI photometer and a "clone" built by PSI for WHOI in 2001 is shown above in Figure 28. A sample of flight intercomparison data for the PSI photometer and the NOAA Aeronomy Laboratory's ozone photometer is shown in Figure 31. Laboratory intercomparison results are shown in Figure 32 for the NOAA photometer and PSI's first prototype, built for JPL and completed in 1997.[6] In all cases, the intercomparison agreement is very good, and none of the PSI instruments show significant negative zero offsets in ozone mixing ratio. The instrument built in the joint effort by PSI and PI for the HIAPER GV aircraft followed these earlier designs very closely, especially in the design and operating characteristics of the photometer measurement cell and associated electronics. Indeed, the only difference in the photometer cell between the HIAPER instrument and the earlier instruments is PI's design of the valve and motor assembly and pressure-tight enclosure. As described by M. H. Proffitt in the PI Operator's Manual (Appendix C), not only the HIAPER instrument but also two other ozone photometers recently built by PI with this design show negative zero offset behavior. As discussed in Appendix C, Proffitt believes this behavior is related to the inherent imbalance of flow rates, pressures, and temperatures between the scrubbed and unscrubbed flows due to the additional pressure drop in the scrubbed path. PSI additionally conjectures that the HIAPER instrument, unlike its predecessors, is susceptible to these flow imbalance effects because of the omission of an o-ring seal on the valve shaft.

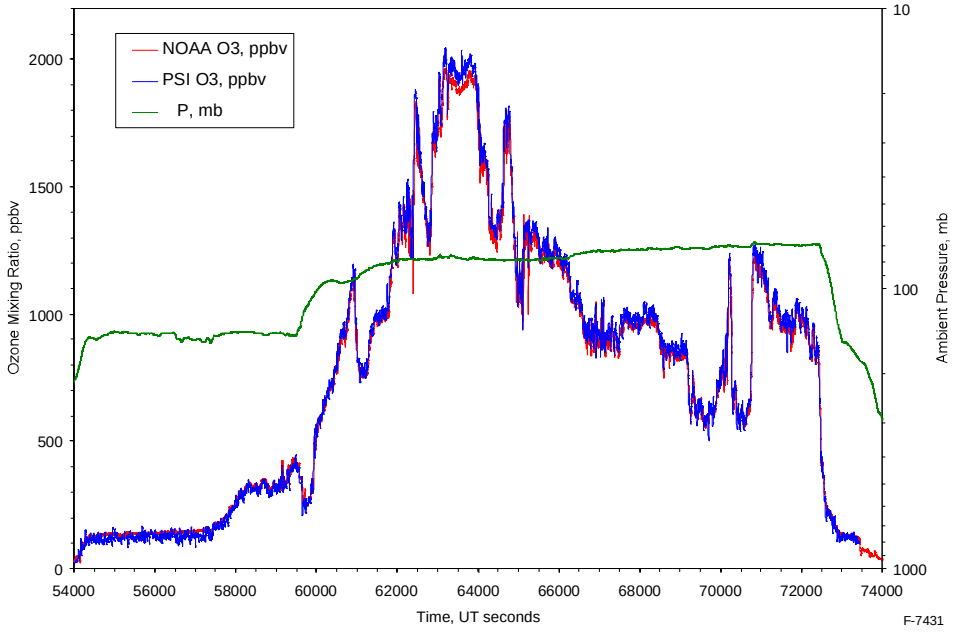

Figure 31. Flight intercomparison of 1-Hz ozone measurements by the NOAA and PSI instruments during a WAM (WB57F) science flight on May 7, 1998, from Houston to an area off the Atlantic coast and back. The ambient pressure is plotted along the right hand axis as a relative indicator of altitude. The outbound flight path followed the tropopause at approximately 14 to 15 km, and the return flight was in the lower stratosphere at 18 to 19 km.

20 New England Business Center □ Andover, MA 01810-1077 □ t 978.689.0003 f 978.689.3232
www.psicorp.com

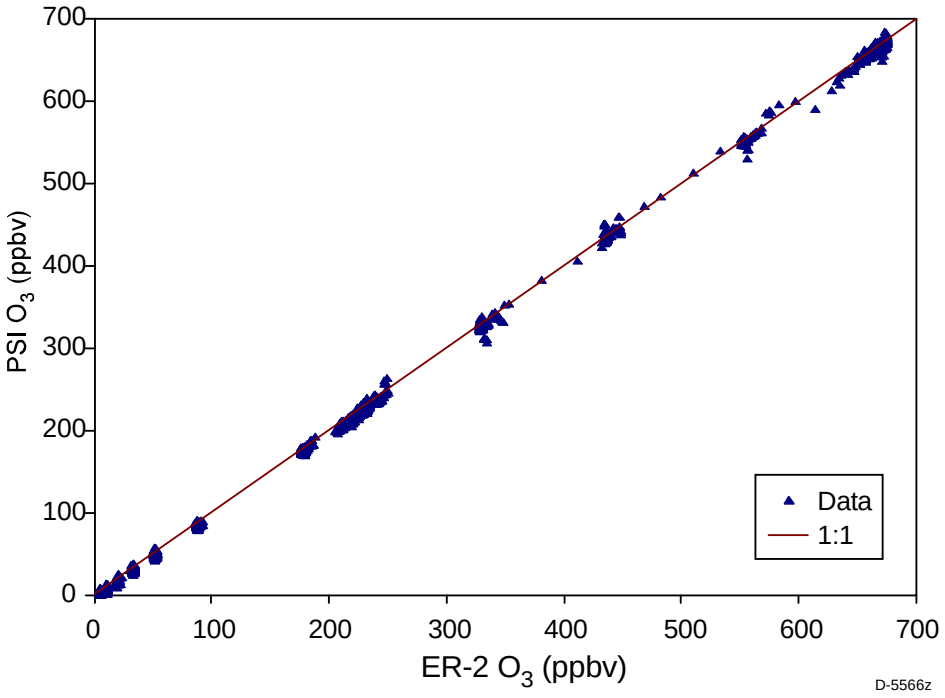

Figure 32. Laboratory intercomparison of ozone mixing ratios measured at 1 Hz by the first PSI prototype and the NOAA/AL ER-2 instruments.

In subsequent work, PSI has resolved the negative offset through extensive redesign and modification of the valve assembly. The modifications and bench test results are described in Sections 9 and 10.

8.2 GV Integration and Flight Tests (July 2007)

The ozone instrument was successfully integrated and flown on the Gulfstream V aircraft at NCAR/RAF. The primary objectives of this task were to ensure that (1) the instrument would be mechanically and electrically compatible with installation and autonomous operation within the aircraft cabin; (2) the instrument would meet NCAR/RAF's certification requirements; and (3) the instrument would function properly in flight over the full operating envelope of the aircraft. These objectives were all met: the instrument was certified and installed on the aircraft, functioned normally throughout four test flights totaling about 20 hours, and neither affected nor was affected by other instrumentation on board. In addition, NCAR/RAF personnel received training on the operation of the instrument and the analysis software. The test flights were used to adjust the sample flow rates for optimum ozone measurement conditions, however the much more demanding goal of quality ozone measurements in flight could not be adequately addressed with such a limited test flight series. In addition, we were not able to test the remote soft-key startup, the IRIG timing interface, and the data feed to the NCAR/RAF on-board data system, as none of these systems were operational at RAF at the time of the flight tests.

20 New England Business Center □ Andover, MA 01810-1077 □ *t* 978.689.0003 *f* 978.689.3232
www.psicorp.com

With assistance from RAF personnel, the instrument was installed on a shelf which was in turn attached to a rack mounted in the aircraft cabin. To attach the housing to the shelf, the instrument on its base plate was first removed from the bottom tray of the housing. Four nut plates were attached to the inside of the tray, and the tray was mounted to the shelf using four ¼-inch aircraft bolts through the bottom of the tray. The instrument was then re-installed in the tray, and the housing cover was attached. The LabWindows data analysis software packages were installed on an RAF laptop computer, which was then strapped to the rack. The instrument inlet and outlet were connected to the aircraft ports using lengths of ½-inch o.d. Teflon tubing. The inlet tubing was attached to an external shrouded HIAPER Modular Inlet (HIMIL) which was mounted on a hard point under the fuselage.

The test flights occurred on 19, 24, 27, and 30 July 2007, and covered altitudes up to ~15 km. The first two flights included interactive operation of the instrument by PSI, and were used to test the basic functionality of the instrument: power stability, computer function, temperature control, pressure stability/leakage, lamp and photometer function, and sample flow rate. The real-time data was monitored on the laptop computer using the "**TELEMETRY**" software package. The flow rate was controlled by a small ball valve on the photometer exhaust. This valve was adjusted throughout the flights to adjust the sample flow rate and observe the effects on the pressure-drop and ozone signals. By examining the pressure data with the valve open and closed at various altitudes, we identified the desired range of absorption cell operating pressure and determined a range of fixed-orifice sizes to try: 0.020", 0.033", and 0.052". These orifices are designed to be inserted in the ½-inch Teflon tubing that connects to the instrument exhaust port. This range of orifice size should provide a good test of the range of flow rates vs. altitude. The 0.033" orifice was installed and was used for the final two test flights. The data sets were analyzed using the "**BATCH**" software and were provided to RAF.

In general, it appeared from the ΔP data that we achieved an acceptable range of sample flow rates, however the ozone signals were extremely noisy and only registered discernible ozone levels at very low altitudes: ~20 ppbv at 2.85 km on the first flight, ~30 ppbv at 1.4 km on the second flight (e.g. Figure 33). We also observed large excursions in the photometric noise levels that were apparently related to changes in angle of attack due to turns and/or changes in elevation. The final two flights used the 0.033" fixed orifice instead of the adjustable valve, and autonomous (unattended) operation of the instrument. The ΔP data indicated flow rates in the desired range at 10-15 km, Figure 34, however there was no valid ozone data in that range. Expected ozone levels at these altitudes are 100-300 ppbv, which should be readily measurable with good signal-to-noise ratios. We believe that this is related not to the negative offset behavior observed on the bench, but rather to extensive catalytic loss of ozone in the external inlet, due to its metal shroud and inadequate Teflon lining and perhaps also to its position beneath the fuselage. The basic conclusion from this limited test flight series is that the instrument functions well during flight, but the establishment of proper sample flow rates and quality ozone measurement results with the HIMIL inlet configuration will require considerably more flight testing.

20 New England Business Center Andover, MA 01810-1077 t 978.689.0003 f 978.689.3232
www.psicorp.com

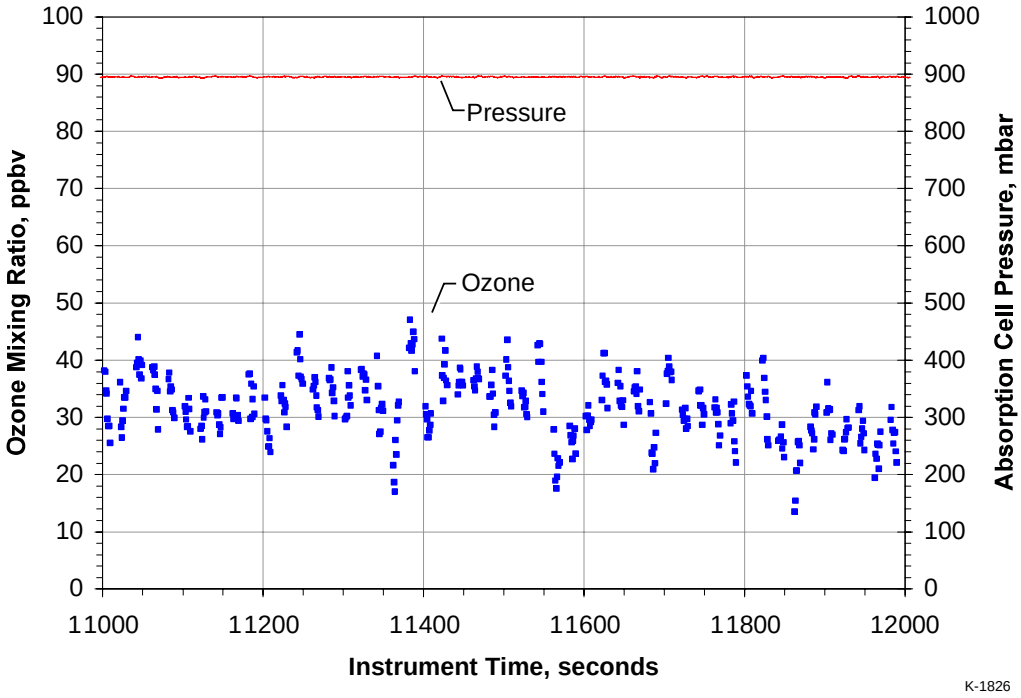

Figure 33. Example ozone data from GV test flight, 24 July 2007, 1.42 km altitude.

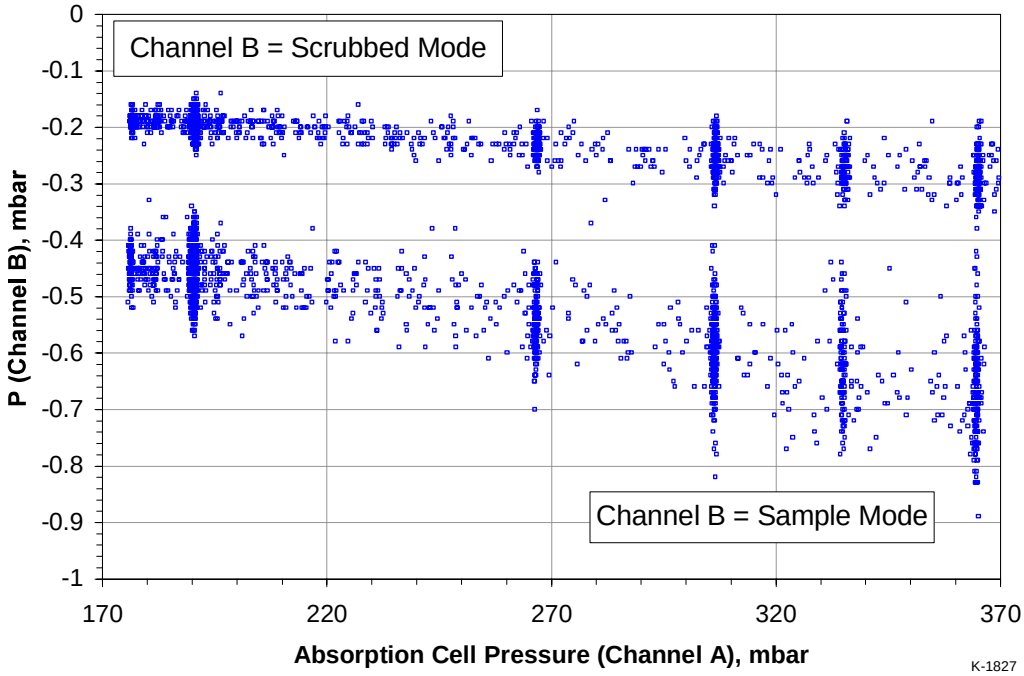

Figure 34. Example ΔP data from GV test flight, 30 July 2007, altitude 10 to 15 km.

20 New England Business Center □ Andover, MA 01810-1077 □ *t* 978.689.0003 *f* 978.689.3232
www.psicorp.com

9. Instrument Modifications (2009)

During the bench and flight tests, we identified two major issues with the instrument performance. First, the Minco temperature controller, originally installed by PI to control the temperature of the absorption cell block, generated a noise spike in the photometric signals every time it turned on. Second, the photometer exhibited large negative signals when sampling clean dry air, and measurements of ozone mixing ratios were correspondingly lower than the values measured by the PSI ozone photometer for the same sample flow stream. After the test flights, the instrument was returned to PSI to resolve these two issues. Both issues have been resolved. This section describes the instrument modifications, and Section 10 describes the final bench tests and results.

9.1 Temperature Controller

The original Minco CT325TF2A1 temperature controller was connected to strip heaters mounted on the absorption cell block and a thermistor imbedded in the aluminum cell body. When the cell temperature was near or below its set point (35 °C), the controller switched power on to the heaters. This switching action caused large spikes in the photometric counter signals, apparently due to EMI pick-up. Once the instrument cover is installed and the instrument is warmed up, the steady-state cell temperature tends to exceed the set point and remain near 36-37 °C, so the controller stayed off and did not affect the bench test or flight test measurements. To resolve the problem, we replaced the Minco controller with a Wavelength Electronics MPT-5000 controller, which is specially designed for low-noise proportional control. We have previously used this controller to regulate the temperatures of diode lasers in high-sensitivity sensor applications, and have had good results with it. The unit measures 1" x 3.55" x 3.5", weighs <0.7 lb, and is mounted on a heat sink. Bench tests established that the controller regulates the cell temperature properly and does not generate noise spikes.

9.2 Valve Shaft Modifications

As noted in Subsection 8.1.3, we traced the negative offset effect to the design of the valve shaft assembly as implemented by PI. Our hypothesis was that an o-ring seal needed to be added on the shaft connecting the valve to the gear motor, to isolate the sample flow from the motor housing volume. This hypothesis was supported by our observations that the PSI instrument, which has an o-ring seal in this location, shows no significant negative offset when the o-ring is in place, but shows a large negative offset similar to the HIAPER results when the o-ring is removed. The primary objective of this modification was to install an o-ring seal on the shaft just above the top of the valve. This required extensive re-design and extension of the shaft assembly, and reverse engineering of the PI installation.

We believe that the offset effect is related to humidity equilibration effects within the absorption measurement channels. Similar effects have been reported for commercial UV ozone photometers, with regard to variations in instrument response when flying through rapid changes in ambient humidity.[7,8] These investigators have presented evidence that adsorption of H_2O

20 New England Business Center □ Andover, MA 01810-1077 □ t 978.689.0003 f 978.689.3232
www.psicorp.com

molecules on the surfaces inside the absorption channel can reduce the low-angle reflectivity of the walls and thereby reduce the intensity reaching the detector from an uncollimated light source. Data were presented for TEI, Dasibi, and 2B Technologies commercial ozone photometers. The PSI and PI chain of instruments is much less sensitive to this effect owing to our use of very low reflectivity black Teflon coatings on the internal surfaces. However, we do observe a small effect when sampling dry air flows. In single-channel experiments with a fixed valve position, we found that admission of a flow of ozone-free dry air results in an increase in the observed light source intensity by a few parts in 10^4. This effect increases with increasing sample air flow rate, and with decreasing cell temperature. Apparently this is because the dry air flow removes some of the adsorbed H_2O, increasing the wall's low-angle reflectivity slightly, and resulting in re-equilibration of the relative humidity within the flow channel (which was previously in equilibrium with the room air). Since the pressure in the unscrubbed channel is a few tenths of a mbar higher than that in the scrubbed channel (due to the additional pressure drop across the scrubber) and the flow rate is consequently somewhat larger, the intensity increase is slightly larger for the unscrubbed channel than for the scrubbed channel. As long as this effect is the same for both the A-sample and B-sample valve configurations, it should cancel out in the dual-channel analysis of the A/B ratio data, and will appear as a small bias between the two channels in the single-channel analysis. This is the case for the PSI ozone instrument.

Several effects can unbalance the dual-channel humidity response. These include (1) large flow rates which induce boundary layer separation (Subsection 8.1.1), (2) lower cell temperatures or a large temperature gradient between the inlet and outlet of the absorption channel, which affect the rate of the humidity re-equilibration, (3) misalignment of the valve holes with the flow channels, producing different pressure drops for the different valve positions, and (4) leakage communication between the absorption cell volume and the ambient air or, in case of the HIAPER instrument, with the motor housing volume which can act as a large H_2O reservoir. Clearly, the larger the pressure drop through the cell, the more sensitive the measurements will be to these effects. Our approach has been the following:

(1) Isolate the absorption cell volume with an o-ring seal on the valve shaft;
(2) Achieve the best possible alignment and control of the valve rotation;
(3) Install a constriction in the unscrubbed flow upstream of the valve to reduce the pressure difference between the scrubbed and unscrubbed flows;
(4) Slightly pre-warm the incoming sample flow in the transfer tubing external to the instrument, to ensure that the absorption cell inlet-to-outlet temperature difference is <1 °C;
(5) Delineate the range of flow rates for which the ozone mixing ratio measurements are accurate.

As described in Section 10, implementation of these measures has eliminated the negative offset effect within the target range of sample flow rates (≤4 slm), resulting in excellent agreement with ozone mixing ratio measurements by the PSI ozone photometer.

20 New England Business Center Andover, MA 01810-1077 t 978.689.0003 f 978.689.3232
www.psicorp.com

A diagram of the modified valve shaft assembly is shown in Figure 35. Not shown in the figure are the gear motor and its aluminum housing cover, which sit on the flange atop the brass housing shown at the top of the figure (cf. Figures 7-9). The aluminum housing cover is mounted on the brass flange with an external o-ring seal. Inside the housing cover and mounted on top of the brass flange are the gear motor and a small circuit board containing the logic circuit that controls the valve rotation. The lower part of the motor housing is made of brass to permit soldering of the electrical feedthroughs for the valve power, control signal, and position sensor returns. The motor shaft connects via a spider coupling to the cylindrical shaft coupling, which in turn connects to the valve core via a small diameter shaft (0.275") containing the added o-ring seal (010 Viton o-ring). The seal is designed so that the shaft rotates within the fixed o-ring. The small shaft is inserted into the cylindrical shaft coupling and is rigidly held in place by two set screws indented into the shaft. The shaft coupling assembly is housed inside an aluminum spool piece with external o-ring seals. The entire volume of the shaft coupling assembly, brass housing, and motor housing is connected to the instrument exhaust flow.

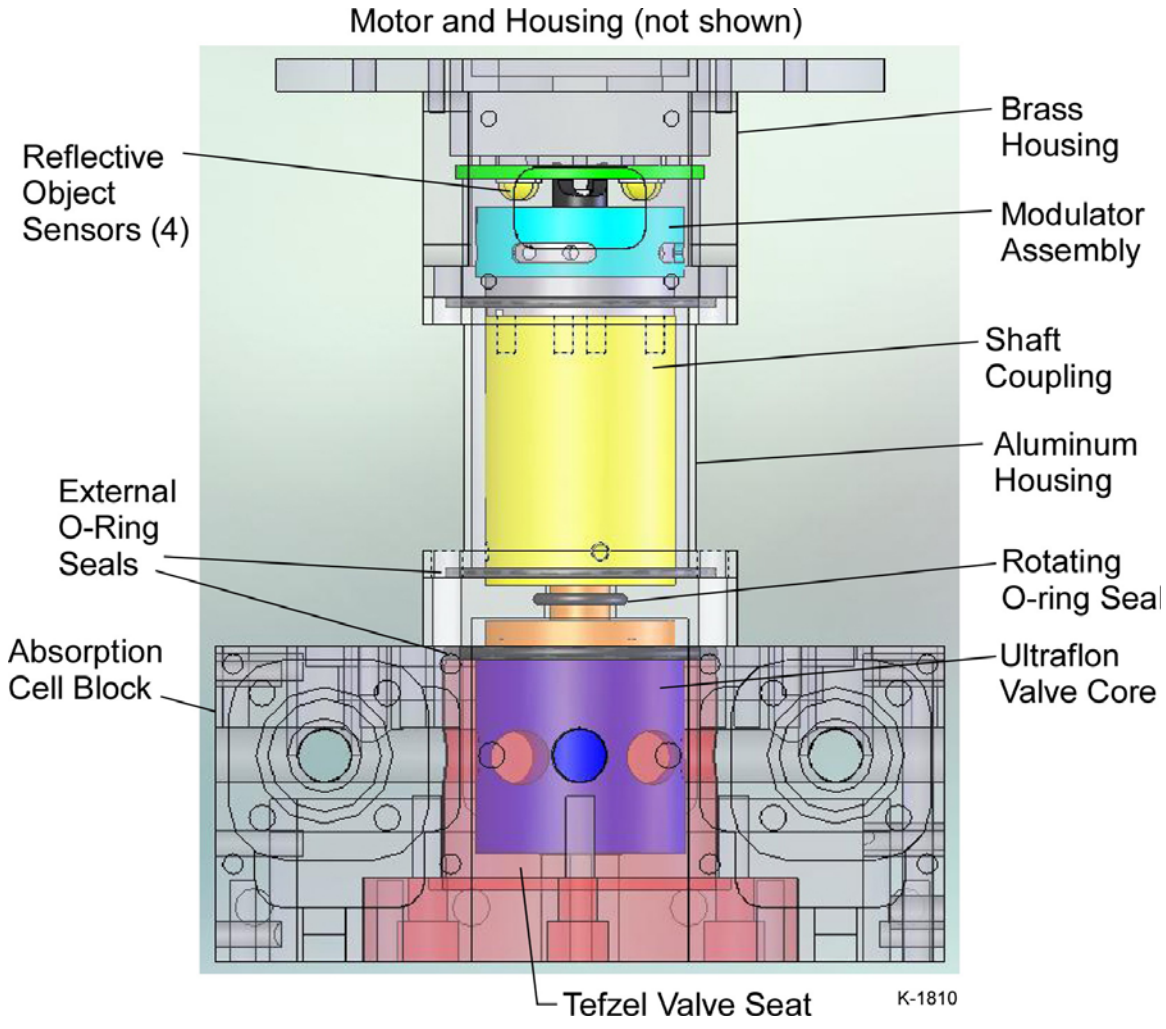

Figure 35. Schematic of modified valve and shaft assembly.

20 New England Business Center Andover, MA 01810-1077 t 978.689.0003 f 978.689.3232
www.psicorp.com

Note that the PSI modifications are designed so that the valve assembly can be returned to the original PI design. In that design, the modulator assembly was mounted directly on top of the Ultraflon valve core and the brass housing was mounted directly on top of the absorption cell body. However, since that design did not work and this one does, we highly recommend retaining the modified configuration.

The installation of the additional shaft couplings and housing necessitated extensive realignment and adjustment of the valve position control system, owing to the highly precise alignment requirements of the valve position sensors. These are four near-infrared reflective object sensors (Clairex Technologies, Inc. CLI700) which look down on the modulator top surface. The sensors are mounted around a circle at 90 degree intervals. These sensors emit light at 880 nm from a small LED and detect the return signal from a reflective surface. The top of the modulator is painted flat black with a ~60° sector of reflective copper tape in one quadrant. As the valve rotates and the reflective tape passes beneath one of the sensors, a signal is triggered which stops the rotation and reports the valve position. The valve position is calibrated by observing the alignment of the valve core holes with the flow channels and adjusting the modulator position with a set screw until the rotations stop at the correct hole alignments. The reflective object sensors are very sensitive to the vertical placement of the reflector, which must be within 0.030" to generate a signal. Thus the rotation of the modulator surface must be precisely in plane and close to the sensors without touching them. This places stringent requirements on the precision of the heights and vertical and horizontal alignment along the axis of the valve core, shaft assembly and motor as well as on the external housing pieces. This precision had been achieved in the original PI assembly, and we designed the inserted shaft assembly and housing pieces to preserve this configuration as closely as possible. Nevertheless, verifying that the sensors functioned and achieving a working valve required considerable investigation and re-engineering of the sensor-to-modulator placement and the operation of the control circuit.

To operate the valve rotation, the data acquisition program commands the computer to send a TTL square wave (Valve Mode) to the motor control board inside the motor housing. This signal alternates between high and low every 10 seconds, and runs a timing circuit to generate the motor power pulse every 10 seconds. The motor power pulse width is controlled by an RC circuit attached to a flip-flop and is about 0.5 s. A series of OR and NAND gates form a logic tree which terminates power to the motor if a signal from the "correct" reflective object sensor is received prior to the end of the motor power pulse. The "correct" sensor signal, as reported by the data acquisition code, must be 1 and/or 3 for Valve Mode = High (A sample mode), and 2 and/or 4 for Valve Mode = Low (B sample mode). If the correct sensor signal is not received during the motor power pulse, the motor stops rotating at the end of the pulse in some random valve position that may or may not produce a position signal. The sensor signal can fail if the sensor is not emitting the light, if the modulator surface does not have sufficient reflectivity, if the surface is too far from or too close to the sensor, or if the sensor sensitivity is too low or too high.

20 New England Business Center Andover, MA 01810-1077 t 978.689.0003 f 978.689.3232
www.psicorp.com

We used an infrared viewer to confirm that all of the sensors were emitting properly, and replaced the original white paint with copper tape to give high reflectivity. Conversely, we found that if the non-reflective part of the surface is reflective enough to produce a signal (or the sensor is too sensitive), the motor will not activate at all. So we applied flat black paint to improve the contrast between the non-reflective and reflective parts of the modulator surface. To increase the sensitivities of the sensors, it was necessary to change out some resistors in the motor control circuit. There is a set of four current-limiting resistors which control the gain on each of the reflective object sensors' detectors. By reducing these resistances, we were able to increase the gains and get the sensors to reliably register the valve position for a modulator-to-sensor gap of approximately 0.020". Several multi-hour tests confirmed that the valve rotation was reliable and highly reproducible.

Full implementation of the valve shaft modifications resulted in significant reduction of the negative offset, but not its complete elimination. We observed that the effect was very sensitive to the valve alignment, and we optimized the alignment accordingly. In addition, we inserted a 3 cm long piece of heavy-wall Teflon tubing, ¼-inch o.d. x 3 mm i.d., into the ¼-inch i.d. unscrubbed-air flow channel upstream of the valve unscrubbed-air inlet. The physical location of this insert in the absorption cell is in the central flow channel, downstream of the split to the scrubber and upstream of the valve inlet for unscrubbed air. This has the effect of increasing the pressure drop for the unscrubbed flow prior to the valve, and reducing the pressure difference between the scrubbed and unscrubbed flows within the absorption chambers by about a factor of 2. The closer matching of the scrubbed and unscrubbed pressures in the absorption paths reduces the sensitivity to the humidity equilibration effects discussed above. Finally, we noted that a small negative offset appeared when the outlet-inlet temperature difference in the absorption paths became greater than about 1.2 °C, and disappeared when that difference was reduced to <1 °C by slight pre-warming of the sample air flow. Brief tests showed that this condition was satisfied for inlet flow rates below about 4 to 5 slm, which is the target flow rate range based on the performance of the PSI instrument and on previous flow noise observations as described in Subsection 8.1.1. More detailed bench tests and intercomparison measurements defining the applicable flow rate range are described in Section 10.

10. Final Bench Tests and Instrument Intercomparisons (September 2009)

Due to the change in the unscrubbed-flow pressure drop, it was necessary to recalibrate the dependence of the ΔP signal on flow rate. This was done using the same setup and procedures described in Subsection 8.1.1. The raw data are plotted in Figure 36, and average values with 1σ standard deviations are plotted in Figure 37. The differences between the upper and lower curves signify the pressure differences between the unscrubbed and scrubbed flow channels, and are about half of the previous values shown in Figure 22. As observed previously, the noise on the ΔP traces increases substantially for flow rates above ~4 slm. We previously ascribed this effect to the onset of boundary layer separation in the flow around the right-angle bends at the absorption chamber inlets. This boundary layer separation causes the formation of vortices and localized recirculation zones which gradually damp out along the absorption flow path. The effect becomes more severe with increasing flow rate. (Note that this effect is not

20 New England Business Center Andover, MA 01810-1077 t 978.689.0003 f 978.689.3232
www.psicorp.com

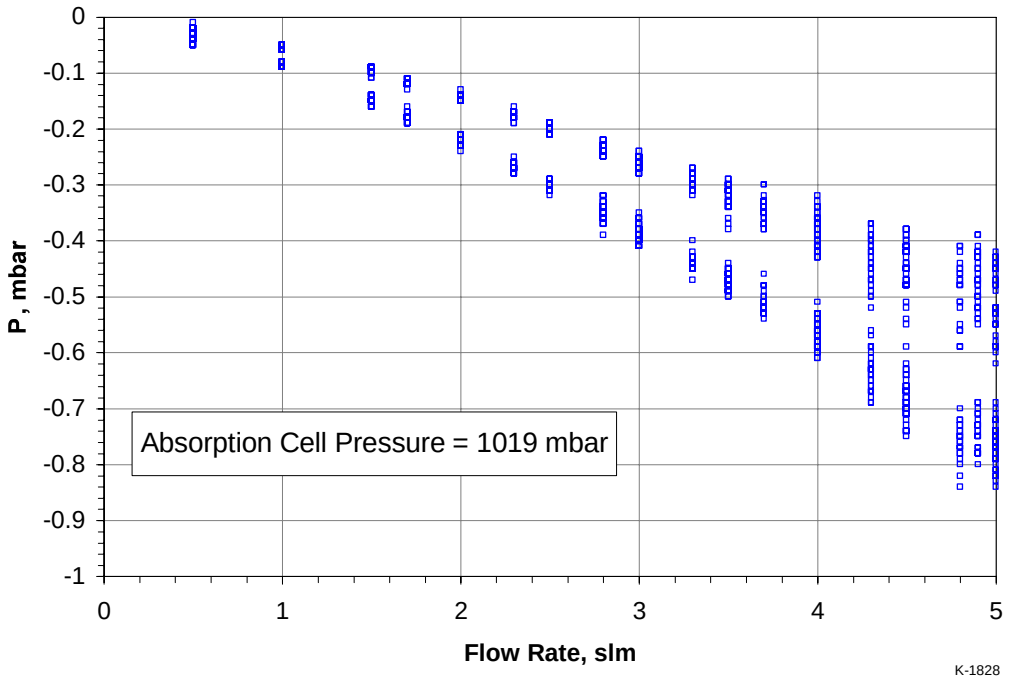

Figure 36. Differential pressure vs. flow rate, modified HIAPER instrument.

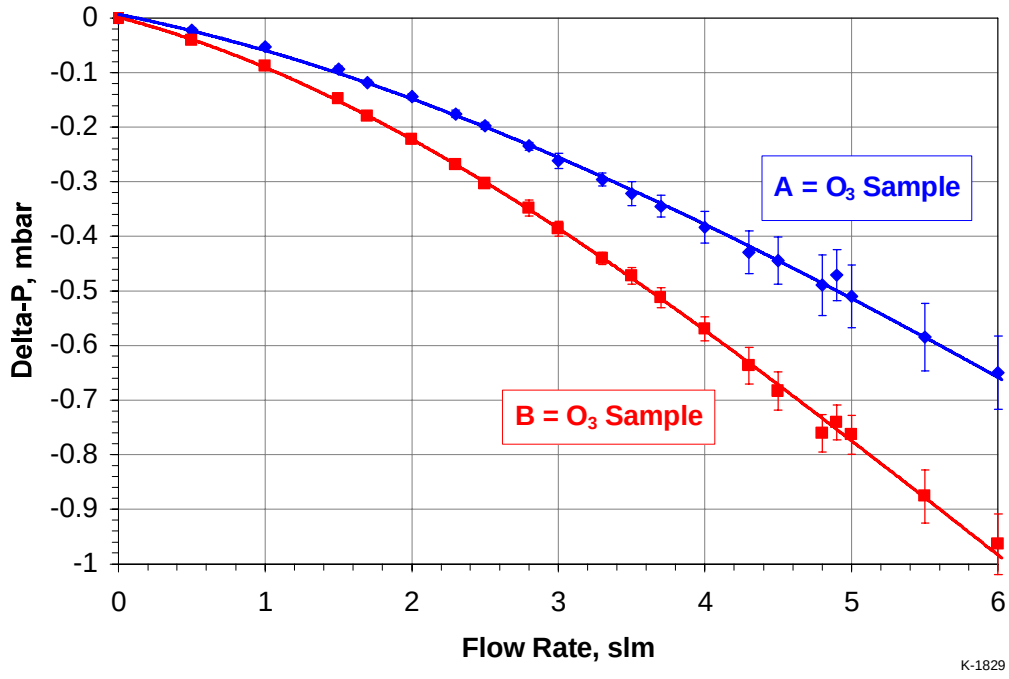

Figure 37. Final flow rate calibration for modified HIAPER instrument.

20 New England Business Center □ Andover, MA 01810-1077 □ t 978.689.0003 f 978.689.3232
www.psicorp.com

related to turbulence, which cannot occur under these conditions. The Reynolds numbers for this range of flow rates are much smaller than values corresponding to turbulent flow.) The onset of this effect at flow rates of 4 to 5 slm is similar to the onset of discrepant ozone measurements as described below, and defines the upper end of the target sample flow rate range.

The plots in Figures 36 and 37 can be directly compared to similar plots from flight measurements to gauge the flow rates achieved in flight. We also used this calibration to determine the fraction of the total flow rate that was sampled by the HIAPER instrument in the intercomparison measurements described below.

Ozone mixing ratio measurements by the PSI and modified HIAPER instruments were intercompared using the setup and procedures described in Subsection 8.1.3. Dry air at several measured total flow rates was passed through a photolytic ozone generator and some 24 inches of ¾-inch and ½-inch Teflon tubing to a tee splitting the flow to each of the two instrument inlets. The tubing between the ozone generator and the HIAPER instrument inlet was gently warmed to roughly 30 °C by heating tape controlled by a Variac at about 20% of full power. About 55% of the flow went to the HIAPER instrument, and the remainder to the PSI instrument. The total flow rate was varied from 5 to 10 slm.

A set of survey measurements by the two instruments at several different total flow rates is shown in Figure 38. The total flow rates are indicated on the plot. At each flow rate, the ozone generator was turned off and on, resulting in measurements of zero ozone and of rapidly increasing ozone production approaching steady state. It is clear that, for total flow rates ≤7.5 slm (~4.1 slm for the HIAPER instrument), there is no significant zero offset and the measurements by the two instruments agree very well. For total flow rates >8 slm (4.4 slm for HIAPER), the zero offset becomes significant and the HIAPER measurements fall below the PSI measurements. Both the zero offset and the measurement discrepancy increase with increasing flow rate above that point. However, the agreement is very good within the target range of flow rates identified by the ΔP measurements. Average values and 1σ standard deviations of the zero-ozone baseline measurements are plotted vs. the individual instrument flow rates in Figure 39. As expected, zero-offset effects become apparent for both instruments above ~4 slm, however there is no significant offset for flow rates below 4 slm. We have observed that the zero-baseline persists for lower flow rates down to <1 slm.

We conducted a series of intercomparison experiments designed to observe several steady-state values of ozone mixing ratio at each of several flow rates. We used total flow rates of 5, 6, 7, 8, and 9 slm (2.8 to 5.0 slm for the HIAPER instrument). At each flow rate, the ozone production rate in the photolysis generator was varied by inserting blocking filters of different sizes between the photolysis lamp and the quartz flow cell. This resulted in seven different ozone mixing ratios at each of the five flow rates. For each mixing ratio, we observed the 1 Hz measurements for 50-100 seconds. The measurements were configured so that each 1-Hz measurement for one instrument was virtually simultaneous with a corresponding measurement by the other instrument. A sample data set for one flow rate is shown in Figure 40. We reduced the data sets to isolate the steady-state portion of each measurement condition, and created

20 New England Business Center Andover, MA 01810-1077 t 978.689.0003 f 978.689.3232
www.psicorp.com

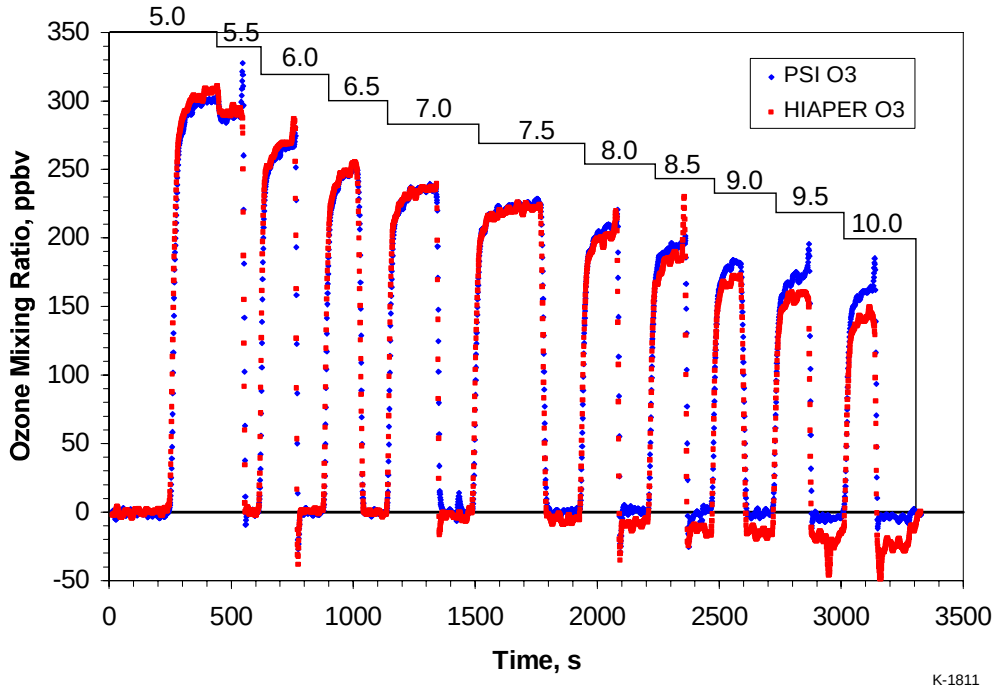

Figure 38. Final ozone intercomparison data: survey of flow rate dependence. Total flow rates to both instruments in slm are labeled on the figure.

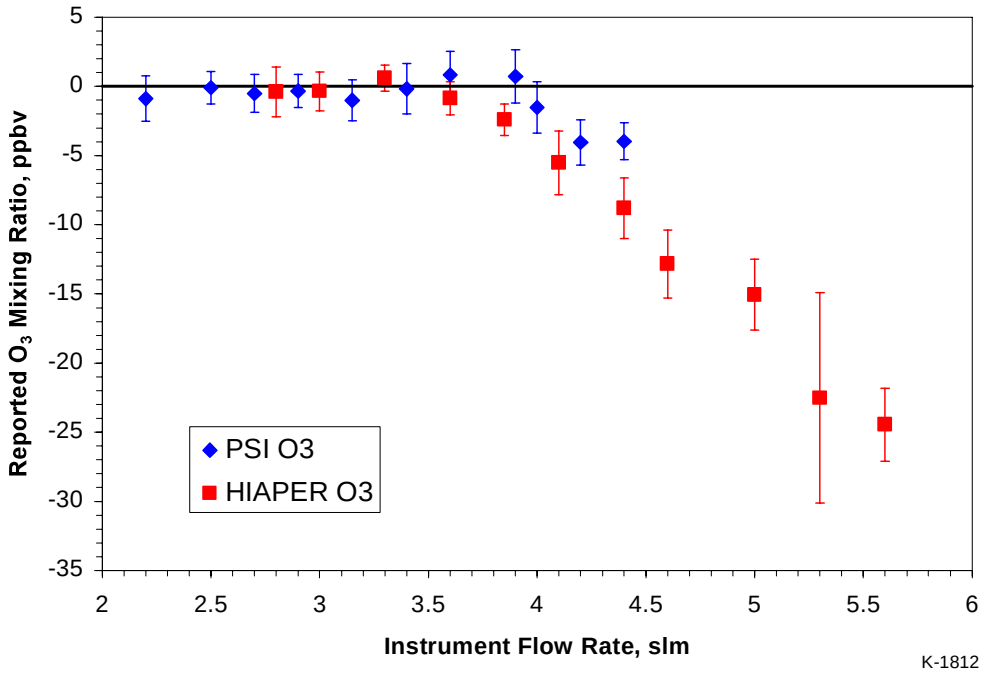

Figure 39. Final ozone intercomparison data: dependence of zero-air baseline on flow rate.

20 New England Business Center □ Andover, MA 01810-1077 □ *t* 978.689.0003 *f* 978.689.3232
www.psicorp.com

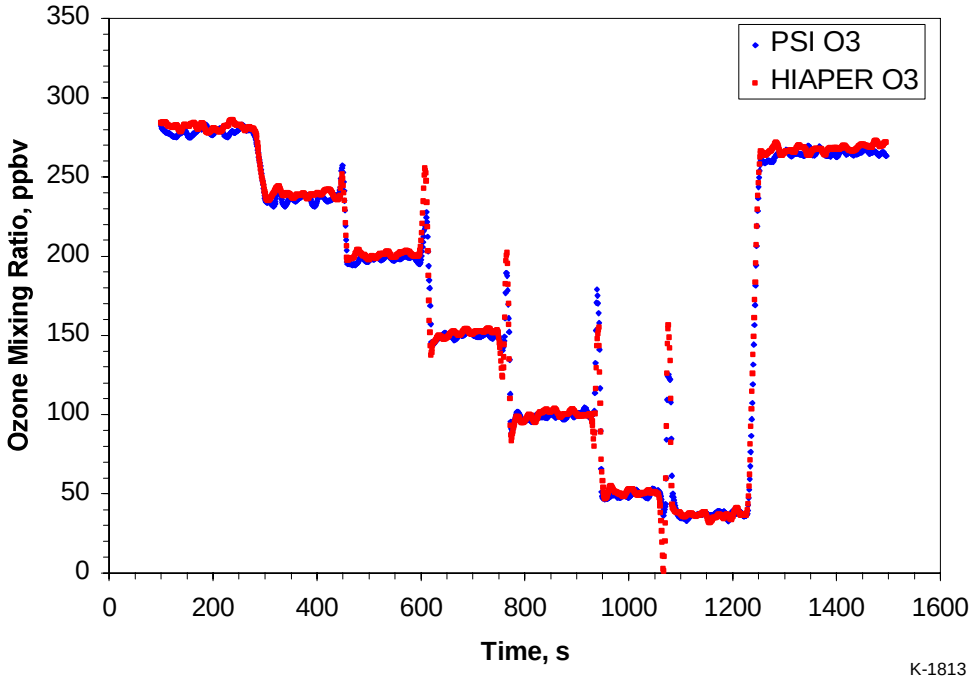

Figure 40. Final ozone intercomparison data: example of data set for total flow rate = 6.0 slm. The figure shows variations in measured ozone levels for different photolysis rates in the ozone generator. The noise spikes are generated when the lamp blocking filters are interchanged in the generator.

correlation plots of the 1-Hz data for one instrument vs. the other. A sample plot for the data of Figure 40 is shown in Figure 41. The correlation of the two measurement sets is excellent. We found that the correlations for HIAPER flow rates of 2.8 to 3.9 slm (total flow rates of 5, 6, and 7 slm) were essentially identical, so we plotted all three data sets together as one. The combined correlation is shown in Figure 42, and again in Figure 43 together with the individual correlations for HIAPER flow rates of 4.4 and 5.0 slm (total flow rates 8 and 9 slm). The composite data have a slope of 1.0142 ± 0.0002, in excellent agreement with a 1:1 correlation. The data for 4.4 slm fall slightly off the 1:1 line, however inclusion of these data in the composite does not substantially alter the fitting results (slope = 1.0052 ± 0.0004). The data for 5.0 slm fall significantly below the composite line, with a ~10 ppbv offset.

We conclude from these results that, at atmospheric pressure, the HIAPER ozone measurements are in excellent agreement with those of the PSI ozone photometer for flow rates ≤4 slm (~3 mmole/s, 0.086 g/s air). The agreement between the two instruments is marginal but probably acceptable between 4 and 4.5 slm, and is poor above 4.5 slm (0.096 g/s). We have identified possible causes for the discrepancies at high flow rates, including flow disturbances, humidity equilibration effects, and differences in scrubbed and unscrubbed pressures and flow rates, which may indeed be interrelated phenomena. We recommend that the HIAPER instrument be implemented with sample flow rates in the range 1 to 4 slm (approximately 0.02 to 0.09 g/s air) for best results.

20 New England Business Center □ Andover, MA 01810-1077 □ t 978.689.0003 f 978.689.3232
www.psicorp.com

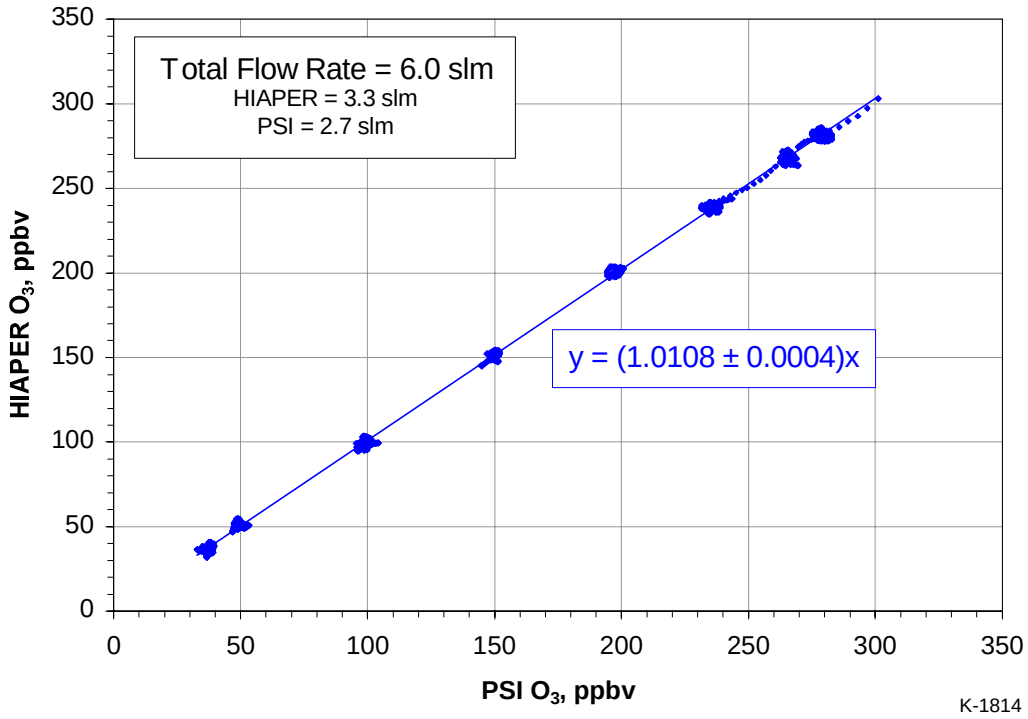

Figure 41. Final ozone intercomparison data: measurement correlation plot for total flow rate = 6.0 slm. The linear least squares fit results are indicated on the plot.

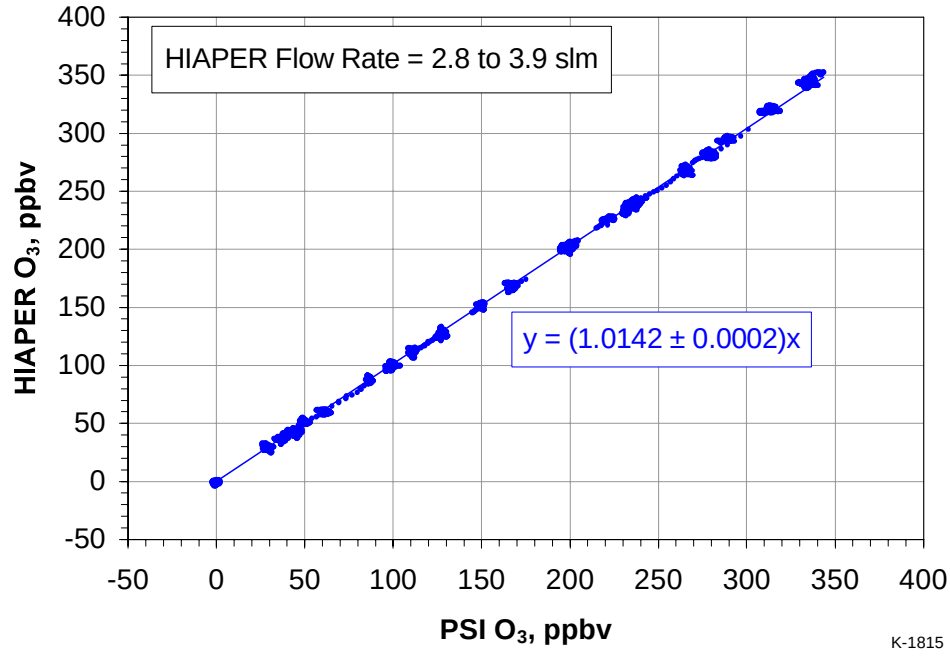

Figure 42. Final ozone intercomparison data: combined correlation plot for HIAPER flow rates 2.8 to 3.9 slm. The linear least squares fit results are indicated on the plot.

20 New England Business Center □ Andover, MA 01810-1077 □ *t* 978.689.0003 *f* 978.689.3232
www.psicorp.com

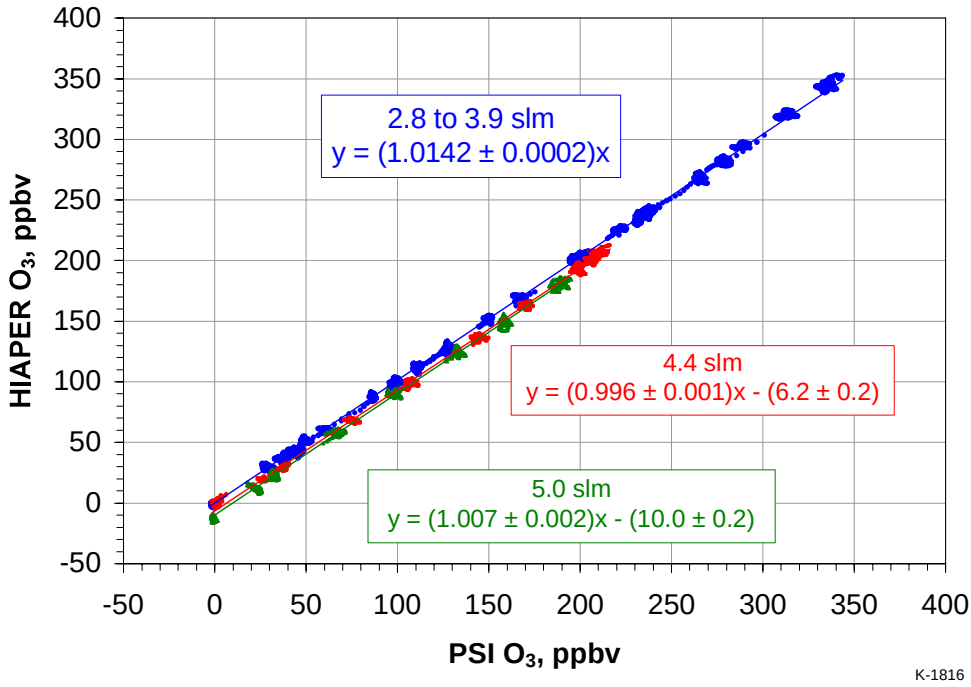

Figure 43. Final ozone intercomparison data: comparison of the data from Figure 42 to correlation plots for HIAPER flow rates 4.4 and 5.0 slm. The linear least squares fit results are indicated on the plot.

11. Summary and Conclusions

We have completed the development, initial bench testing, certification, aircraft integration, and initial flight testing of the HIAPER GV Ozone Photometer. Based on the initial testing results, we performed substantial modifications to the instrument to eliminate noise sources and to resolve discrepant ozone mixing ratio measurements. Final bench testing at atmospheric pressure confirmed the success of the modifications and acceptable accuracy of the instrument for ozone measurements, and delineated the operating regime for the instrument. The HIAPER ozone instrument operating characteristics are as follows:

- Accuracy ± 5% for ozone mixing ratios > 50 ppbv
- Measurement precision (photometric noise limit) ± 5 x 10^{10} molecules/cm^3 at 1 Hz
- Sample air flow rates 0.02 to 0.09 g/s
- T (cell outlet) - T (cell inlet) < 1°C

As a result of the modification effort, we have identified several operational conditions which can potentially affect the measurement accuracy at higher flow rates, most significantly related to fluid dynamic and/or humidity effects. Future flight tests should address the establishment of useful sample flow rates as a function of altitude, and non-destructive sampling of ambient ozone through the external inlet and transfer tubing to the instrument. A set of recommended flight operation procedures is given in Appendix H.

20 New England Business Center □ Andover, MA 01810-1077 □ t 978.689.0003 f 978.689.3232
www.psicorp.com

12. References

1. H. Schlichting, Boundary Layer Theory, J. Kestin, transl., Fourth Edition, McGraw-Hill, New York, 1960.
2. R.I. Crane and R.L. Evans, "Inertial Deposition of Particles in a Bent Pipe," *J. Aerosol Sci. 8,* 161-170, 1977.
3. Y.S. Cheng and C.S Wang, "Motion of Particles in Bends of Circular Pipes," *Atmospheric Environment 15,* 301-306, 1981.
4. D.Y.H. Pui, F. Romay-Novas, and B.Y.H. Liu, "Experimental Study of Particle Deposition in Bends," *Aerosol Sci. Technol. 7,* 301-315, 1987.
5. E.J. Hintsa, G. P. Allsup, C. F. Eck, D. S. Hosom, M. J. Purcell, A. A. Roberts, D. R. Scott, E. R. Sholkovitz, W. T. Rawlins, P. A. Mulhall, K. Lightner, W. W. McMillan, J. Song, and M. J. Newchurch, "New ozone measurement systems for autonomous operation on ocean buoys and towers," *J. Atmos. Oceanic Tech. 21,* 1007-1016, 2004.
6. W.T. Rawlins, D.M. Sonnenfroh, D.A. Palombo, P.A. Mulhall, A.H. Burbo, H.C. Murphy, G. Dippel, M.R. Malonson, S.D. Sewell, R.H. Krech, and M.H. Proffitt, "Lightweight Ozone Photometer for Balloon and Aircraft Atmospheric Measurements," PSI-2328/TR-1503, Final Report for NASA Jet Propulsion Laboratory, Contract NAS7-1381 (Dr. J. J. Margitan, COTR), July 1997.
7. K.L Wilson and J. W. Birks, "Mechanism and Elimination of a Water Vapor Interference in the Measurement of Ozone by UV Absorbance," Environ. Sci. and Technol. 40, 6361-6367 (2006).
8. K.L. Wilson, "Water Vapor Interference in the UV Absorption Measurement of Atmospheric Ozone," Ph.D. Thesis, University of Colorado, Boulder, CO, 2005.

20 New England Business Center Andover, MA 01810-1077 *t* 978.689.0003 *f* 978.689.3232
www.psicorp.com

20 New England Business Center Andover, MA 01810-1077 *t* 978.689.0003 *f* 978.689.3232
www.psicorp.com

Appendix A

Mechanical Loads Analysis

We carried out a mechanical loads analysis, specifically focused on Emergency Landing Loads (ELL) as specified in the NSF/NCAR GV Investigator's Handbook. Since the HIAPER instrument's structural configuration is almost identical to that of the PSI WB-57F ozone instrument previously approved by NASA for flight, we expected large safety margins, as confirmed by this quantitative analysis. At 29 lb or less, the instrument is relatively light, with the heaviest single component being the 6.5 lb absorption cell.

We used the safety factors and emergency landing loads specified in the NSF/NCAR GV Investigator's Handbook. We took the mechanical properties for the fasteners and materials from the MIL-HDBK-5J (January 2003) document, also specified in the GV handbook. The NCAR handbook ELL load specifications and HIAPER ozone instrument weights are listed in Table A-1. We focused our analysis on the highest ELL load scenarios, namely the forward shear (9 G) and downward tensile (6 G). Clearly all the other ELL loads are less than these, and there is no inherent asymmetry in the instrument structure that would cause any components to be more likely to fail in one direction than in another. Our analysis addressed the following failure modes:

(1) Failure of the mounting bolts that attach the instrument to the airplane instrument rack. These consist of four ¼-28 bolts. For a conservative calculation, we have assumed Grade 1 bolts for this analysis, however we intend to use higher-grade bolts for this attachment.
(2) Failure of the mounting screws that attach the instrument assembly and bottom plate to the base of the housing. These consist of eight 10-32 screws spaced around the perimeter of the bottom plate. Again we have assumed Grade 1 screws for a lower bound, but we will use higher-grade screws for the actual assembly.
(3) Failure of the mounting screws and/or stand-off brackets that attach the absorption cell to the bottom plate. The cell is mounted on four stainless steel standoff brackets, which are attached to the bottom plate by four 8-32 screws. As above, we have assumed Grade 1 screws for a lower bound, but we will use higher-grade screws for the actual assembly.
(4) Penetration of the housing by the heaviest possible loose component, i.e. the 6.5 lb aluminum absorption cell. For this analysis, we assumed the full 9 G forward impact force, with point loading on a 0.01 in^2 area on the housing. The housing is a COTS aluminum 6061 enclosure from Zero Manufacturing, Inc., with a wall thickness of 0.09 inch.

20 New England Business Center Andover, MA 01810-1077 t 978.689.0003 f 978.689.3232
www.psicorp.com

Table A-1. GV Ozone Photometer Mechanical Stress Criteria

Margins		
Factor of Safety	1.50	
Equipment Mass Factor	1.25	
Fitting Factor Quick Change	1.33	
Combined Factor Multipliers	2.5	
Emergency Landing Load Factors		
Up	3.0	G
Forward	9.0	G
Sideward	4.0	G
Downward	6.0	G
Rearward	1.5	G
Inertial Load Factor		
Nose thru Mid Cabin	6.3	G
	-3.3	G
Aft Cabin and Baggage	7.0	G
	-4.0	G
Tail Compartment	-8.9	G
	-5.9	G
Masses		
Baseplate and Data System	13.0	pounds
Photometer Cell	6.5	pounds
Instrument Total	19.5	pounds
Zero Housing Top	2.5	pounds
Zero Housing Bottom	7.0	pounds
Zero Housing Total	9.5	pounds
Total Instrument and Housing	29.0	pounds

The NCAR GV handbook defines the Margin of Safety (MS) as follows:

$$MS = \left(A \,/\, \left(B\, \Pi F_i\right)\right) - 1 \qquad \text{(A-1)}$$

20 New England Business Center □ Andover, MA 01810-1077 □ *t* 978.689.0003 *f* 978.689.3232
www.psicorp.com

where A is the "allowable stress" or strength of the member or fastener, B is the actual maximum load determined from the ELL specifications and the mass, and the F_i are the analytical safety factors relevant to the application. Table 5.1 in the NCAR GV handbook lists five analytical factors. Three are relevant to this analysis: the Factor of Safety (1.50), the Equipment Mass Factor (1.25), and the Fitting Factor for Quick Change Items (1.33). The product of these three factors gives an overall safety factor of 2.50. For ELL conditions, the value of MS must exceed 0.0 to be acceptable (i.e. A/B > 2.5).

The results of the analysis are summarized in Table A-2. In all cases, the allowable stress is well in excess of the factored load, resulting in MS values well in excess of 0.0. Indeed, in each of the shear and tensile load cases, the MS is positive even for a single Grade 1 screw. The MS values will be even larger for the lesser sideward (3 G) and rearward (1.5 G) ELL factors. Since we plan to use higher-grade screws and bolts, it is clear that the safety margins are very large for all of the ELL conditions. We conclude that the instrument is secure in all specified ELL load conditions with maximum safety factor.

Table A-2. Mechanical Loads

	Factored Load (lb)	**Allowable Stress (lb)**	**MS**	**Required MS**
Instrument Installation				
- Forward Shear	652	6860	9.5	0
- Downward Tensile	435	7340	15.9	0
Instrument to Housing				
- Forward Shear	439	7936	17.1	0
- Downward Tensile	293	7952	26.2	0
Cell to Baseplate				
- Forward Shear	146	2956	19.2	0
- Downward Tensile	98	2692	26.6	0
- Brackets (forward)	146	4000	26.4	0
Housing Penetration (forward)	146	400	1.74	0

20 New England Business Center Andover, MA 01810-1077 t 978.689.0003 f 978.689.3232
www.psicorp.com

20 New England Business Center Andover, MA 01810-1077 *t* 978.689.0003 *f* 978.689.3232
www.psicorp.com

Appendix B

Parts Lists

Table B-1. COTS Parts

Description	Source	Material
16 chan 12 bit A/D	Diamond Model DMM-NA-XT	COTS
Counter/timer board	Diamond Model QMM-5	COTS
CPU	Diamond Prometheus model PR-Z32-EA-ST	COTS
Front panel	Diamond Model PBEC-05-K	COTS
20 GB Hard drive	Seagate #ST92011A,	COTS
Panel I/O board	Diamond #Model PNL-Z32-EA	COTS
VGA board	Diamond Model ACC-VGA-02	COTS
SMA to SMA coax for Detector bds	L-Com #ccsr316-2	COTS
Pressure sensor, absolute	All Sensors #683-15PSIA4V	COTS
Pressure sensor, differential	All Sensors #683-1INCHD4V	COTS
Temperature Controller	Minco #CT325TF2A1	COTS
Heater strips 78.4 ohm	Minco #HK5164R78.4L12B	COTS
Heater strips 52.3 ohm	Minco #HK5165R52.3L12B	COTS
Silicone photodiodes S1336-8BQ	Hamamatsu	COTS
254 NM filters	Barr Associates	COTS
UV Beamsplitter	Esco #PLT-UV-25.4x25.4	COTS
Quartz windows, 1/2D x 1/8 thick	Esco #WD-CQF-S1-AS.7DIA2.18TH	COTS
UV Mirror	Thorlabs #PF10-03-F01	COTS
Faulhaber motor#1727U012CL 86:1+X0814C	MicroMo	COTS
5 V @ 4 amp ±12 V @0.5 amp PS	Wall SIW24T12-30	COTS
±15 V @ 1 amp PS	Wall SIW24 D15-30	COTS
12 V @ 1.25 ams PS	Wall LCSW 2412-15	COTS
24 V PS	Wall LANH 524ND	COTS
Lamp PS	BHK #68-0020-04	COTS
Circulation Fan	Rotron FE12H3	COTS
Low pressure Mercury Lamp	BHK #80-1025-33	COTS
Ozone scrubber cartridge	Tanabyte #SCN001	COTS
Spider gear (aluminum)	Berg #CO46-1B	COTS

H-6622

20 New England Business Center □ Andover, MA 01810-1077 □ t 978.689.0003 f 978.689.3232
www.psicorp.com

Table B-2. Mechanical Parts

Description	Source	Material
CELL	PSI	6061 Aluminum
FILTER RETAINER	PSI	6061 Aluminum
LH INLET PORT	PSI	6061 Aluminum
RH INLET PORT	PSI	6061 Aluminum
END CAP	PSI	6061 Aluminum
HEAT STRIP MOUNT 1	PSI	6061 Aluminum
HEAT STRIP MOUNT 2	PSI	6061 Aluminum
ELECTRICAL COVER PLATE	PSI	6061 Aluminum
D SUB MOUNT 1	PSI	6061 Aluminum
D SUB MOUNT 2	PSI	6061 Aluminum
BASE PLATE	PSI	6061 Aluminum
DIODE COVER	PSI	6061 Aluminum
COVER	PSI	6061 Aluminum
WINDOW COVER	PSI	6061 Aluminum
DIODE MOUNT	PSI	6061 Aluminum
VALVE SHAFT	PSI	6061 Aluminum
MOTOR MOUNT	PSI	6061 Aluminum
MOTOR COVER	PSI	6061 Aluminum
OPTICAL MOUNT	PSI	6061 Aluminum,black anodized
OPTICAL MOUNT COVER	PSI	6061 Aluminum,black anodized
MODULATOR	PSI	6061 Aluminum,black anodized
THERMISTER SOLDER MOUNTS	PSI	Brass
PORT COVER	PSI	Brass
MOTOR CONTROL HOUSING	PSI	Brass
REFLECTIVE DIODE RETAINER	PSI	Delrin
PC BOARD MOUNT LEFT	PSI	Delrin
PC BOARD MOUNT RIGHT	PSI	Delrin
CHANNEL END PLUG	PSI	Glass filled teflon
SIDE PASSAGE CAP	PSI	Glass filled teflon
LAMP HOUSING	PSI	Glass filled teflon
RETAINING RING	PSI	Steel
VALVE BLOCK	PSI	Tefzel HT2004, 25% glass
VALVE INSERT	PSI	Ultraflon CFX
Angle brackets to mount data system	PSI	Steel
Parker A-LOK fittings	MSC	Brass
Screws, angle brackets & standoffs	MSC	Stainless steel

H-6623

20 New England Business Center Andover, MA 01810-1077 t 978.689.0003 f 978.689.3232
www.psicorp.com

Table B-3. Connectors, Wiring, Tubing, etc.

Description	Source	Material
MicroCom cable connectors, 4 conductors	Comtronic #CMR-02-B-04S	Brass Teflon insulator
MicroCom panelconnectors, 4 conductors	Comtronic #CMR-02-E-04P	Brass Teflon insulator
9, 15, 25, 37 pin D connectors	SPC Type DExPMP x=pins	Steel shell, glass reinforced PBT
Connectors, 2 & 4 pin	Winchester JF Series	Molded diallyl phthalate
Teflon tubing	Various	PFA Teflon
Teflon insulated wire	Belden #83002 &#83026	TFE Teflon, stranded
Teflon fittings	Swagelok FC LF series	TFE Teflon
CELL chambers teflon coated	PCM	PFA Teflon
Ribbon cables with connectors	PI	Various
Detector board	PSI	PC board with various electronic components
Valve controller board	PI	PC board with various electronic components
Interface board	PI	Circuit board with various electronic components
Pressure seal	Parker O-Rings	Viton
Resistors	Most Mil style RN55 metal film	Nickel-chrome alloy and epoxy
Capacitors	Ceramic conformally coated	Epoxy encpsulated
Heat shrink tubing	Insulating tubing	Polyolefin
83002 Belden hookup cable, 26 AWG	Allied Electronics	MIL-W-16878/4: TFE insulator, SPC conductor
83026 Belden hookup cable, 22 AWG	Allied Electronics	MIL-W-16878/5: TFE insulator, SPC conductor
10612 Cheminax twin axial cable	Raychem	MIL-W-22759: ETFE insulator, SPC conductor

H-6624

20 New England Business Center □ Andover, MA 01810-1077 □ t 978.689.0003 f 978.689.3232
www.psicorp.com

20 New England Business Center Andover, MA 01810-1077 *t* 978.689.0003 *f* 978.689.3232
www.psicorp.com

Appendix C

Operator's Manual for Dual-Beam Ozone Photometer

Michael H. Proffitt
Proffitt Instruments Inc.

20 New England Business Center Andover, MA 01810-1077 *t* 978.689.0003 *f* 978.689.3232
www.psicorp.com

Operator's Manual for Dual-Beam Ozone Photometer

Table of Contents

20 New England Business Center Andover, MA 01810-1077 *t* 978.689.0003 *f* 978.689.3232
www.psicorp.com

Operator's Manual for Dual-Beam Ozone Photometer

Under subcontract agreement between PSI and Proffitt Instruments, Inc. (PI)

Introduction

The UV absorption method for the measurement of ozone concentration and mixing ratios is often considered to be an "absolute" measurement. That is, the calibration for the method is provided by a well established laboratory measurement of the absorption cross section of ozone at the 254 nm mercury line wavelength, and is generally agreed to be accurate to 2% or better. This method relies upon the well known Beer-Lambert expression for determining gas concentrations within a sample chamber. In our case,

$C_S = \ln(I_o/I)/L\sigma$

where C_S is the concentration (number density) of ozone in the chamber, $\ln(I_o/I)$ is the measured absorbance, L is the chamber length, and σ is the absorption cross section of ozone at the 254 nm mercury line. To obtain a value for C_S only an accurate measure of the absorbance, L and the usual laboratory value for σ at 254 nm (1.147×10^{-17} cm^2/molecule) are required. The measured intensity values for I and I_o require no calibration in any absolute sense, and the quantity calculated as the absorbance is simply the natural log of the ratio.

To convert the concentration measurement of ozone (C_S) to mixing ratios, measurements of the pressure and temperature of air in the sample chamber are required. That is, where χ is the atmospheric mixing ratio in parts per billion by volume (ppbv), T is the temperature of the air in the sample chambers in units of Kelvin, P is the pressure of the air in the sample chambers in units of mbar, and C_S is in units of molecules of ozone per cm^3,

$\chi = 1.379 \times 10^{-10} \times C_S \times T/P$.

The custom designed instrument described in this manual is a dual-beam absorption photometer and was modeled after earlier designs, but built specifically for *in-situ* atmospheric ozone measurements from the NCAR HIAPER aircraft. The complete instrument is an assembly of three modules: a photometer module, a data system module, and an interface and power supply module. These three modules are described in the following section as assemblies of units with related components. A table summary of this description and instrument specifications can be found in Appendix A and B, while schematics and replacement parts are found in Appendix C, Appendix D, and Appendix E. Appendix G includes recent information on instrument upgrades now available from PI.

Instrument modules and units

The **photometer module** is an assembly of 7 units:

20 New England Business Center Andover, MA 01810-1077 *t* 978.689.0003 *f* 978.689.3232
www.psicorp.com

1. The **body unit** consists of a custom built temperature-controlled aluminum block that contains two 20 cm long, 0.25 in. diameter, absorption chambers and a sample "pre-warming" chamber. Air to be sampled is brought from outside the aircraft into the Teflon coated pre-warming chamber through Teflon tubing. This chamber brings the sample temperature to the body unit temperature, which is temperature controlled to about 34 °C. The inlet sample flow is then split into two paths, one containing the air sample to be introduced into one of the absorption chambers and the second containing an air sample that first passes through an ozone scrubber before entry into the other chamber. A four-port rotating valve directs the scrubbed (ozone-free) and un-scrubbed (ozone-laden) air flows into the two sample chambers. Switching of the valve position every 10 seconds interchanges the scrubbed and un-scrubbed paths between the two chambers. The flow through the chambers is driven during flight by aircraft "ram" pressure and its rate must be optimized to ensure it is just fast enough for complete exchange of the air in the chambers in one second. It is important that this flow is slow enough to assure the temperature of the air entering the chambers has equilibrated to near the temperature of the aluminum body. By so optimizing the flow rate it will also avoid turbulence in the chambers that may produce noise in the optical absorbance measurements. After the sampled air passes out of the chambers it is exhausted from the aircraft. It is important to note that only materials that do not destroy ozone have been used in the flow path that is ozone-laden.

2. **The optics unit** consists of a low pressure mercury lamp with mount, a black anodized optical mount with UV mirror and beamsplitter, two 254 nm narrow band filters and four quartz windows. The quartz windows effectively seal the ends of the 20 cm sample chambers from cabin air and allow 254 nm UV radiation to pass through the chambers. UV radiation from the low pressure mercury lamp is precisely directed by the beamsplitter and mirror through the two sample chambers. After passing the length of the chambers, narrowband filters allow only the 254 nm radiation to pass for detection by photodiodes (see detector unit). Each filter/photodiode mount also holds a quartz window in place on the body unit.

3. The **detector unit** consists of two amplifier printed circuit boards, two photodiode detectors with mounts, and a detector interface board. Each amplifier provides a signal proportional to the 254 nm signal intensity striking a photodiode that is mounted together with a narrowband filter (also see optical unit). The signal current from each photodiode is processed by a low-noise amplifier that is fed to a high-precision voltage-to-frequency converter. Each printed circuit board is embedded within the aluminum base unit to minimize electromagnetic pick up. The frequencies of the V/F converters are sampled at 1 Hz by the counter/timer board of the data system module and stored in a data file.

4. The **valve unit** is a 4-port rotating valve that directs the scrubbed and un-scrubbed air flows into the two sample chambers. It consists of a gear motor with mount, a drive train, a valve sleeve with rotating insert, a valve position sensor, a valve controller board, a brass mount for the motor, electrical feed-throughs, and reflective object sensors, and a pressure can. The Tefzel valve sleeve is fitted into a cavity in the body and the sleeve

20 New England Business Center Andover, MA 01810-1077 *t* 978.689.0003 *f* 978.689.3232
www.psicorp.com

precisely fits with the rotating insert. Once every 10 seconds, the DC gear motor quickly rotates the valve 90° via a spider coupling and the valve shaft attached to the rotating insert. Also attached to the valve insert is a flat black disk "modulator" with a small white reflective section that rotates along with the valve insert and allows sensing of the valve position by the four reflective object sensors. These sensors are equally spaced from the valve axis and in quadrature so they will detect when the valve has moved 90 degrees from its previous position. The valve controller PC board is mounted inside the pressure can and turns the motor on and off, accurately positioning the valve as indicated through signals detected by the reflective object sensors. The controller board also senses when the valve is in the correct position for the flow condition required by the data system. Although there are 4 valve positions, two are redundant. That is, there are only two possible modes for a chamber: scrubbed and un-scrubbed. The pressure can is connected to the common chamber exhaust for sampled air and provides a small pressure decrease from the pressure inside chambers. This eliminates possible contamination of the air being sampled by valve leakage.

5. The **pressure unit** consists of an absolute pressure gauge and a differential pressure gauge. The pressure at the midpoint of one of the absorption chambers is monitored by the absolute pressure gauge, while a differential pressure gauge monitors the pressure drop between the midpoint of the other chamber and the common chamber exhaust. The absolute pressure measurement is required to calculate the ozone mixing ratio in ambient air and the differential measurement is only used as an indication of the rate of air flow through the chambers.

6. The **temperature unit** consists of 11 temperature sensors and a temperature controller with resistive heaters. Four of the temperature sensors are mounted onto vacuum feed-throughs, and are located within the sample flow, three temperature sensors are positioned on the body unit, and the remaining four are located in various positions around the data system and interface & power supply modules. Air sample thermistors are placed in the sample air flow near the chamber inlets and exhausts and used for ozone mixing ratio calculations. Other temperature measurements are for diagnosing instrument operation and considered as housekeeping data. All temperatures are measured using high-precision thermistors. The photometer body temperature is controlled near 34°C using resistive heaters.

7. The **flow unit** consists of all other components directly in the sample flow path. These are the ozone scrubber, Teflon and brass tube fittings, two aluminum exhaust ports, and various Teflon parts within the un-scrubbed air sample path.

The **data system module** consists of a PC 104 format data system and a hard drive for data storage. The PC104 units consist of a CPU, a counter/timer board, 16 single ended and 8 differential A/D channels, a VGA board to allow connection of a monitor during checkout, a front panel for external connections from the data system, and a counter interface board. The PC104 components are stacked to minimize size and weight. Attached to this stack is the counter

20 New England Business Center Andover, MA 01810-1077 *t* 978.689.0003 *f* 978.689.3232
www.psicorp.com

interface board that connects the detector signals to the counter/timer board. The data are stored on a removable "notebook" hard drive and are analyzed after flight to determine ozone mixing ratios.

The **interface and power supply module** includes an interface board with various cable connections, power supplies, a baseplate and a circulation fan. This is the component that provides power to the other modules and is where the various units are inter-connected. The interface board was built to accommodate the particular needs of the HIAPER instrument. It is hand wired with cables attached and must be handled with care. Removal of the board from the aluminum baseplate is not recommended and is not necessary for servicing of the instrument. If it becomes necessary to remove it or disconnect it from other modules, a procedure is outlined in the section on general care and cleaning. Information on the electrical interconnections within this module can be found in Appendix C and Appendix D.

Operating environment

Aircraft cabin temperature should be above 0 °C but not more than 25°C. Higher temperatures may not allow for the instrument temperature control needed for best instrument operation. Low instrument temperatures prior to operation may cause an erratic behavior of the rotating valve during the initial warmup period, and a warmup time of more than the usual 20 minutes may be required. Sampled air temperature can be from as high as 40 °C at ground level to below -60 °C at flight altitudes, as long as the temperature of the sample air is pre-heated to near 30 °C at the instrument inlet. Cabin pressure of more than 600 mbar and sample pressure of not less than 100 mbar should be maintained during instrument operation.

Instrument setup

The photometer is a stand alone package and requires less than 3 amps of 28 VDC power. When power is connected, the temperature controller will apply heat to the body unit until the nominal set point of 34 °C is attained. In the event the body is initially above the set point or heat generated within or near the instrument warms the body above that set point, the temperature of the instrument will not be controlled. This situation should be avoided if optimal instrument operation is needed. The entire photometer, including its mercury lamp, the valve control circuitry, plus the data system are also powered when 28 VDC is applied.

The inlet design and its placement on the aircraft are critically important if the full measurement capabilities of the PI photometer are to be achieved. The instrument inlet must be constructed to assure the sample is taken within the free air stream, well away from the aircraft boundary layer and local turbulence from other inlets and aircraft protrusions. If turbulence surrounding the aircraft is transferred into the photometer, there may be excessive noise in the 1 second data. Clean Teflon materials should be used exclusively for all sample inlet lines to minimize ozone loss on surfaces before the air enters the sample chamber. The inlet and connecting tubing are not provided by PI.

20 New England Business Center Andover, MA 01810-1077 *t* 978.689.0003 *f* 978.689.3232
www.psicorp.com

The instrument inlet flow rate must be about 1 liter/minute (l/m) to completely flush both chambers in one second. Much higher flow rates may result in incomplete pre-warming of the air before entry into the sample chambers or in non-laminar flow, and as was discussed earlier should be avoided.

Instrument operation and pre-flight performance check

After application of 28 VDC power, the data system immediately boots up on its DOS 6.22 operating system which starts the Quick Basic data acquisition program within about 1 minute. Two modes of operation are possible following boot up: unattended data acquisition and preflight checkout. Both modes use the same data acquisition program and in both cases, data are written to the hard drive. Data formats have been set by PSI and are available in PSI documentation.

In checkout mode, a monitor must be connected to the front panel of the data system before power up. It is recommended that a 30 minute pre-flight performance check using an external monitor be made before each flight to be certain that all instrument components are functioning properly.

These will normally be performed without a flow of sample air through the chambers. In less than 30 minutes, the operation of the essential measurements can be verified and other housekeeping data can all be observed on the monitor (see Appendix F). At startup these checks include:

1. Data system is operational and data are being recorded
2. The lamp, detectors and detector boards are operating
3. Valve rotation is occurring
4. Pressure sensors are operating
5. Temperature sensors in the sample chambers are operating
6. Temperature controller is operating
7. Power supply and reference voltages are appropriate
8. Circulation fan is operating

After 20 minutes of warmup other checks can be made. These include:

1. UV signals are stable
2. Temperature of the photometer is under control

No additional pre-flight checks are necessary unless there is reason to believe the instrument has been contaminated, either in the laboratory or during a previous flight. If contamination has occurred, the entire flow path must be cleaned by trained personnel as discussed under the section General care and cleaning.

Following the successful checkout and prior to the anticipated flight, the instrument should be powered down and the monitor connection removed from the front panel. After the flight, data files stored on the hard drive can be conveniently downloaded to other computers by removing the hard drive from the data system and using a USB IDE enclosure for notebook hard drives to make the transfer of data to a flight analysis computer.

20 New England Business Center Andover, MA 01810-1077 *t* 978.689.0003 *f* 978.689.3232
www.psicorp.com

Other preflight procedures may be required on a flight to flight basis if the instrument is routinely removed from the aircraft. In this case, power, sample inlet and exhaust must be reconnected. Other electrical connections to the aircraft that may also be required, such as RS232 or IRIG, are not provided by PI, but may need to be reconnected.

The accuracy of the temperature measurement is assured for the life of the instrument by their careful installation into the air flow near the chambers inlets and exhausts. However, the accuracy of the absolute pressure measurements should be periodically checked to assure its zero pressure value and span have not changed. In general, the span is very stable and should not require additional calibration. Never-the-less, when an accurate reference gauge is available, span checks during zero checks are recommended. The original calibration constants can be found in Appendix A.

General care and maintenance

The instrument should be stored and operated in a clean environment and never be in a smoky environment. All contaminants that might cause carbon or oil deposits on the optical, pressure or flow related components of the instrument must be avoided. Importantly, engine exhaust and smoking near the instrument can adversely affect instrument operation. The sensitive components include all optics and Teflon materials that are in contact with the sample flow. Note that most optical components are open to cabin air where smoking may occur. These include windows, beamsplitter, mirror, photodiodes, narrow-band filters and lamp. Care should also be taken to protect the inlet and connecting tubing from contamination. Ozone losses occur on contaminated surfaces that the sample air contacts. Additionally, small particles of debris that enter and become lodged in the sample chambers, can cause excessive noise.

All of the **optical components** are sensitive to other contamination as well, such as the oil deposited when touched with fingers. Cleaning of optical components must be done by trained personnel or risk permanent damage to these sensitive components.

It is normal for a **mercury lamp** to give an occasional brief spike in intensity that can be observed for one or two seconds in the recorded data. These spikes are caused by a quick movement of the emitting plasma within the lamp, but should not occur more than about once per hour. If spikes are observed to be more frequent, the lamp may need to be replaced. Although a good lamp should last for thousands of operating hours, as it is used, its intensity will decline gradually. Eventually the UV intensity will decrease sufficiently to either require gain adjustments on the detector boards, or replacement of the lamp itself. If the lamp requires replacement, it should be done only by personnel trained in servicing the instrument. Replacement may require careful gain adjustments on the highly sensitive detector boards. The **mercury lamp** is particularly sensitive to abuse and should remain in its original orientation and position within its Teflon housing. For example, touching the Vicor shield of the mercury lamp could permanently reduce the UV output of the lamp if it is not cleaned before operation. And if the lamp is broken and releases the mercury onto or around the instrument, it may be impossible to clean the chambers and other flow related components sufficiently to obtain

20 New England Business Center Andover, MA 01810-1077 *t* 978.689.0003 *f* 978.689.3232
www.psicorp.com

original instrument specifications. Also, if the set screws that lock the lamp into position are loosened and the lamp is reinserted without regard to its original orientation, the detected lamp intensity may change sufficiently to adversely affect instrument sensitivity, or in some cases, render the instrument inoperable.

In the event the lamp is not uniformly illuminated and the plasma within the lamp forms beads of light that move quickly within the lamp, the result is excessive noise in the absorbance. That is, the ratio of lamp intensities entering the two chambers averaged over one second will change from second to second which is evident as noise in the absorbance. If the lamp is noisy, it must be replaced with a lamp that is not. Such lamp illumination fluctuations and inhomogenieties also can be observed visually if the UV is filtered for eye safety. **Caution: Direct viewing of the lamp radiation must be avoided or eye damage will occur. Please carefully read the safety considerations section in this manual for more information on mercury lamps and their power supplies.**

Each **pressure gauge** behaves somewhat differently so only experience with your particular gauge will give confidence in how often to check for changes. In some cases, where care has been taken with the instrument, the zero will remain sufficiently stable for years. Keep in mind that pressure gauges should not be exposed to large sudden changes in pressure, such as quickly opening a gauge to atmospheric pressure after a vacuum zero check. Although the zero check may have been made successfully, if the vacuum is suddenly released, the zero may change substantially.

Both the **zero and the span** for the pressure sensor require calibration. Their initial values were measured before instrument delivery to PSI and set within the data acquisition software provided (see Appendix A). Adjustment to these calibrations can be made through the data reduction software provided by PSI. Keep in mind that a 1% error in the pressure measurement results in a 1% error in the ozone mixing ratio.

A photograph and the physical layout of the components on the interface board are given in Appendix C. Information helpful in checking the electronic integrity of the various instrument modules is provided by this layout and the tables in Appendix D. Appendix C includes a scaled version of the actual board and a photograph of the interface and power supply unit, including connector labels. Appendix C is intended to present complimentary information to the tabular lists of connector interconnections given in Appendix D. Together, they provide necessary information on interconnections between these components in the event that an electronic problem arises. Resistor and capacitor values are not given, but can be read directly from the board itself. This is done to avoid inaccurate labeling of component values where changes may occur during the installation of the instrument on the aircraft. Please note that the potograph in Appendix C differs in two ways from the board delivered by PSI. The DIP switch in the photo is replaced by a 2 position switch and a pot was added to the board. The pot is also not on the schematic. It is a preset adjustment for the valve and requires no service, i.e. do not change its setting.

20 New England Business Center Andover, MA 01810-1077 *t* 978.689.0003 *f* 978.689.3232
www.psicorp.com

In the event that the interface board must be removed or disconnected from other modules, there are many connectors to make allowance for. They must be carefully labeled so they can be properly reconnected. See Appendix C and D for details. The connectors on the interface board are:
J1: 37 pin D connector to the data system CPU (front panel 50 pin connector)
J2: 25 pin D connector to the data system 12 bit A/D board (50 pin connector on board edge)
J3: 9 pin D connector (male) that sends power to the interface board and the 28 VDC to the power supplies
J4: 9 pin D connector (female) that connects to the valve 9 pin D connector on the body
J5: 9 pin D connector (female) (two) that connect to the detector 9 pin D connectors on the body
J6: 15 pin D connector (female) that connects to the thermistor 15 pin D connector on the body
J7: 9 pin D connector (female) that connects to the pressure/heater 9 pin D connector
J8: 2 conductor circular connector that powers the data system (5 volts)
J9: 2 pin connector that connects the lamp to the lamp power supply
J10: 2 pin connector that connects the instrument to the 28 volt power supply
J11: 4 pin connector that connects power and the thermistor to the temperature controller
J12: 2 pin connector that connects the 12 volt power to the circulating fan
J13-J16: 2 pin connectors (four) that connect to thermistors for the circulating fan, the power supply panel, the air surrounding the instrument (box temperature), and the front panel of the data system.

When reconnecting these connectors, care must be taken to be certain the correct connections have been made. In particular, J4, J5 and J7 are all identical 9 pin female connectors and could be inadvertently interchanged. If this occurs, it may cause serious damage to the various instrument components. Similarly, J10 is not polarized, and this must be carefully connected to be sure that the 28 volt power line is connected to the red wire on J10. J12 uses an identical 2 pin connector and should also be connected with the proper polarity to avoid damage to the fan. Particular care must also be taken to be certain that the 50 pin connectors on the data system are correctly connected **before power is applied, or the data system will be damaged**.

In general, the instrument requires little or no regular maintenance and disassembly should not be necessary. However, if the instrument is contaminated it will need to be cleaned by a person trained for the job and with knowledge of the assembly and disassembly of the body and associated components. **This must not be attempted without detailed training from PI or PSI. Many critical components can be seriously damaged by improper cleaning or handling and render the instrument inoperable, and perhaps seriously damaged. When cleaning is required, it should be arranged through PI.**

Safety considerations

There are very few safety issues with the PI Dual-Beam Ozone Photometer, and all are involved with the low pressure mercury lamp. The manufacturer represents the lamp as containing less than 3 milligrams of mercury, much less than is generally found in a single fluorescent bulb. This

20 New England Business Center Andover, MA 01810-1077 *t* 978.689.0003 *f* 978.689.3232
www.psicorp.com

amount of mercury is not generally considered to be a hazard to the environment if disposed of properly.

More importantly, the lamp emits UV radiation, and can cause eye damage. If the lamp is to be viewed directly, appropriate precautions must be taken to eliminate the most harmful UV components by viewing through goggles that block all UV radiation.

The lamp's power supply operates near 200 VAC. Care should be taken to avoid contact with these high voltage terminals.

Intellectual property

PI retains all right, title and interest in and to all pre-existing PI Intellectual Property, which includes, but is not limited to, all versions, derivative works, updates, improvements, modifications, enhancements and releases thereof. PI retains all rights to instrument data acquisition source code.

Warranty

PI makes no warranties, express or implied, as to any matter whatsoever, including, without limitation, the condition of the research or any invention(s) or product(s), whether tangible or intangible, conceived, discovered, or developed under the subcontract with PSI; or the ownership, merchantability, or fitness for a particular purpose of the research or any such invention or product. PI shall not be liable for any direct, consequential, or other damages suffered by any licensee or any others resulting from the use of the research or any such invention or product.

This User Manual describes the capabilities, operation, and care of a dual-beam ozone photometer developed by Proffitt Instruments, Inc. (PI) and Physical Sciences, Inc. (PSI). It is based upon a working flight prototype that has been extensively tested and used by PSI. PI has led the design and fabrication effort, including implementation of the pressure tight valve. PSI has provided the mechanical parts, the detector printed circuit boards and is the leader for the bench-testing, intercomparison validation, aircraft integration and flight testing of the photometer. PI is solely responsible for the content of this Operator's Manual.

PSI, under contract with the University Corporation for Atmospheric Research, entered into a Sub Contract Agreement with PI on February 3, 2005, that included PI to deliver a fully functional ozone photometer. The photometer was delivered to PSI on December 27, 2005. On January 12, 2006, after satisfactory lab tests, delivery of the instrument was accepted by PSI. Important follow-up instrument checks have been performed by PI and are discussed in the Addendum of this User Manual.

20 New England Business Center Andover, MA 01810-1077 *t* 978.689.0003 *f* 978.689.3232
www.psicorp.com

PI Appendix A: Photometer and measurement specifications

- Total weight: 7 kg (includes all units and baseplate)
- Dimensions: 44 x 29 x 17 cm (instrument on baseplate, no housing)
- Power: 28±2 VDC (70 watts max, intermittent; 17 Watts minimum)
- Ozone measurement time resolution: 1 second (each 10 second data interval includes nine 1 second measurements and a 1 second interval for the valve rotation)
- Precision of measurement: 3 x 10^{10} molecules/cm^3 (about 1 ppbv at STP under laboratory conditions)
- Length of chambers: 20.0 cm
- Absolute pressure sensor calibration constants: span = 258.26 mbar/volt offset = 59.55 mbar
- Differential pressure sensor calibration constants: span = 1.25 mbar/volt offset = 2.25 mbar

20 New England Business Center Andover, MA 01810-1077 *t* 978.689.0003 *f* 978.689.3232
www.psicorp.com

PI Appendix B: Summary of modules and units

VI. Photometer module
- A. Body unit
- B. Optics unit
  1. Mercury lamp with mount
  2. Black anodized optical mount
  3. UV mirror
  4. Beamsplitter
  5. 254 nm narrow-band filter (2)
  6. Quartz windows (4)
- C. Detector unit
  1. Amplifier printed circuit boards (2)
  2. Photodiode detectors with mounts (2)
  3. Detector interface board
- D. Valve unit
  1. 4-port valve (sleeve and rotating insert)
  2. Gear motor and mount
  3. Motor drive train
  4. Valve position sensor
  5. Reflective object sensors (4)
  6. Valve controller printed circuit board
  7. Brass mounting with electrical feedthroughs
  8. Pressure can
- E. Flow unit
  1. Ozone scrubber
  2. Teflon tubing
  3. Teflon and brass tube fittings
  4. Various Teflon parts
  5. Aluminum exhaust ports

VII. Data system
- A. CPU board
- B. Counter/timer board with interface
- C. A/D converters
- D. VGA (video board)
- E. Front panel
- F. Hard drive

VIII. Interface and power supply module
- A. Interface board
- B. +5 volt and ±12volt DC power supply
- C. +12volt DC supply for lamp HV power supply
- D. Lamp HV power supply
- E. Circulation fan
- **F.** Baseplate

20 New England Business Center □ Andover, MA 01810-1077 □ *t* 978.689.0003 *f* 978.689.3232
www.psicorp.com

PI Appendix C: Interface board

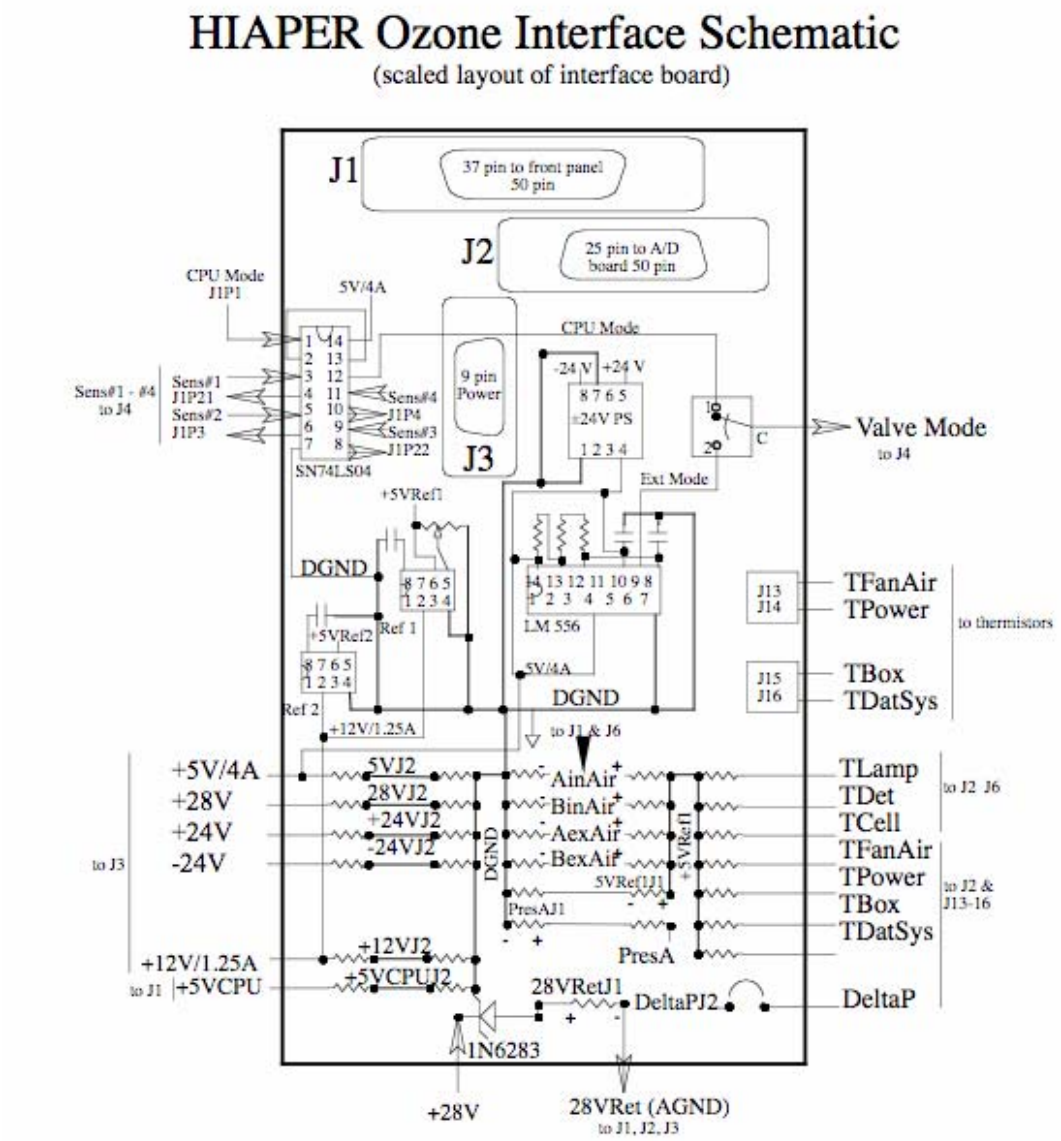

20 New England Business Center □ Andover, MA 01810-1077 □ t 978.689.0003 f 978.689.3232
www.psicorp.com

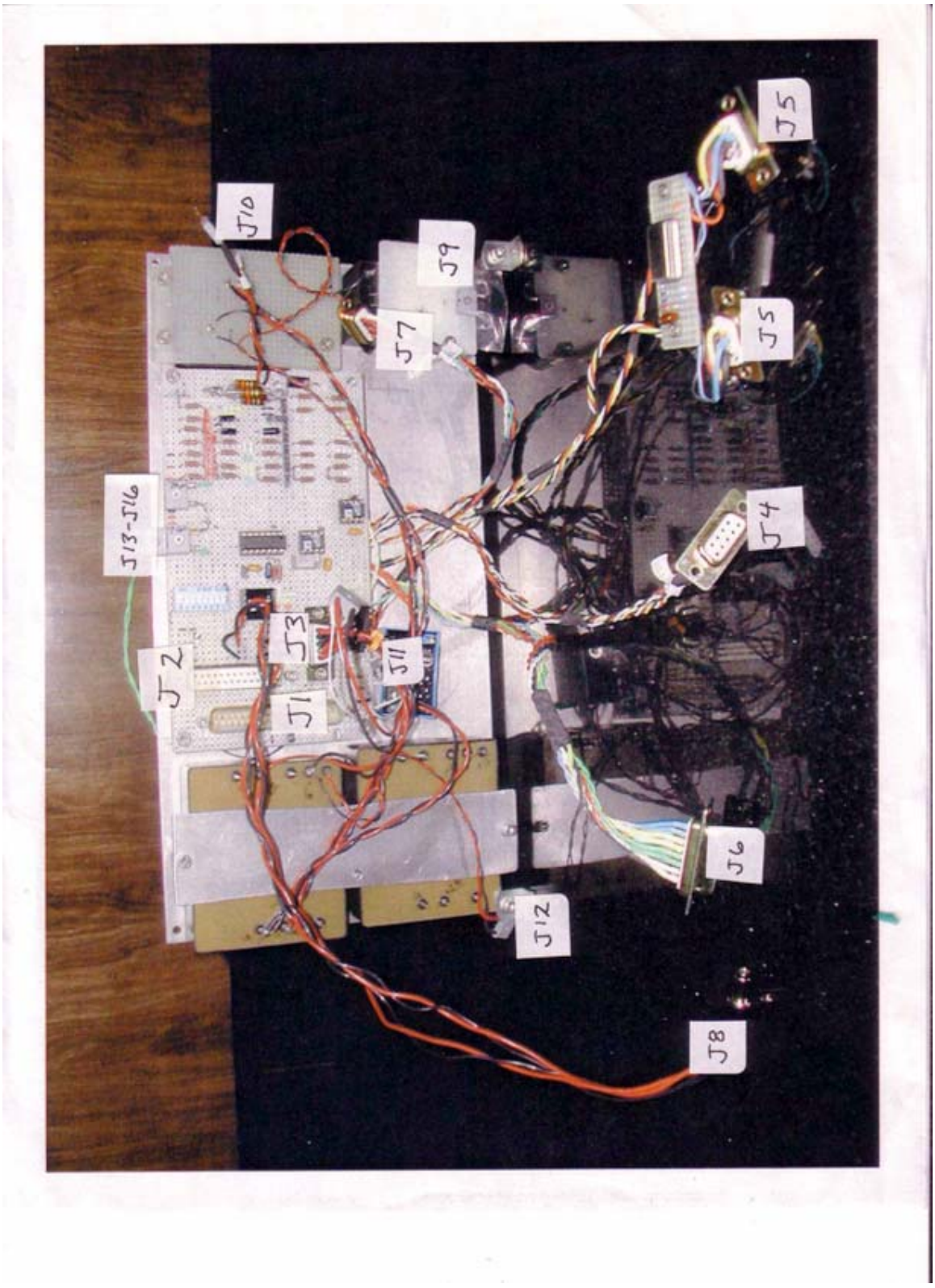

20 New England Business Center □ Andover, MA 01810-1077 □ t 978.689.0003 f 978.689.3232
www.psicorp.com

PI Appendix D: Connectors

A/D CH	JUNCTION NAME	FRONT PANEL 50 PIN	J1 37 PIN D CONN
	UNUSED	1..13	
	CPUMode	14	1
	UNUSED	15..16	
	ObjSens#1	17	21
	ObjSens#2	18	3
	ObjSens#3	19	22
	ObjSens#4	20	4
	DGND	21..24	23,5,24,6
	UNUSED	25,26	
	+5VCPU	27	26
	DGND	28	8
	UNUSED	29..33	
	AGND	34	11
#0 +DIF	+AInlAir	35	30
#0 -DIF	-AInlAir	36	12
#1 +DIF	+BInlAir	37	31
#1 -DIF	-BInlAir	38	13
#2 +DIF	+AExhAir	39	32
#2 -DIF	-AExhAir	40	14
#3 +DIF	+BExhAir	41	33
#3 -DIF	-BExhAir	42	15
#4 +DIF	+5VRef1J1	43	34
#4 -DIF	-5VRef1J1	44	16
#5 +DIF	+PresAJ1	45	35
#5 -DIF	-PresAJ1 (DGND)	46	17
#6 +DIF	+PresBJ1	47	36
#6 -DIF	-PresBJ1 (DGND)	48	18
#7 +DIF	+28VRet	49	37
#7 -DIF	-28VRet (AGND)	50	19

A/D CH	JUNCTION NAME	A/D BOARD 50P	J2 25 PIN D CONN
#15 SNG	+5VCPUJ2	1	1
#7 SNG	DeltaPJ2	2	14
#14 SNG	+12VJ2	3	2
#6 SNG	TDatSys	4	15
#13 SNG	-15VJ2	5	3
#5 SNG	TBox	6	16
#12 SnG	+15VJ2	7	4
#4 SNG	TPower	8	17
#11 SNG	-24VJ2	9	5
#3 SNG	TFanAir	10	18
#10 SNG	+24VJ2	11	6
#2 SNG	TCell	12	19
#9 SNG	+28VJ2	13	7
#1 SNG	TDet	14	20
#8 SNG	+5VJ2	15	8
#0 SNG	TLamp	16	21
	AGND	17	9..12
	UNUSED	18,20,22	13
	AGND	19,21,23	9..12
	UNUSED	24..26	22..25
	AGND	27	9..12
	UNUSED	28,29	UNUSED
	DGND	30	UNUSED
	UNUSED	31..49	UNUSED
	DGND	50	UNUSED

20 New England Business Center □ Andover, MA 01810-1077 □ t 978.689.0003 f 978.689.3232
www.psicorp.com

NAME OF WIRE	POWER J3 9P	VALVE J4 9P	DETEC J5 9P (2)	THERM J6 15P	PRES/HEAT J7 9P	CPU 5 V J8 2P	LAMP 12V J9 2P	28 V PS J10 2P	T CONT J11 4P	FAN J12 2P	THERM J13..J16
+28V	1							A			
+5V/4A	4	1	3			CENTER					
+12V/1.25A	5						A				
+15V/1A	6										
+12V_TS	7									A	
-12V_TS	8										
-15V/1A	9										
+28VRet								B			
-28VRet (AGND)	2										
DGND		5	7	11,13,15	2						A
AGND	3	2	2,4,6,9			GND	B			B	
+AInAir				1							
-AInAir				2							
+BInAir				3							
-BInAir				4							
+AExAir				5							
-AExAir				6							
+BExAir				7							
-BExAir				8							
TDatSys											B
Tbox											B
Tpower											B
TFanAir											B
TCell				14							
TDet				12							
TLamp				10							
+12Vvalve		**3**									
ValveMode		4									
Sens#1		6									
Sens#2		7									
Sens#3		8									
Sens#4		9									
-24V			1								
+24V			5								
8MHzClk			8								
+5VRef2					1						
Heater					3,5				A		
HeaterCom					4				B		
PresB					6						
DeltaP					7						
ThermTempCtrl1					8				C		
ThermTempCtrl2					9				D		
UNUSED				9							

20 New England Business Center Andover, MA 01810-1077 *t* 978.689.0003 *f* 978.689.3232
www.psicorp.com

PI Appendix E: Replacement parts

Part Name	Part number	Manufacturer
CPU & 16 bit A/D	Prometheus PR-Z32-EA-ST	Diamond Systems
Panel I/O board	PNL-Z32-EA	Diamond Systems
12 bit A/D	DMM-NA-XT	Diamond Systems
Counter/timer board	QMM-10	Diamond Systems
Front panel	PBEC-05-K	Diamond Systems
VGA	ACC-VGA-02	Diamond Systems
Hard drive	Notebook e.g. Seagate 20 Gb #ST92011A	Various
Absolute pressure sensor	683-15PSIA4V	All Sensors
Differential pressure sensor	DeltaP 683-1INCHD4V	All Sensors
Temperature Controller	CT325TF2A1	Minco Products
Thermistor for temp controller	31-TS665TFY40B(A)	Minco Products
Heater strips 78.4 ohm	HK5164R78.4L12B	Minco Products
Heater strips 52.3 ohm	HK5165R52.3L12B	Minco Products
Silicone photodiodes	S1336-8BQ	Hamamatsu
UV Beamsplitter	PLT-UV-25.4x25.4	Esco Products
Quartz windows	WD-CQF-S1-AS.7DIA2.18TH	Esco Products
UV Mirror	PF10-03-F01	Thorlabs
DC gear motor	1727U012CL 86:1+X0814C	Faulhaber
Spider gear	CO46-1B	W M Berg
5 V @ 4 amp ±12 V @0.5 amp PS	SIW24T12-30	Wall Industries
±15 V @ 1 amp PS	SIW24 D15-30	Wall Industries
12 V @ 1.25 ams PS	LCSW 2412-15	Wall Industries
±24 V PS	LANH 524ND	Wall Industries
Low pressure Mercury Lamp	80-1025-33	BHK
Lamp PS	68-0020-04	BHK
Valve controller	Valve controller board	PI
Detector board	Detector PC board	PSI
Circulation Fan	FE12H3	Rotron
Hex Inverter	SN74LS04N	Various
5 volt reference	AD586LN	Analog Devices
Dual timer	LM556CN	Various
Thermistors, general use	192-103LET-A01	Fenwal
Ozone scrubber cartridge	SCN001	Tanabyte Engineering

Source Address (Manufacturer)

Diamond Systems, 1255 Terra Bella, Mountain View, CA

Mouser Electronics, 1000 N Main St, Mansfield, TX (All Sensors)

Minco Products, 7300 Commerce Lane, Minneapolis, MN

Hamamatsu, 360 Foothill Rd, Bridgewater, NJ

Esco Products, 171 Oak Ridge Road, Oak Ridge, NJ

ThorLabs, 435 Route 206, Newton NJ

MicroMo, 14881 Evergreen Ave, Clearwater, FL (Faulhaber)

W.M. Berg, 499 Ocean Ave, East Rockway, NY

Wall Industries, 5 Watson Brook Rd, Exeter, NH

BHK, 1480 N Claremont Blvd, Claremont CA

PI, 1122 Enclave Sq East, Houston TX

PSI, 20 New England Business Center, Andover, MA

Newark InOne, 4801 N. Ravenswood Ave, Chicago, IL (Rotron, AD, Fenwal)

Tanabyte Engineering, 1210 W. Burbank Blvd, Burbank, CA

20 New England Business Center Andover, MA 01810-1077 t 978.689.0003 f 978.689.3232
www.psicorp.com

PI Appendix F: Monitor screen

Pre-flight check out data are available by directly viewing the monitor (see *Instrument operation and pre-flight performance checks*). The monitor displays information in the following format by line number:

0: IRIG Time: hour: minute: second.millisecond
1: Counter A: counter A freq, freq change during last sec, secs since start (CPU clock)
2: Counter B: counter B, freq change during last sec, # of 1 sec cycles (data sys clock)
3: Ratio A/B: counter A/counter B, Ratio change during last second
4: Chamber Temps: chamber A in, chamber B in, chamber A out, chamber B out
5: Lamp, Det, Scrub: Temp near Lamp, Temp near Detector , Temp near Scrubber
6: Fan, PS Panel, Box, Proc: fan air temp, PS panel temp, box, temp, data sys temp
7: 5V Ref, 5V PS, 5V PC, +12V: Ref 5V for A/D's, 5V PS, 5V on data sys, +12V
8: +24 V, -24v, +28V, 28V I: ±24V PS, 28V main supply, 28V current
9: Delta Pres, Atmos Pres: difference between chamber A and common exhaust, pressure in chamber B
10: ValveQuad, ExpectQuad, Skips, Stops: Valve position observed by reflective sensors, valve position expected by computer, number of times valve skipped a valve position, number of times valve did not advance.
11: % of time needed during last second, maximum % of time since start
12: Data written to Data file: HIAPER.DAT

20 New England Business Center Andover, MA 01810-1077 *t* 978.689.0003 *f* 978.689.3232
www.psicorp.com

PI Appendix G: Recent instrument upgrades available from PI

1) Interface board available as a printed circuit board. This replaces the hand wired interface board on the present instrument and incorporates commercial cables for connection to other instrument components.

2) Improved brass mount for valve. Redesign of the brass valve mount allows easy access to valve components.

3) Printed circuit board for mounting the pressure sensors. This replaces the current hand wired version.

4) Printed circuit board to replace detector interface board. This replaces the current hand wired version.

5) Printed circuit board to replace counter interface board. This replaces the current hand wired version.

6) Improved mounting for the silicon photodiodes. This is to eliminate grounding problem of photodiode and better protect the detectors.

7) Improved vacuum seals of thermistor feed-throughs. This improves the vacuum integrity of the instrument.

These seven upgrades should significantly improve the prototype instrument you have, including the virtual elimination of hand wiring on the interface board and improved vacuum integrity.

Other upgrades now under development:

1) balance scrubbed and unscrubbed flow rates

2) electronic positioning and brake for valve

3) controlled warming chamber for scrubber air

4) improved temperature controller for body unit

5) redesign of optical mount to improve heat distribution from lamp

6) Detector boards redesign for noise reduction and improved heat dissipation

Proffitt Instruments, Inc.
Attention: Mr Rod Hotz
1122 Enclave Square East
Houston, TX 77077-7616
USA

Email: proffitt@uolsinectis.com.ar

PI Addendum concerning photometer offsets, time response, and temperature control

PI hand delivered the completed instrument to PSI on December 27, 2005. Although basic bench tests were performed by PI prior to delivery, to meet the required schedule, tests with sample air flow tests were not made. This was agreeable to PSI since they would perform a thorough bench test before accepting the instrument, and their experience with earlier versions of the instrument indicated that as long as tests without flow were passed, there were no special concern under sample flow conditions. Immediately after delivery, PI assisted PSI with final bench tests in their labs. PSI accepted the completed instrument on January 12, 2006. At that time it appeared the instrument was performing well, although PSI did not find it necessary to perform instrument tests with sample air flow. The instrument was not tested again before January 2007.

During 2006, PI built and delivered a "clone" of the HIAPER instrument to a second customer. Upon delivery in late 2006, flow tests were made by the customer who found there were unacceptable offsets in the calculated ozone concentrations. That is, with ozone free air being sampled, large "negative ozone" values were indicated. This was a big surprise to all of us. Instruments #1 (the original PSI/PI instrument from 1998) , #2 (the HIAPER Aircraft version), and #3 (the HIAPER clone delivered in 2006) are nearly identical, with primary differences being that #2 and #3 have a modified valve motor/drive mechanisms that is pressure sealed to accommodate operation in an aircraft cabin. These modifications were necessary to prevent contamination of the sample chambers with cabin air and they were the responsibility of PI with PSI assisting.

As already pointed out, earlier experience of PSI with instruments #1 and the newer ground based instrument built by PSI, identified no such offsets when intercompared under sample flow conditions in the PSI labs. After making some basic checks of #3, and considering the PSI tests with earlier instrument versions, the valve became the main suspect. We conjectured the valve and/or its pressure housing were possibly leaking into the sample chambers and somehow causing the offsets. A second possible cause was found by simple tests that showed both positive and negative offsets could be produced by warming or cooling the scrubbed air path. However, it was reasoned that if the offsets resulted from flow path asymmetries, they should also be evident in instruments #1 and #2. Since they were not observed in #1, this option was immediately shelved in favor of exploring the valve as the cause. This decision was confirmed in early 2007 when PSI also found excessive offsets when testing the #2 HIAPER instrument under sample flow conditions.

The approached used by PI to investigate the source of the offsets was to build another "clone" of the HIAPER instrument for testing in house. Fortunately, PI had already begun building another instrument which was completed on February 1, 2007 (instrument #4). Most of February, March and April were spent testing the valve design and investigating how it might cause offsets. These tests identified no problem with the valve, as long as it is accurately positioned after each valve rotation. To aid in positioning of the valve, PI designed and implemented an addition to the valve controller circuit that allows electronic valve position adjustment using a variable resistor.

20 New England Business Center Andover, MA 01810-1077 *t* 978.689.0003 *f* 978.689.3232
www.psicorp.com

However, accurate adjustment had little or no effect on the magnitude of the offsets, although large misalignment was observed to change the offset.

By mid May, and after many tests, PI had all but abandoned the valve tests in favor of testing flow path asymmetries that may affect temperatures in the chambers. This approach was supported by experiments in the early 1980s demonstrating that temperature of sample air as it enters the chambers should be near the chamber wall temperature or offsets could occur. Those lab tests showed the offsets in these early instruments were generally less than 1 ppbv but occasionally up to 5 ppbv. Both positive and negative offsets were seen, but always much less than the ±10-20 ppbv commonly observed in instruments #2,#3, and #4. To minimize offsets one early instrument for use on balloons included a temperature controlled "pre-warming" volume for sample flow immediately before it is introduced into the chambers.

PI has performed tests on #4 that indicate flow related design problems are causing the large offsets. Asymmetries between the two flow paths (scrubbed and un-scrubbed) are more pronounced in the design used for instruments #1, #2, #3 and #4 than in the very early instruments from 1980s, and these asymmetries appear to be much more important than originally thought. There are three asymmetric components considered here.

First, the long curved connection between the scrubber and the valve (0.15 inch inside diameter and about 5 inches long) is more restrictive than the short direct connection between the un-scrubbed air and the valve (¼ inch diameter and about 1.5 inches long). The scrubber itself also contributes to this difference, but tests show its contribution is relatively small. The restriction in the tubing connection results in a large change in flow rate within a chamber when switching between scrubbed and un-scrubbed modes. Judging from differential pressure gauge measurements under flow conditions, it appears the HIAPER instrument flow ratio of un-scrubbed to scrubbed is about 3:1. That is, if the instrument has a total flow rate of 2 l/m, only 0.5 l/m are flowing in the scrubbed chamber while 1.5 l/m is flowing in the un-scrubbed.

Second, the scrubber connection is external to the aluminum temperature controlled body, so the air temperature entering the scrubbed port of the valve will be near the temperature of the external tubing rather than the temperature of the body. If the flow is not excessive, the un-scrubbed air temperature will be very near the temperature of the photometer body.

Third, the position of the lamp on the A chamber side of the photometer body contributes to heat asymmetrically. This is at least partially compensated for by asymmetry in the resistive heaters on the body, but heat is applied only as needed to control the body temperature, and control is not linked to the lamp temperature. This differential heating between the two chambers my cause different offsets in the two chambers.

In various tests, it has been consistently observed that the counts (i.e. signal intensity) measured for a chamber increase as flow rate increases. To explore this observation and the offsets found in instruments #2,#3,and #4 a "stop/flow" test using #4 was conducted that eliminates some of the measurement variables. This test was conducted with chamber B exhaust capped, thus testing

20 New England Business Center Andover, MA 01810-1077 t 978.689.0003 f 978.689.3232
www.psicorp.com

only one chamber. An ozone scrubber was placed on the chamber A inlet, and a diaphram pump was used to draw clean ozone free ambient air into the chamber. A flow meter followed by needle valve were inserted down stream of the photometer to change and accurately measure flow rate through chamber A.

The instrument was set-up without a temperature controller, and housed inside a highly insulated box. The only heat sources were the lamp, the detector electronics and a small circulating fan. All other instrument components were outside the insulated box. This produced a highly uniform and stable temperatures around and within the aluminum body (at about 30 C). The photometer was turned on and allowed to temperature stabilize over-night. The valve was first rotated into quadrant 1, one of the two un-scrubbed quadrants, before a sequence of 10 flow/no-flow data sets were taken. The flow rate through chamber A was set to one of 10 predetermined values between 0.5 l/m and 5 l/m. Each time the desired flow value was set, data were taken for about 150 seconds. Then the flow was abruptly cut to zero, again taking data for about 150 seconds. A new flow rate was then set and this "stop/flow" procedure was repeated a total of 10 times. This same sequence was repeated for quadrants 2 (scrubbed), 3 (un-scrubbed) and 4 (scrubbed). The difference in counts where the flow was abruptly cut to zero flow was calculated, then plotted as a function of flow rate. These data revealed that the two scrubbed quadrants were virtually identical, and the two un-scrubbed quadrants were as well. However, the scrubbed data plots differed substantially from the un-scrubbed data plots. These data are summarized in the figure below, including their quadratic fits.

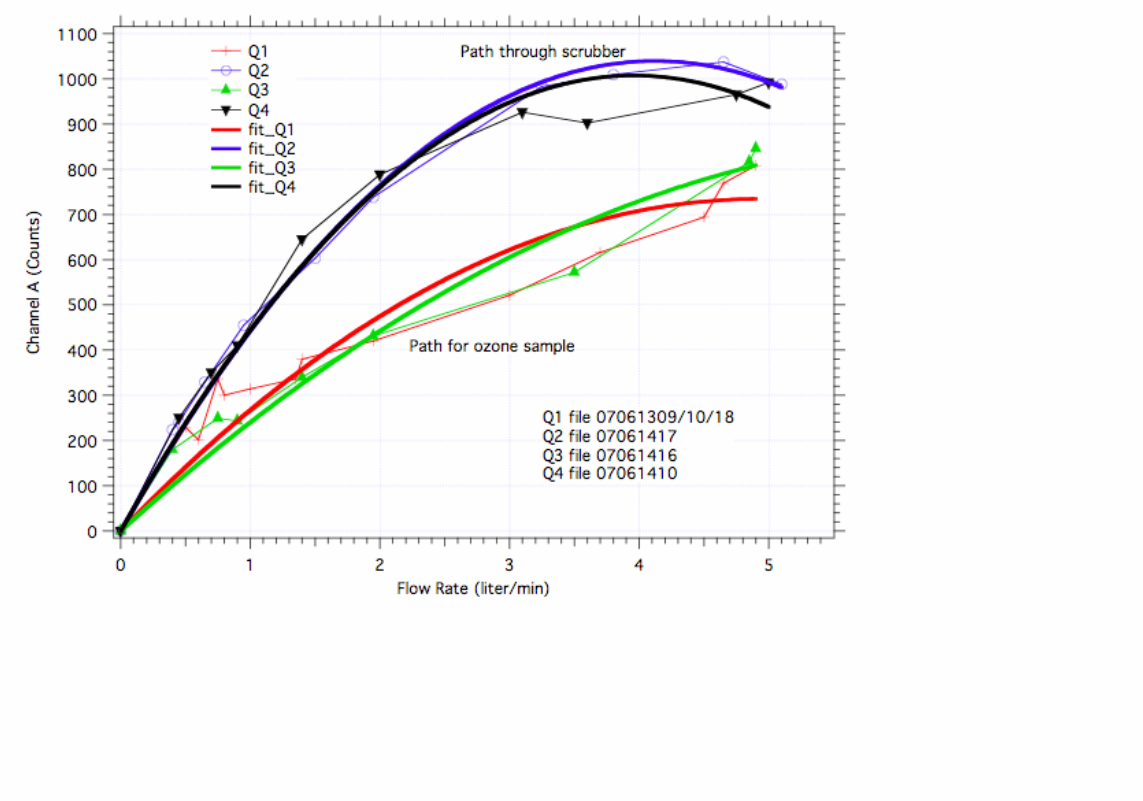

20 New England Business Center Andover, MA 01810-1077 t 978.689.0003 f 978.689.3232
www.psicorp.com

The data for quadrants 2,3, and 4 in the figure are taken with a chamber temperature of 29.3 C. Quadrant 1 tests were run again 8 hours later to confirm their consistency, once at 29.3 C and the other was at 30.5 C. The two sets for quadrant 1 were found to be mutually consistent, and all of these data points are included in the figure. The differences between the scrubbed and the un-scrubbed data demonstrate how strongly the counts are affected by flow asymmetry. The plot shows how positive, negative and zero offsets can result from various conditions. First consider that the flow rate is constant for the scrubbed and un-scrubbed mode. Then the un-scrubbed signal will be somewhat greater than the scrubbed, producing a substantial positive offset. Now consider where the flow rates are very different, with the scrubbed flow 0.5 l/m and the un-scrubbed flow rate 2 l/m. This changes the offset to negative since the un-scrubbed counts are higher than the scrubbed. And finally, if the un-scrubbed is 2 l/m and the scrubbed is 1 l/m, the offset observed would be near zero, since the count increases are nearly the same.

Clearly, these curves will differ between instruments. As demonstrated in this figure, the differences in the curves will depend strongly upon the relative flow restrictions in the two flow paths. However, they should be nearly identical if their flow paths are also nearly identical, just as the curves for the scrubbed and un-scrubbed quadrant pairs are nearly identical. It seems reasonable that the curves will also change with various temperature scenarios, however confirmation will be difficult before the flow rate ratio is corrected from 2 or 3 in the current instrument design, to near 1 and the temperature of the scrubbed air is better controlled. It also may be that the curves for chamber B will be different from chamber A, since chamber A is nearer the lamp heat source.

PI received new information from PSI on July 5, 2007 that detailed some of their findings regarding the offsets. The document is titled “WTR Notes from HIAPER Ozone Instrument Bench Testing and Intercomparisons-May-June 2007” and will accompany the instrument delivery. This document provides some additional information that is useful in evaluation of the instrument. PSI has come to different conclusions than PI regarding the cause of the offsets that should be considered. PI is particularly interested in the intercomparisons provided in this report, as it presents evidence that the HIAPER instrument showed substantial offsets not found in #1 and another ground-based instrument built by PSI. Considering our analysis above, and that #1 is practically identical to #2 and #3, the lack of large effects in #1 is a mystery. It may be solved by identifying a fortuitous combination of factors present in that instrument resulting in one of the many possible zero offset flow conditions discussed above.

In July 2006, PI discovered that the detector boards had a time response of 2 to 3 seconds. We found that capacitors on the input amplifier were not the original design value. After replacing these capacitors, the time response became less than 1 second.

Additional tests on #3 revealed that the instrument temperature was not controlled as well as expected from manufacturer specifications. This creates changes in the offset values that are correlated with the temperature controller cycling. The present controller must be replaced and PI is currently exploring alternate controllers.
July 7, 2007

20 New England Business Center Andover, MA 01810-1077 t 978.689.0003 f 978.689.3232
www.psicorp.com

Appendix D

QBASIC Output Subroutines, psi-irig.exe

D.1 Output to Video Monitor Screen

```
SUB WRITETOSCREEN
      PRINT "IRIG Time"' = (hh:mm:ss:ms)"
      PRINT "hh:mm:ss.ms"
      PRINT USING "##:##:##.###"; HH; MM; SS + MS / 1000!
      PRINT ""
      PRINT "COUNTER A", freqa&, DELTAFREQA&, "TIME =",
      PRINT USING "######.#"; ENDTIME# - STARTTIME#
      PRINT "COUNTER B", freqb&, DELTAFREQB&, "CYCLE NO. =", cycleno#
      PRINT "RATIO A/B ",
      PRINT USING "###.######"; FREQRATIO#; PREVRATIO# - FREQRATIO#
      PRINT "CHAMBER TEMPS         ",
      PRINT USING "#####.##"; TEMPERATURE#(1); TEMPERATURE#(2);
TEMPERATURE#(3); TEMPERATURE#(4)
      PRINT "LAMP, DET, SCRUB",
      PRINT USING "#####.##"; TEMPERATURE#(5); TEMPERATURE#(6);
TEMPERATURE#(7)
      PRINT "FAN, PS PANEL, BOX, PROC",
      PRINT USING "#####.##"; TEMPERATURE#(8); TEMPERATURE#(9);
TEMPERATURE#(10); TEMPERATURE#(11)
      PRINT "5V REF, 5V PS, 5V PC, +12V",
      PRINT USING "#####.##"; VOLTAGE#(1); VOLTAGE#(2); VOLTAGE#(9);
VOLTAGE#(8)
      PRINT "+24V, -24V, +28V, 28V I",
      PRINT USING "#####.##"; VOLTAGE#(4); VOLTAGE#(5); VOLTAGE#(3);
CURRENT#(1)
      PRINT "DELTA PRES, ATMOS PRES",
      PRINT USING "#####.##"; PRESSURE#(1); PRESSURE#(2)
      CALL FINETIMER
      PCTTIME% = 100 * MICSECS# / 1000000
      IF PCTEXPIRED% > MAXPCT% THEN MAXPCT% = PCTEXPIRED%
      PRINT "VALVEQUAD%, EXPECTQUAD%, SKIPS, STOPS) ";
      PRINT USING "#######"; VALVEQUADRANT%; EXPECTQUADRANT%; VALVESKIPPED%;
VALVESTOPPED%
      'PRINT USING "#######"; VALVEPOS%; EXPECTQUADRANT%; VALVESKIPPED%;
VALVESTOPPED%
      PRINT USING "###.#"; PCTTIME%;
      PRINT "%  OF 1 SECOND TIME WAS USED: MAX USED WAS";
      PRINT USING "###.#"; MAXPCT%;
      PRINT "%"
END SUB
```


20 New England Business Center Andover, MA 01810-1077 t 978.689.0003 f 978.689.3232
www.psicorp.com

D.2 Output to Hard Drive (**C:/DATA**)

```
SUB WRITETODISK

      'date, time, cycle number
      PRINT #1, ""
      PRINT #1, DATE$, TIME$, cycleno#

      'IRIG time
      PRINT #1, USING "##:##:##.###"; HH; MM; SS + MS / 1000!

      'Delta P, Cell P (mbar)
      PRINT #1, USING "#####.##"; PRESSURE#(1); PRESSURE#(2)

      'counts/s Channel A, Channel B
      PRINT #1, USING "########"; freqa&; freqb&

      'Air flow temperatures (C), A Inlet, B Inlet, A Outlet, B Outlet
      PRINT #1, USING "####.##"; TEMPERATURE#(1); TEMPERATURE#(2);
TEMPERATURE#(3); TEMPERATURE#(4);

'housekeeping data every 5 seconds
IF cycleno# MOD 10 = 0 OR cycleno# MOD 10 = 5 THEN
       'Temperatures:  lamp end, detector end, cell body
       PRINT #1, USING "####.##"; TEMPERATURE#(5); TEMPERATURE#(6);
TEMPERATURE#(7);

       'fan, power supply panel, box, processor
       PRINT #1, USING "####.##"; TEMPERATURE#(8); TEMPERATURE#(9);
TEMPERATURE#(10); TEMPERATURE#(11)

       'Voltages:  5V ref, 5V supply, 28V, +24V, -24V, vacant, vacant,
       '    +12V, 5V for PC104
       PRINT #1, USING "####.##"; VOLTAGE#(1); VOLTAGE#(2); VOLTAGE#(3);
VOLTAGE#(4); VOLTAGE#(5); VOLTAGE#(6); VOLTAGE#(7); VOLTAGE#(8); VOLTAGE#(9)

       'Total 28V current (mA)
       PRINT #1, USING "#####"; CURRENT#(1);

       'Valve quadrant, expected quadrant, skips, stops
       PRINT #1, USING "#######"; VALVEQUADRANT%; EXPECTQUADRANT%;
VALVESKIPPED%; VALVESTOPPED%
       CALL FINETIMER
       PCTEXPIRED% = 100 * MICSECS# / 1000000

       '% time used for each second of data recording
       PRINT #1, USING "###.#"; PCTEXPIRED%
END IF
END SUB
```


20 New England Business Center Andover, MA 01810-1077 t 978.689.0003 f 978.689.3232
www.psicorp.com

D.3 Output to Serial Port (RS232)

```
SUB WRITETOSERIAL

        'date, time, cycle number
        PRINT #2, DATE$, TIME$, cycleno#

        'IRIG time
        PRINT #2, USING "##:##:##.###"; HH; MM; SS + MS / 1000!

        'counts/s channel A, channel B
        PRINT #2, USING "########"; freqa&; freqb&;

        'delta-P, cell pressure (mbar)
        PRINT #2, USING "#####.##"; PRESSURE#(1); PRESSURE#(2);

        'Temperatures (C):  Air flow A inlet, B inlet, A outlet, B outlet
        'lamp end, detector end, cell body
        'fan, power supply panel, box, processor
        PRINT #2, USING "####.##"; TEMPERATURE#(1); TEMPERATURE#(2);
TEMPERATURE#(3); TEMPERATURE#(4);
        PRINT #2, USING "####.##"; TEMPERATURE#(5); TEMPERATURE#(6);
TEMPERATURE#(7);
        PRINT #2, USING "####.##"; TEMPERATURE#(8); TEMPERATURE#(9);
TEMPERATURE#(10); TEMPERATURE#(11);

        'Voltages:  5V Ref, 5V PS, 5V PC, +12V
        '+24V, -24V, +28V
        PRINT #2, USING "####.##"; VOLTAGE#(1); VOLTAGE#(2); VOLTAGE#(9);
VOLTAGE#(8);
        PRINT #2, USING "####.##"; VOLTAGE#(4); VOLTAGE#(5); VOLTAGE#(3)

        'Total 28V current (mA)
        PRINT #2, USING "#####"; CURRENT#(1)

        'valve flag (0 or 1), valve quadrant, expected quadrant, skips, stops
        PRINT #2, USING "#######"; VALVEPOS%; VALVEQUADRANT%; EXPECTQUADRANT%;
VALVESKIPPED%; VALVESTOPPED%

END SUB
```


20 New England Business Center Andover, MA 01810-1077 t 978.689.0003 f 978.689.3232
www.psicorp.com

20 New England Business Center Andover, MA 01810-1077 *t* 978.689.0003 *f* 978.689.3232
www.psicorp.com

Appendix E

C++ Algorithm for Ozone Mixing Ratio Determination

The following is a listing of selected portions of the "**O3BATCHPRO**" C++ code relevant to the calculation of O_3 mixing ratios from the data generated by **psi-irig.exe**. The mixing ratios are determined from both dual-channel (ratiometric) and single-channel analyses, using a 5-point linear segment fitting method to detrend time drifts in the signal levels and A/B ratio values. The dual-channel algorithm is also used in the real-time "**TELEMETRY**" code.

The flow switching valve interchanges the ozone-laden and ozone-free flows every 10 seconds. The valve transition point for each 10-second period is defined to be $x = 1$, counter value *IPTR*. The raw data for points 1 and 2 are corrupted by the valve transition; values for these points are interpolated in the dual-channel analysis and are omitted in the single-channel analysis. The linear segment fitting algorithm uses linear least squares fits to points 5 through 10 of the previous 10-second period and points 3 through 7 of the current period. In the algorithm, points 5 to 10 of the previous period, which are plotted to the left of the valve switching point in a plot vs. time, are numbered $x = 2$ *to* 6 from right to left, while points 3 through 7 of the current period are numbered $x = 3$ *to* 7 from left to right. The general linear least squares equations for N points with slope m and intercept b are:

$$y = mx + b$$

$$m = (N\Sigma xy - \Sigma x\Sigma y)/(N\Sigma x^2 - (\Sigma x)^2)$$

$$b = (\Sigma y\Sigma x^2 - \Sigma x\Sigma xy)/(N\Sigma x^2 - (\Sigma x)^2)$$

For the forward marching fit (to the right of the valve change), $x = 3$ *to* 7, the fitting parameters are $N = 5$, $\Sigma x = 25$, $\Sigma x^2 = 135$, *and* $(N\Sigma x^2 - (\Sigma x)^2) = 50$. For the backward marching fit (to the left of the valve change), $x = 2$ *to* 6, the fitting parameters are $N = 5$, $\Sigma x = 20$, $\Sigma x^2 = 90$, *and* $(N\Sigma x^2 - (\Sigma x)^2) = 50$. The analysis determines the value of the response parameter F_{CAL} at each valve transition point, i.e. every 10 seconds. The values of $F_{CAL}(i)$ at each 1-second point are linearly interpolated from the adjacent 10-second values. The absorbance and/or ozone mixing ratio at each point is then determined from $F_{CAL}(i)/\{value\}(A,i)$ (Channel A in sample mode), or $\{value\}(B,i)/F_{CAL}(i)$ (Channel B in sample mode), where *{value}* represents either the A/B ratio or the single-channel A or B signal. The sample mode is determined from the value of *ValveFlag*, which is 0 for A-sample and 1 for B-sample. In the single-channel algorithm, the variable name "*fcal*" is replaced by "*fzero*".

```
#define IP6       IPTR+6
#define IP5       IPTR+5
#define IP4       IPTR+4
#define IP3       IPTR+3
#define IP2       IPTR+2
#define IP1       IPTR+1
```


20 New England Business Center □ Andover, MA 01810-1077 □ t 978.689.0003 f 978.689.3232
www.psicorp.com

```
#define IM1       IPTR-1
#define IM2       IPTR-2
#define IM3       IPTR-3
#define IM4       IPTR-4
#define IM5       IPTR-5

#define SIGMA     1.147e-17       //absorption cross section in cm2
#define PATH      20              //optical path length in cm
#define ACONST    1.3802E-10      //conversion to mixing ratio in ppbv

NaN = 99999.0;               //signifies no data value for this point

      cycle[ptr] = cyclenum;
      ratio[ptr] = (float)countsA / (float)countsB;
      counta[ptr] = countsA;
      countb[ptr] = countsB;
      tempA[ptr] = (tinA+toutA)/2. + 273.15;
      tempB[ptr] = (tinB+toutB)/2. + 273.15;
      totalpressure[ptr] = totpress;  //cell pressure in mbar


......

//ratiometric dual channel analysis:  loop on IPTR

sumYright = ratio[IP2] + ratio[IP3] + ratio[IP4] + ratio[IP5] + ratio[IP6];
sumXYright = 3.0*ratio[IP2] + 4.0*ratio[IP3] + 5.0*ratio[IP4] +
6.0*ratio[IP5] + 7.0*ratio[IP6];
sloperight = (5.0*sumXYright-25.0*sumYright)/50.0;
interceptright = (135.0*sumYright-25.0*sumXYright)/50.0;


sumYleft = ratio[IM1] + ratio[IM2] + ratio[IM3] + ratio[IM4] + ratio[IM5];
sumXYleft = 2.0*ratio[IM1] + 3.0*ratio[IM2] + 4.0*ratio[IM3] + 5.0*ratio[IM4]
+ 6.0*ratio[IM5];
slopeleft = (5.0*sumXYleft-20.0*sumYleft)/50.0;
interceptleft = (90.0*sumYleft-20.0*sumXYleft)/50.0;

fcalright = sloperight+interceptright;
fcalleft = slopeleft+interceptleft;

if (fcalright<0)
      fcalright = 1.0;

if (fcalleft<0)
      fcalleft = 1.0;

fcal[IPTR] = sqrt(fcalright * fcalleft);
ratio[IPTR] = fcalright;
ratio[IP1] = fcalright + sloperight;

//interpolate to find 1-second fcal values
```


20 New England Business Center Andover, MA 01810-1077 t 978.689.0003 f 978.689.3232
www.psicorp.com

```
for (i=1; i<IPTR; i++)
      fcal[i] = ((IPTR-i)*fcal[0] + i*fcal[IPTR]) / IPTR;

//Single Channel Analysis:
//find the FZero (fcal) values for each individual channel

if (ValveFlag==0) {                          //Channel A
      sumYright = counta[IP2] + counta[IP3] + counta[IP4] + counta[IP5] +
counta[IP6];
      sumXYright = 3.0*counta[IP2] + 4.0*counta[IP3] + 5.0*counta[IP4] +
6.0*counta[IP5] + 7.0*counta[IP6];

      sumYleft = countb[IM1] + countb[IM2] + countb[IM3] + countb[IM4] +
countb[IM5];
      sumXYleft = 2.0*countb[IM1] + 3.0*countb[IM2] + 4.0*countb[IM3] +
5.0*countb[IM4] + 6.0*countb[IM5];

      slopeleft = (5.0*sumXYleft-20.0*sumYleft)/50.0;
      interceptleft = (90.0*sumYleft-20.0*sumXYleft)/50.0;

      sloperight = (5.0*sumXYright-25.0*sumYright)/50.0;
      interceptright = (135.0*sumYright-25.0*sumXYright)/50.0;

      fzeroa[IPTR] = sloperight+interceptright;
      fzerob[IPTR] = slopeleft+interceptleft;

      fzeroa[IP1] = 2*sloperight+interceptright;

}
else {                                       //Channel B
      sumYright = countb[IP2] + countb[IP3] + countb[IP4] + countb[IP5] +
countb[IP6];
      sumXYright = 3.0*countb[IP2] + 4.0*countb[IP3] + 5.0*countb[IP4] +
6.0*countb[IP5] + 7.0*countb[IP6];

      sumYleft = counta[IM1] + counta[IM2] + counta[IM3] + counta[IM4] +
counta[IM5];
      sumXYleft = 2.0*counta[IM1] + 3.0*counta[IM2] + 4.0*counta[IM3] +
5.0*counta[IM4] + 6.0*counta[IM5];

      slopeleft = (5.0*sumXYleft-20.0*sumYleft)/50.0;
      interceptleft = (90.0*sumYleft-20.0*sumXYleft)/50.0;

      sloperight = (5.0*sumXYright-25.0*sumYright)/50.0;
      interceptright = (135.0*sumYright-25.0*sumXYright)/50.0;

      fzeroa[IPTR] = slopeleft+interceptleft;
      fzerob[IPTR] = sloperight+interceptright;

      fzerob[IP1] = 2*sloperight+interceptright;

}

//Interpolate to find 1-second fzero values
```


20 New England Business Center Andover, MA 01810-1077 t 978.689.0003 f 978.689.3232
www.psicorp.com

```
for (i=1; i<IPTR; i++) {

      if (ValveFlag==0)
            fzeroa[i] = ((IPTR-i)*fzeroa[0] + i*fzeroa[IPTR]) / IPTR;
      else
            fzerob[i] = ((IPTR-i)*fzerob[0] + i*fzerob[IPTR]) / IPTR;
}
;
for (i=0; i<IPTR; i++) {
      if (ValveFlag==0) {
            tcell[i] = tempA[i];

            //dual-channel absorbance, A sample:
            absorp[i] = log(fcal[i]/ratio[i]);

            //single-channel mixing ratio, Channel A:
            ppbva[i] =
log(fzeroa[i]/counta[i])*6.0166e5*tcell[i]/totalpressure[i];
            ppbvb[i] = NaN;
      }
      else {
            tcell[i] = tempB[i];

            //dual-channel absorbance, B sample:
            absorp[i] = log(ratio[i]/fcal[i]);

            //single-channel mixing ratio, Channel B:
            ppbva[i] = NaN;
            ppbvb[i] =
log(fzerob[i]/countb[i])*6.0166e5*tcell[i]/totalpressure[i];
      }

//single-channel analysis:  no value for first two array points
      if (i <= 1) {
            ppbva[i] = NaN;
            ppbvb[i] = NaN;
      }

//ratiometric 1-Hz ozone concentrations and mixing ratios:
      concentration[i] = absorp[i]/SIGMA/PATH;
      ppbv[i] = ACONST*concentration[i] * tcell[i]/totalpressure[i];
}
```


20 New England Business Center Andover, MA 01810-1077 t 978.689.0003 f 978.689.3232
www.psicorp.com

Appendix F

Example Pages for "TELEMETRY" Graphical User Interface

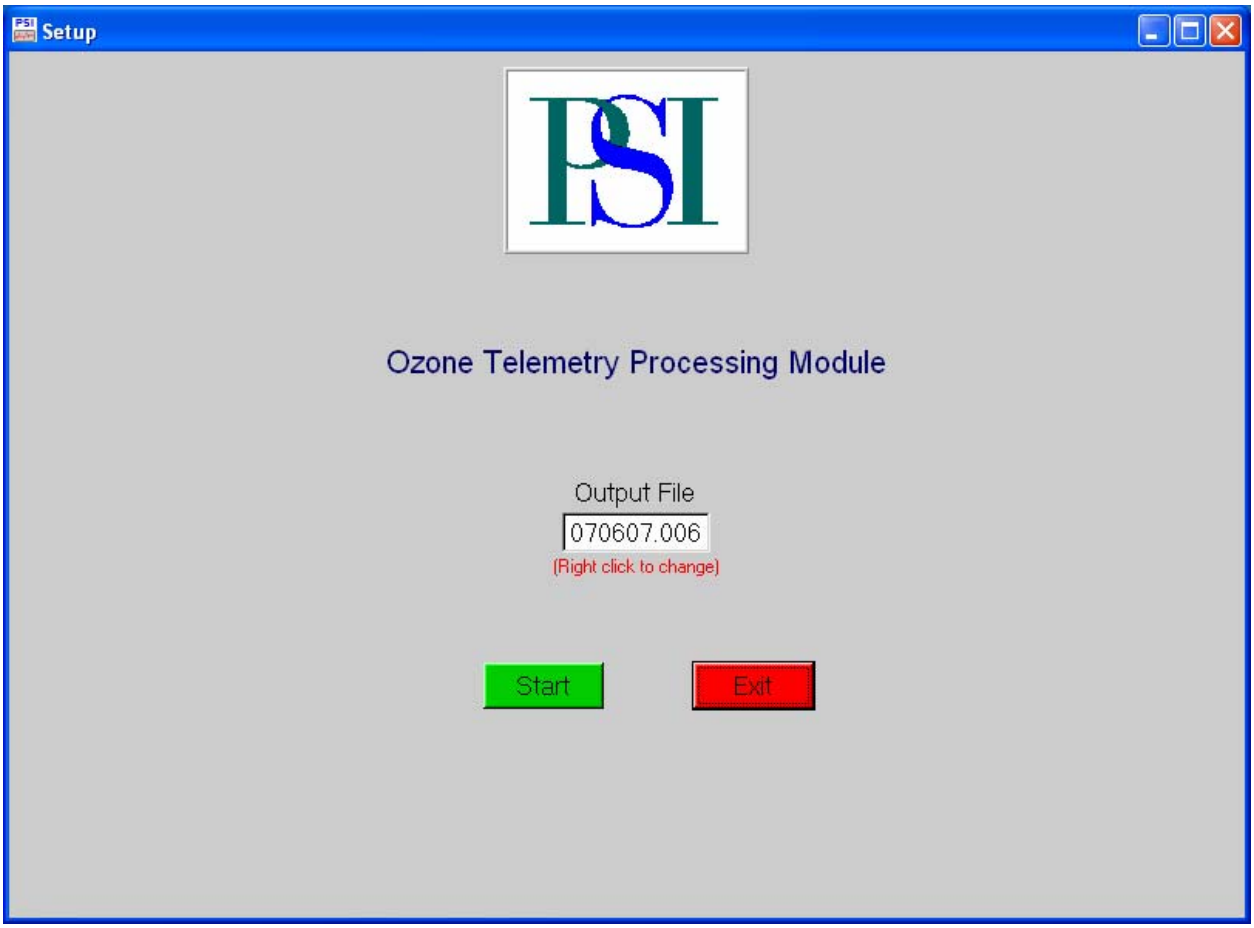

F-1. **TELEMETRY** Setup Page: set up file names and folders.

20 New England Business Center □ Andover, MA 01810-1077 □ *t* 978.689.0003 *f* 978.689.3232
www.psicorp.com

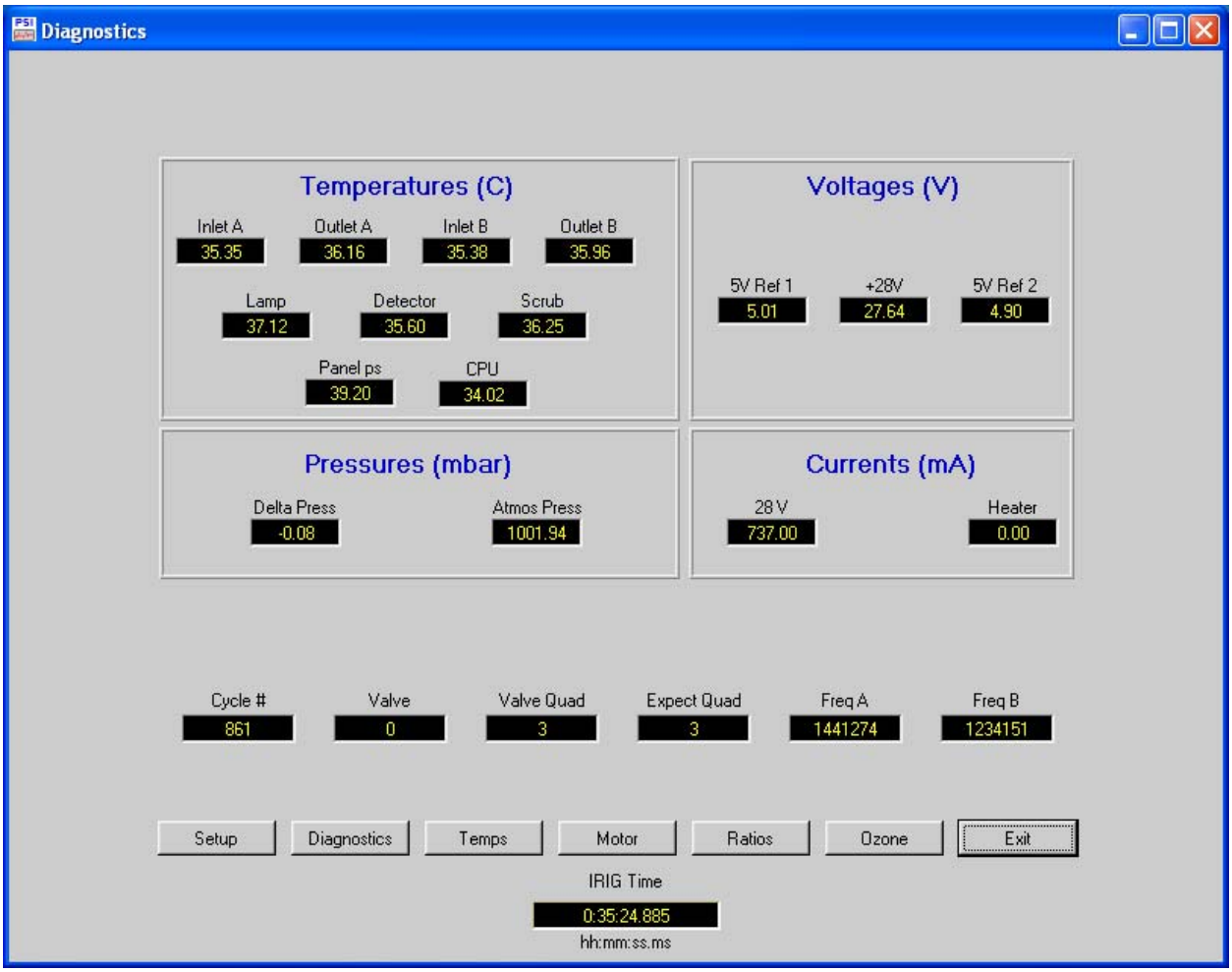

F-2. **TELEMETRY** Diagnostics Page: housekeeping data display (real time).

20 New England Business Center □ Andover, MA 01810-1077 □ *t* 978.689.0003 *f* 978.689.3232
www.psicorp.com

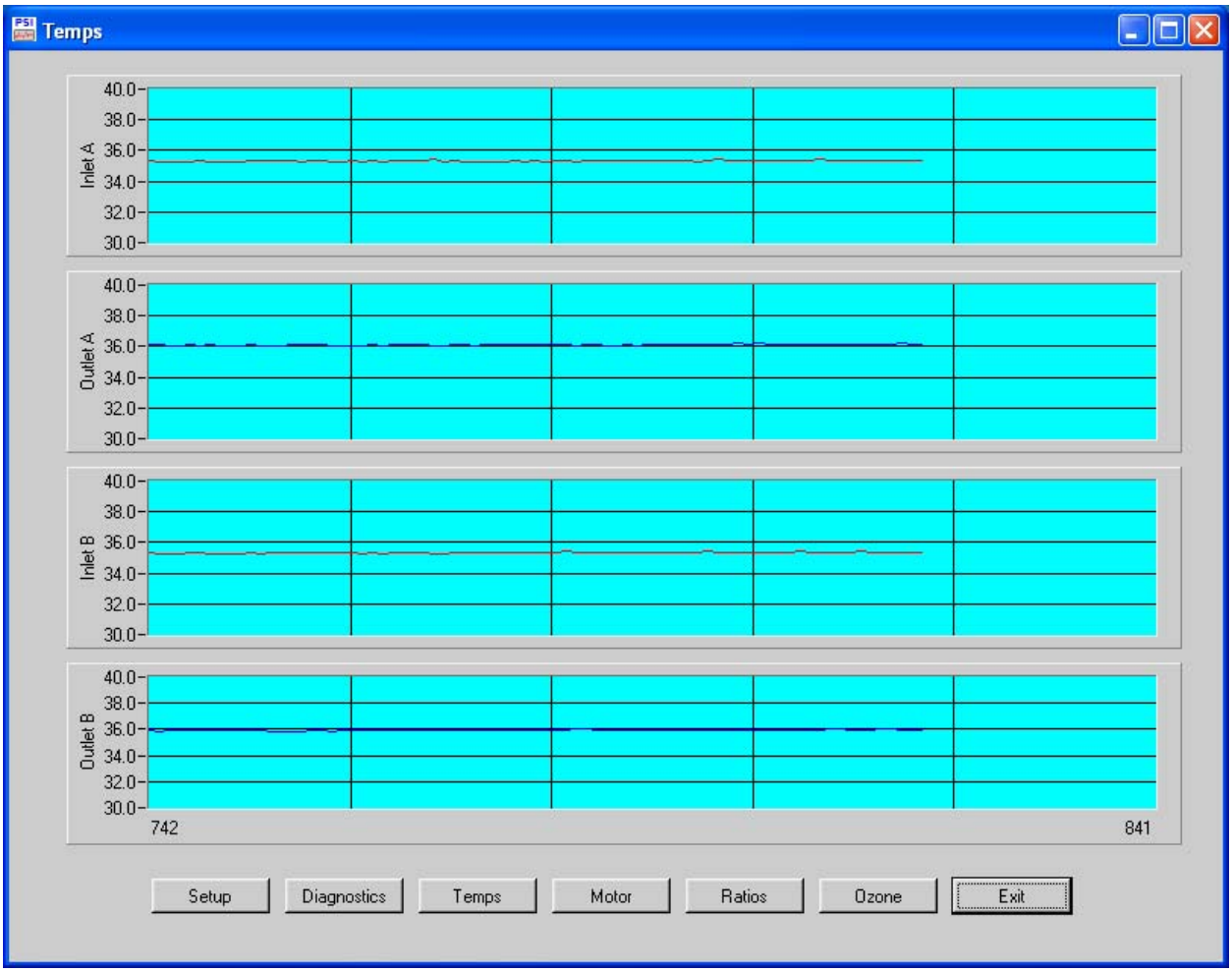

F-3. **TELEMETRY** Temperature Plots: sample air inlet and outlet temperatures for Channels A and B (real time)

20 New England Business Center □ Andover, MA 01810-1077 □ *t* 978.689.0003 *f* 978.689.3232
www.psicorp.com

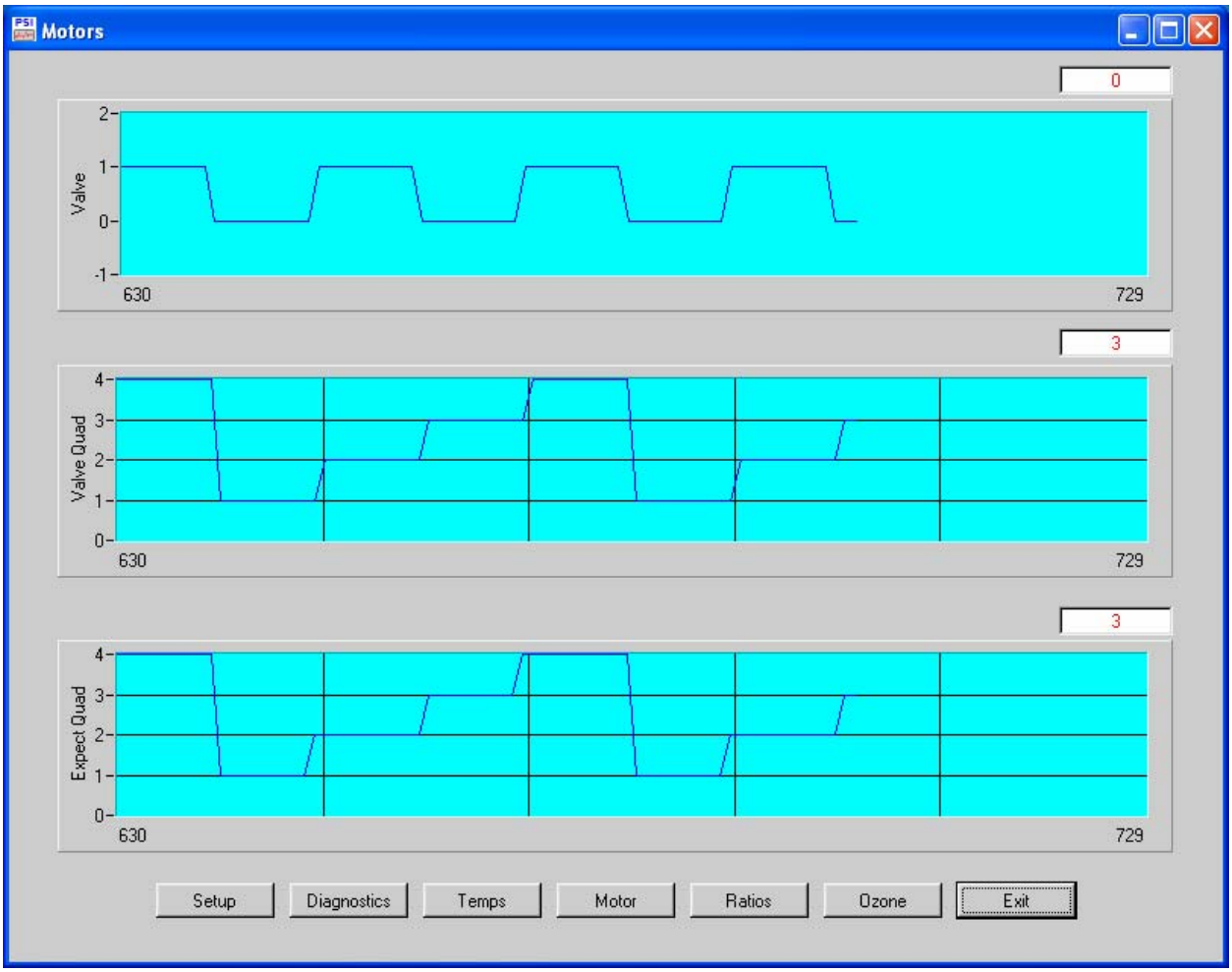

F-4. **TELEMETRY** "Motor" Plots: valve rotation data (real time).

20 New England Business Center □ Andover, MA 01810-1077 □ *t* 978.689.0003 *f* 978.689.3232
www.psicorp.com

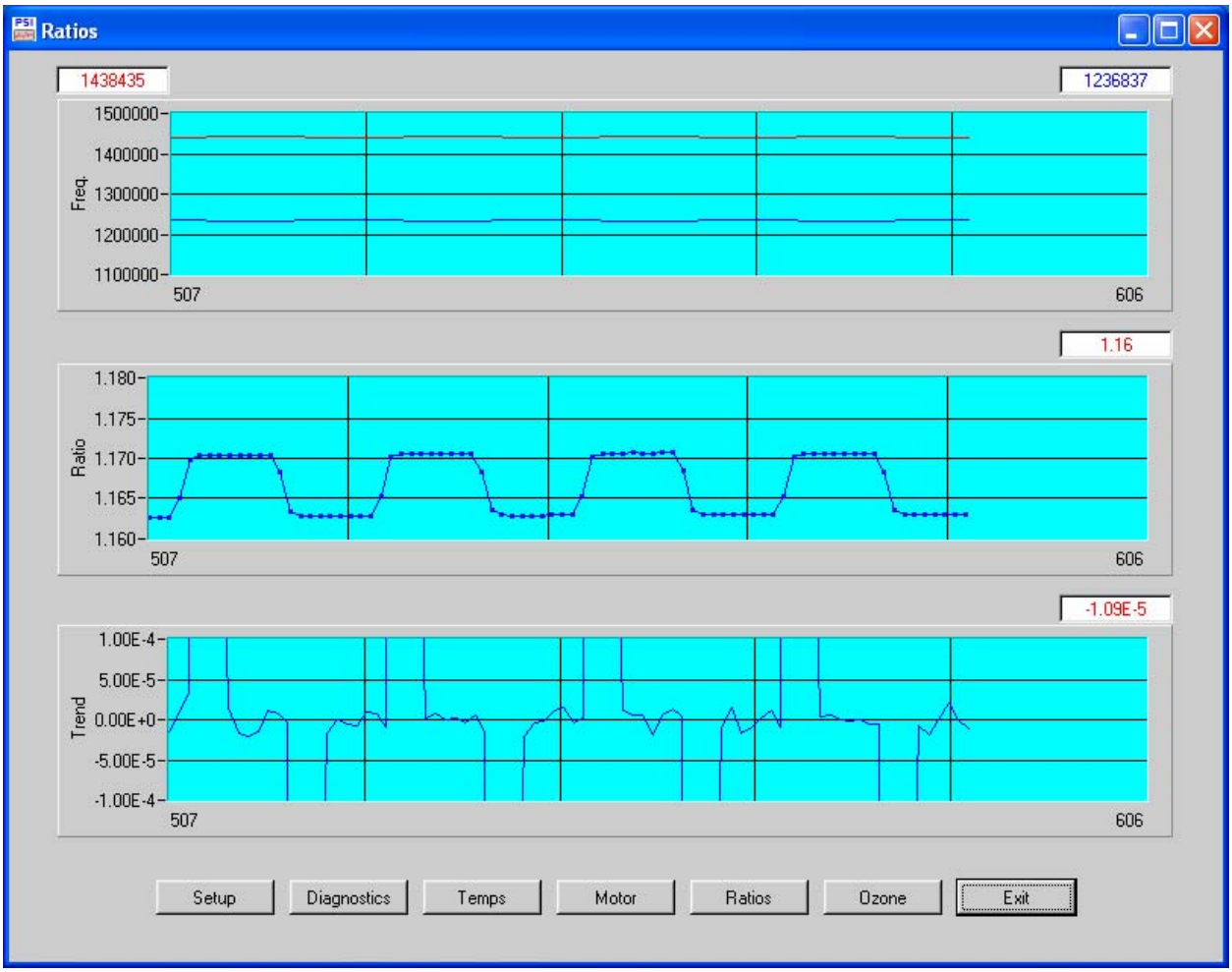

F-5. **TELEMETRY** "Ratio" Plots: photometer signals, signal ratios, and running derivative of ratios ("Trend") (real time).

20 New England Business Center □ Andover, MA 01810-1077 □ *t* 978.689.0003 *f* 978.689.3232
www.psicorp.com

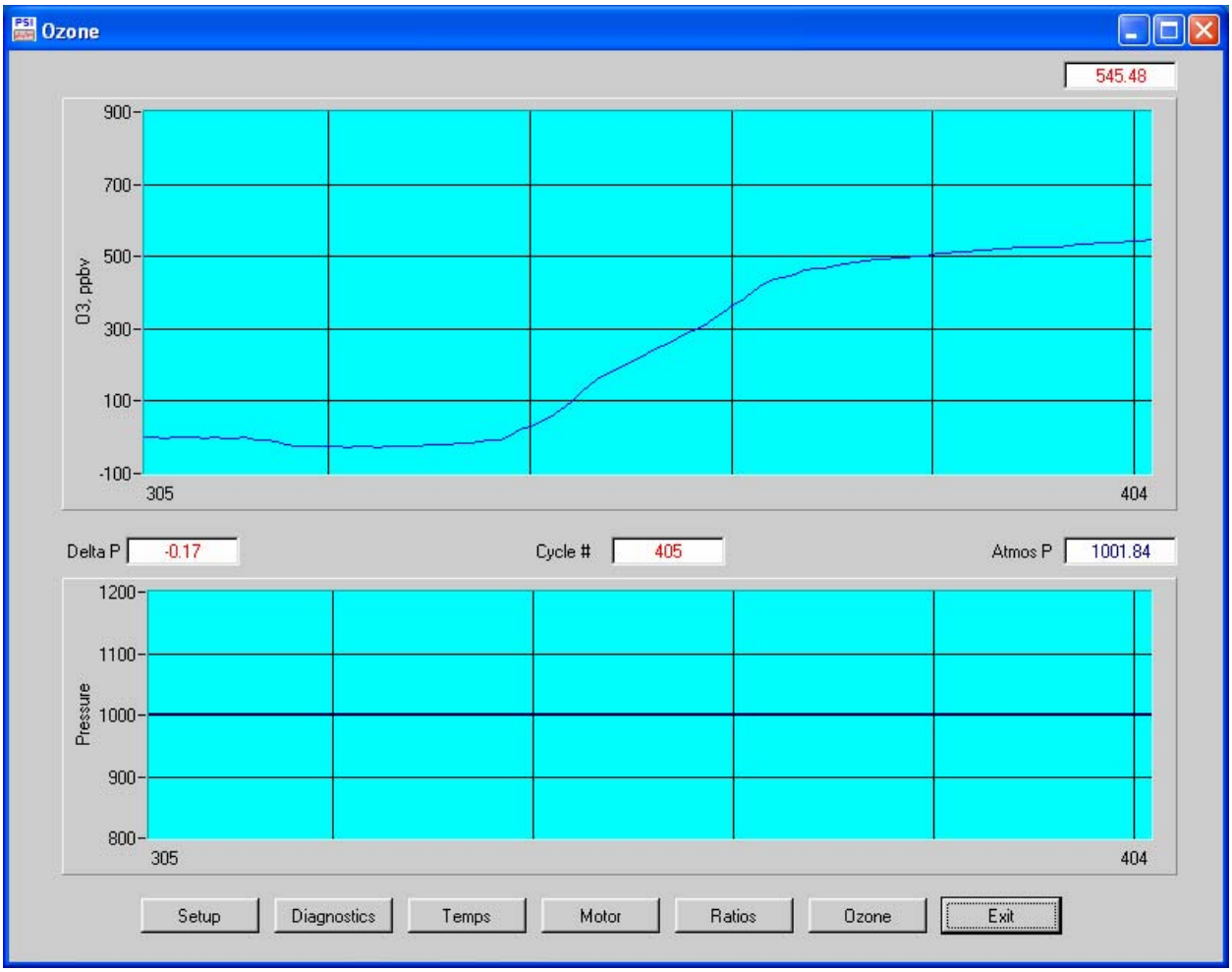

F-6. **TELEMETRY** "Ozone" Plots: 1-Hz dual-beam ozone mixing ratio (upper plot), pressure and differential pressure (lower plot) (20 seconds behind real time).

20 New England Business Center Andover, MA 01810-1077 *t* 978.689.0003 *f* 978.689.3232
www.psicorp.com

Appendix G

Example Pages for "BATCH" Graphical User Interface

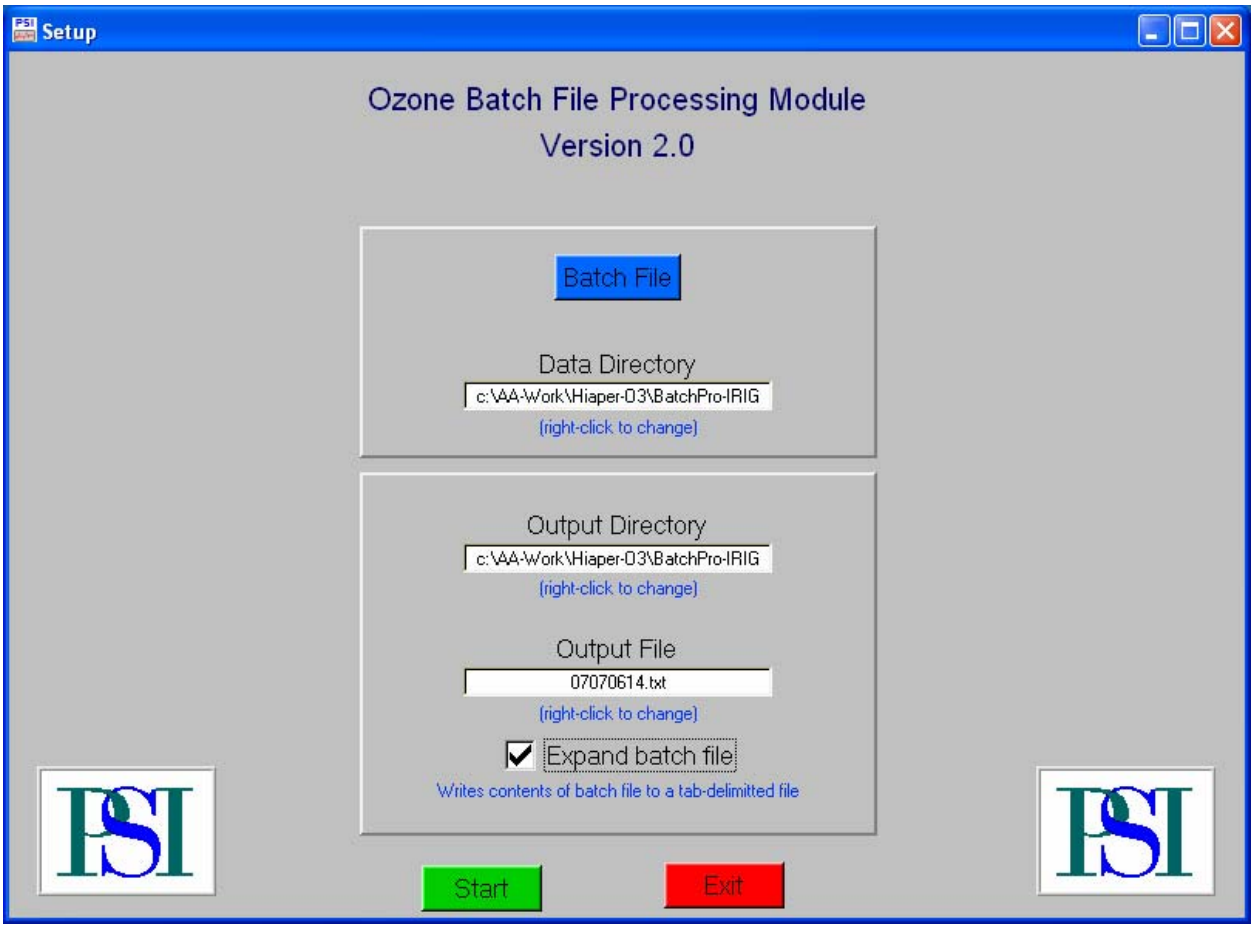

G-1. **BATCH** Setup Page: set up file names and folders.

20 New England Business Center □ Andover, MA 01810-1077 □ *t* 978.689.0003 *f* 978.689.3232
www.psicorp.com

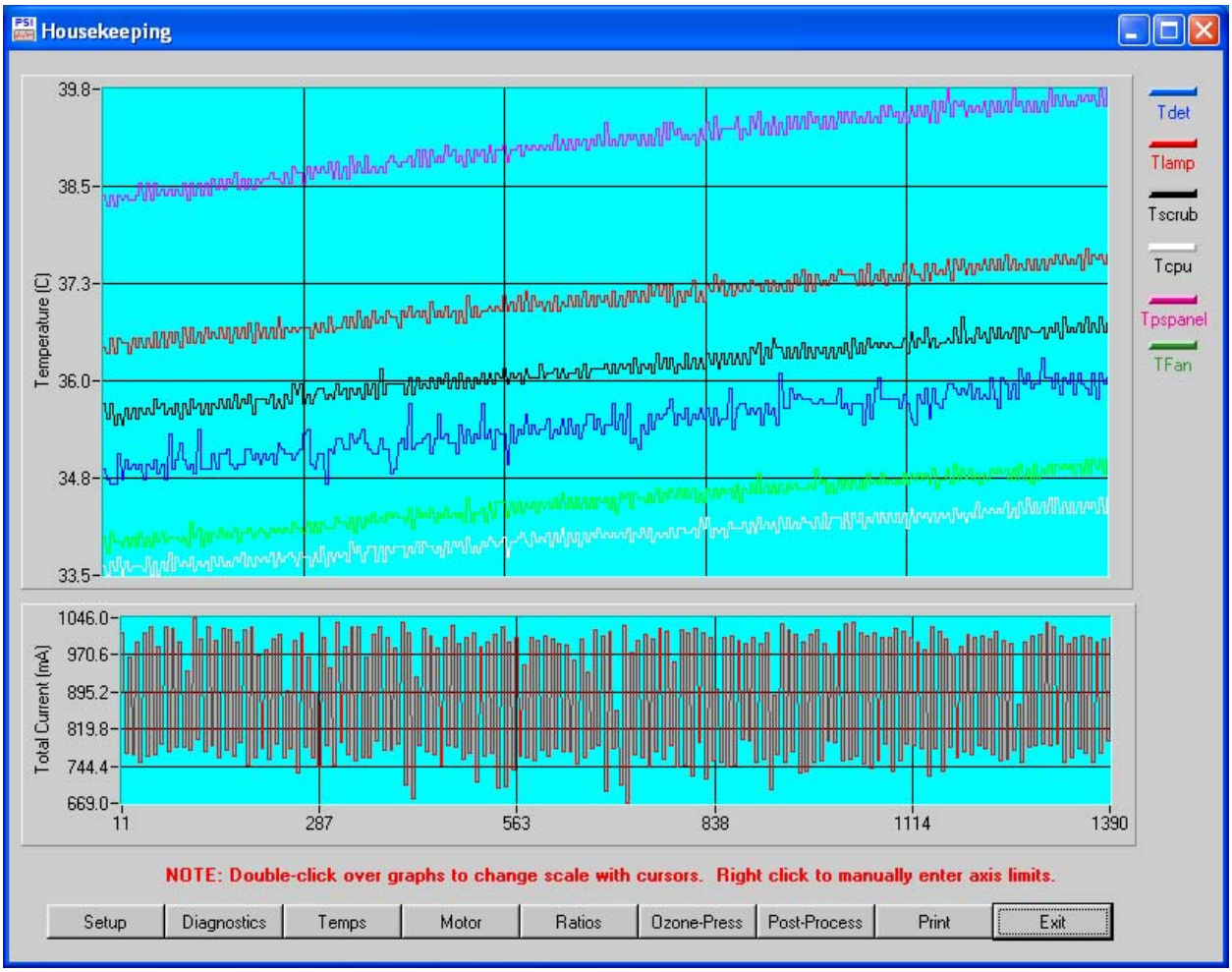

G-2. **BATCH** Diagnostics Plots: housekeeping temperatures and total current.

20 New England Business Center □ Andover, MA 01810-1077 □ *t* 978.689.0003 *f* 978.689.3232
www.psicorp.com

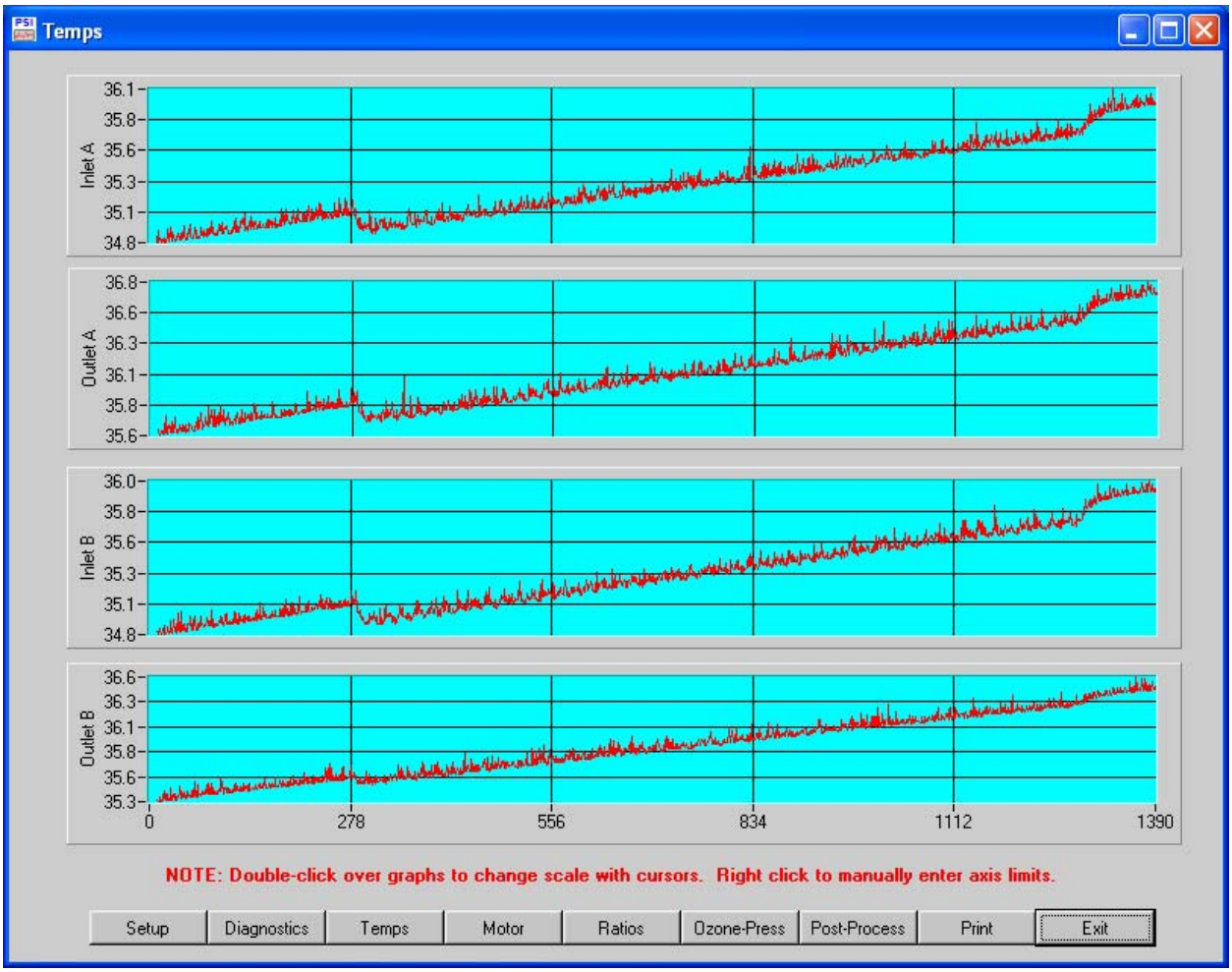

G-3. **BATCH** Temperature Plots: sample air inlet and outlet temperatures for Channels A and B.

20 New England Business Center □ Andover, MA 01810-1077 □ *t* 978.689.0003 *f* 978.689.3232
www.psicorp.com

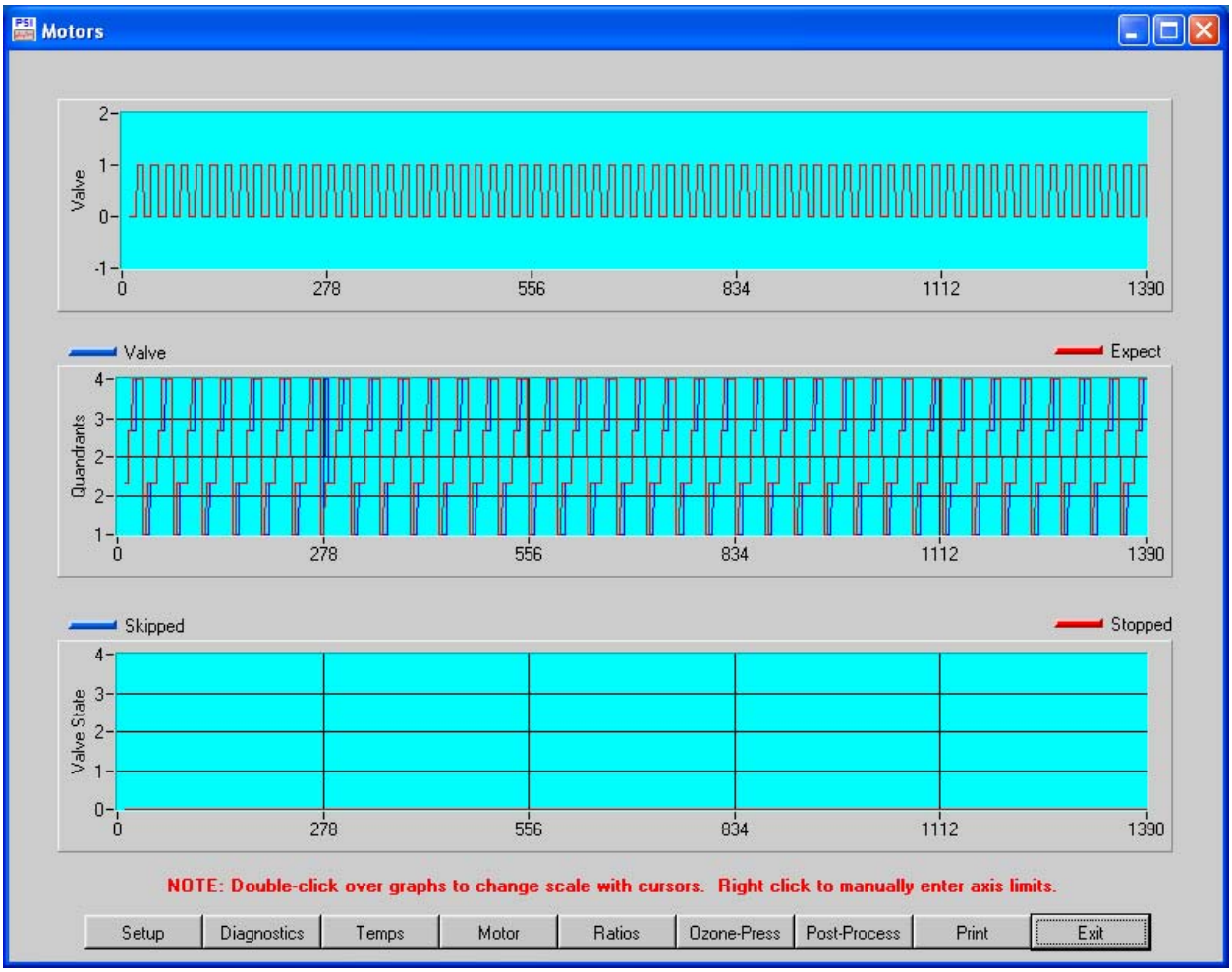

G-4. **BATCH** "Motor" Plots: valve rotation data.

20 New England Business Center □ Andover, MA 01810-1077 □ *t* 978.689.0003 *f* 978.689.3232
www.psicorp.com

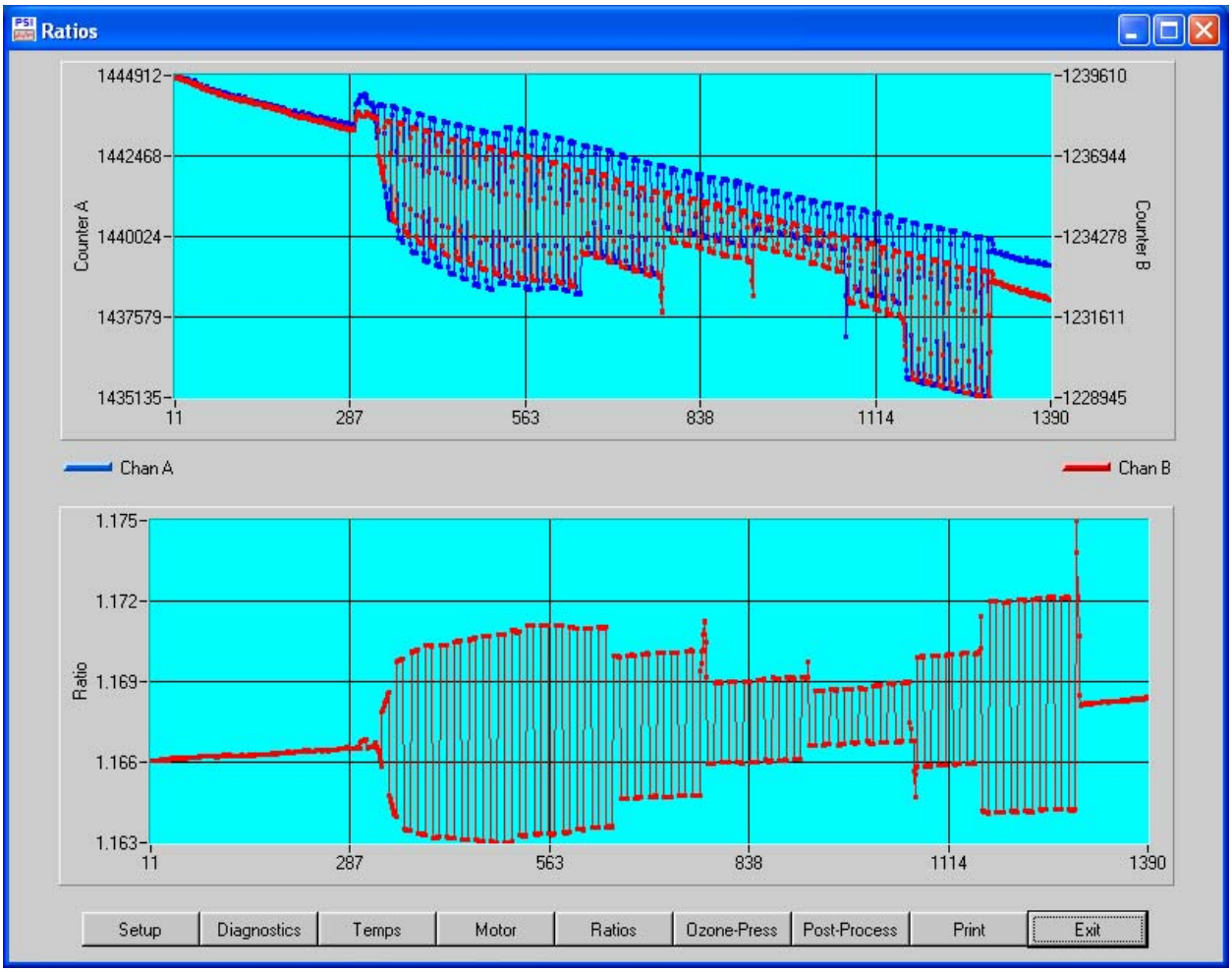

G-5. **BATCH** "Ratio" Plots: single-channel signals (upper plot) and A/B ratios (lower plot).

20 New England Business Center □ Andover, MA 01810-1077 □ *t* 978.689.0003 *f* 978.689.3232
www.psicorp.com

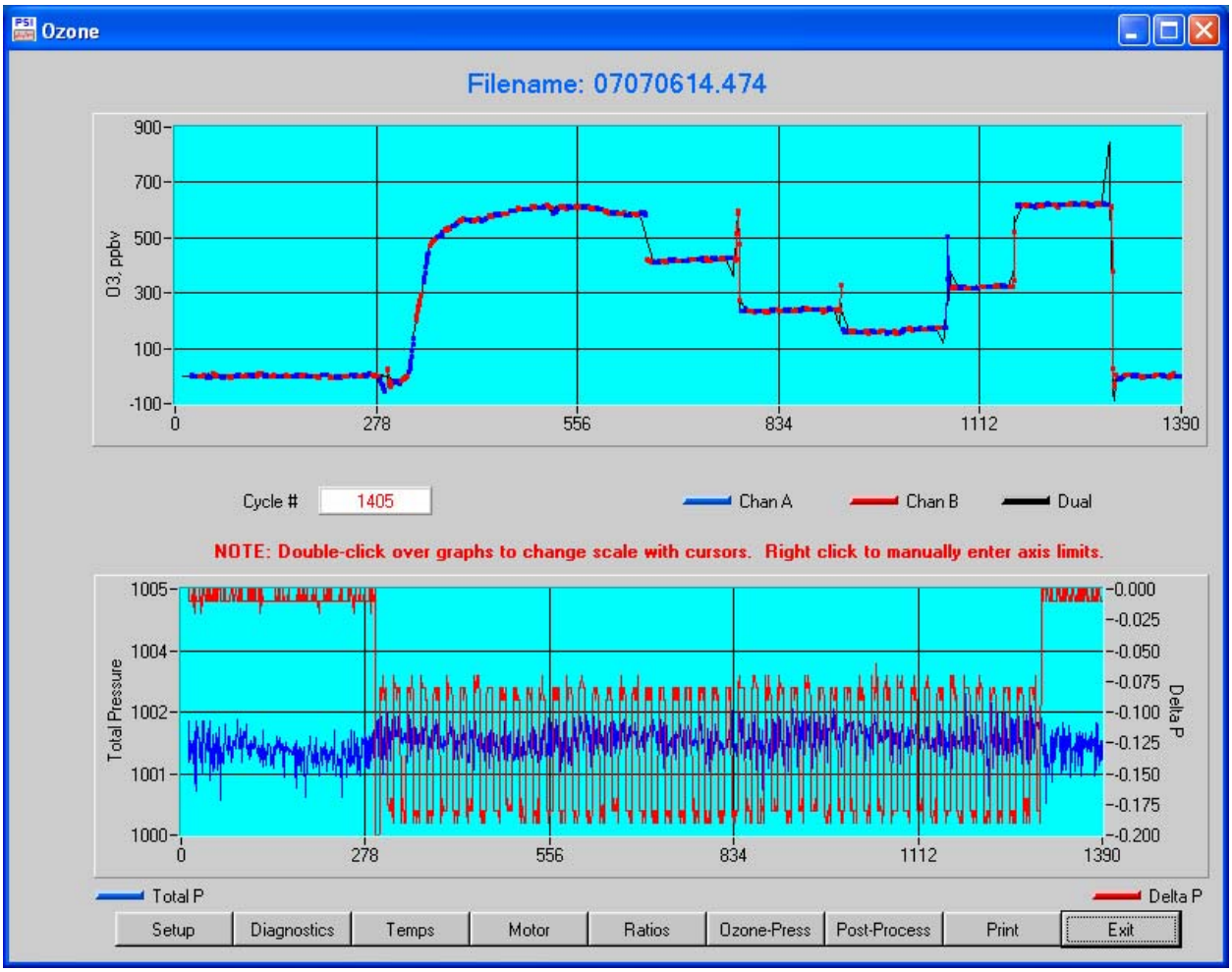

G-6. **BATCH** "Ozone-Press" Plots: 1-Hz ozone mixing ratios for single-channel and dual-channel analysis (upper plot), pressure and differential pressure (lower plot).

20 New England Business Center □ Andover, MA 01810-1077 □ *t* 978.689.0003 *f* 978.689.3232
www.psicorp.com

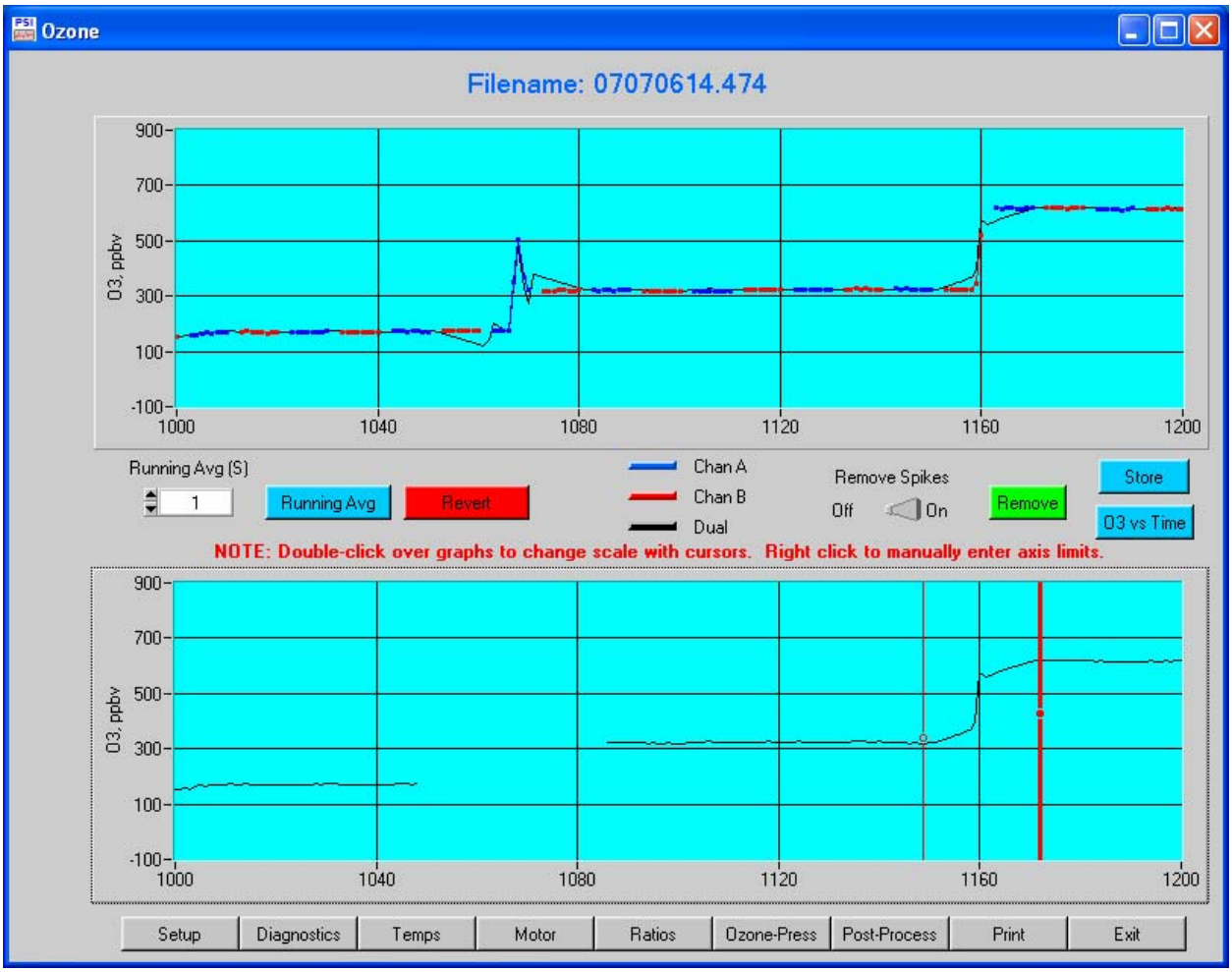

G-7. **BATCH** "Post-Process" Page: running average and spike scrubbing of ozone data.

20 New England Business Center □ Andover, MA 01810-1077 □ *t* 978.689.0003 *f* 978.689.3232
www.psicorp.com

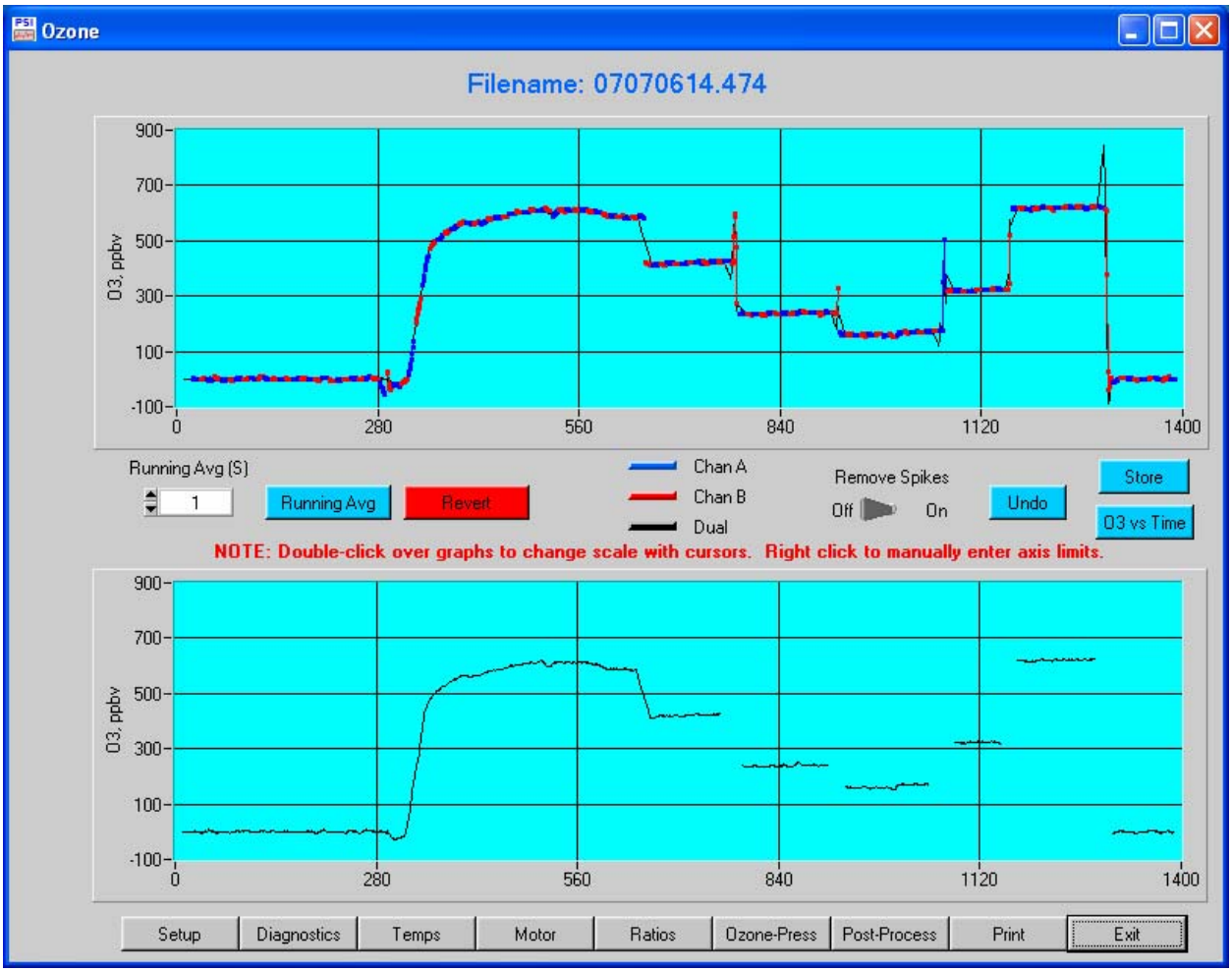

G-8. **BATCH** "Post-Process" Page: example of unprocessed (upper plot) and processed (lower plot) ozone data.

20 New England Business Center □ Andover, MA 01810-1077 □ *t* 978.689.0003 *f* 978.689.3232
www.psicorp.com

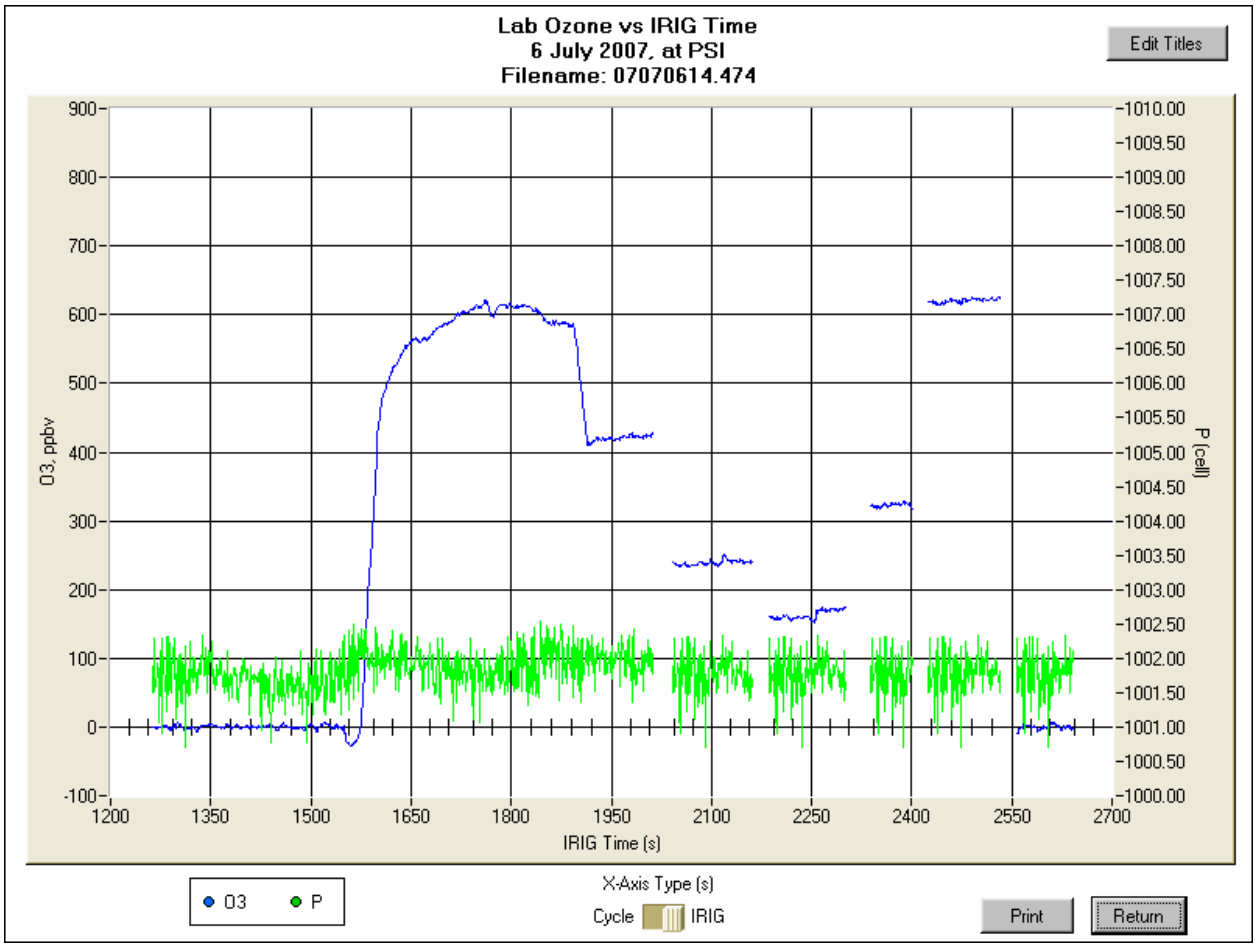

G-9. **BATCH** "O3 vs Time" Page: Example of print-ready archival plot of ozone mixing ratios and cell pressure vs. IRIG time.

20 New England Business Center □ Andover, MA 01810-1077 □ *t* 978.689.0003 *f* 978.689.3232
www.psicorp.com

20 New England Business Center Andover, MA 01810-1077 *t* 978.689.0003 *f* 978.689.3232
www.psicorp.com

Appendix H

Recommended Flight Operation Procedures

To install and operate the instrument on the GV aircraft:

- Read and understand the Proffitt Instruments manual (Appendix C) before using this instrument.
- Optional bench checkout:
  - Remove the computer panel cover, and then remove the instrument cover by removing the bolts around the base. (It is easier to get the instrument cover off if the computer panel cover is removed first.) Make sure to detach any connecting cables first.
  - Examine the internal components to make sure that the connectors are properly attached and the air flow tubing is tightly connected.
  - Connect a video monitor and keyboard, turn the instrument on, and make sure that the computer boots and the data acquisition software runs.
  - Observe the data display on the screen to make sure that the values are correctly reported and that all of the instrument subsystems are operating normally. (For example, an anomalous temperature reading could signify an open circuit.)
  - Observe that the valve rotates through all four positions in sequence.
  - The data display checkout can usually be accomplished in about 5 minutes or less. Terminate the program with the ESC key.
  - Look at the C:/DATA drive to make sure that the data file is correctly stored and that there is adequate hard drive space.
  - Disconnect the monitor and keyboard from the computer panel. Carefully replace the cover and all of the bolts, and replace the computer panel cover. (The computer panel cover should be left on during flight, but may be removed for pre- and post-flight access to the computer panel.)
- Rack installation and pre-flight checkout:
  - Align the four holes in the bottom of the instrument housing with the bolt holes in the mounting shelf for the rack. The instrument is located near one end of the shelf, with the inlet and outlet nearest the end of the shelf.
  - Attach the four ¼-inch aircraft bolts from the bottom to secure the instrument to the shelf, and mount the shelf to the rack.
  - When the rack is in position inside the aircraft, attach the inlet and outlet tubing.
  - We recommend wrapping a length of heating tape around a section of the inlet tubing immediately upstream of the instrument inlet to allow the option of pre-warming the sample flow to maintain <1 °C temperature difference between the absorption cell inlet and outlet. The temperature of this pre-heated section should be no higher than roughly 30 to 35 °C.
  - Install the appropriate flow-limiting orifice in the ½-inch tubing at the connection to the exhaust outlet.

20 New England Business Center Andover, MA 01810-1077 t 978.689.0003 f 978.689.3232
www.psicorp.com

  - **Note that all inlet tubing and connections MUST be Teflon with no metal exposed to the sample flow;** outlet and exhaust connections may be of any material.
  - If desired, mount a laptop equipped with the data analysis software on the rack.
  - Attach the AC power cable to the 4-pin Bendix connector labeled "115 VAC" on the switch panel.
  - If available, attach the DC soft-key cable to the 2-pin Bendix connector labeled "VDC". When the switch on the panel is in the UP position, the soft-key control is enabled (or the instrument is OFF when there is no soft-key connection). When the switch is in the DOWN position, the instrument is on manual power and is ON.
  - If available, connect the IRIG signal cable to the 9-pin D connector labeled "IRIG IN".
  - Connect either the on-board data system or the laptop computer serial port to the 9-pin D connector labeled "COM1" using a null-modem cable.
  - Switch the instrument on and observe the RS232 data stream on the laptop (using the "**TELEMETRY**" software, Subsection 7.2.2) or on the on-board data system to make sure that everything is working properly.
- Warm-up and flight measurements:
  - The instrument requires about 30 minutes warm-up for best valve operation and lamp stability.
  - During flight, the instrument may be operated autonomously, or interactively by monitoring the real-time RS232 data stream on the external computer. Interactive operation would allow for rapid adjustments such as restarting if something goes awry, or changing out the flow-limiting orifice if the flow rates are too high.
  - When data acquisition is completed, turn off the instrument power. Allowing the instrument to continue to run after useful data acquisition is completed will simply build up a large and cumbersome data file.
  - The instrument can either be disconnected and removed from the aircraft or left on board for the next flight.
- Post-flight data download:
  - Connect a video monitor and a keyboard to the instrument computer panel.
  - With the instrument power off, connect the portable "Mad Dog" USB hard drive to the lower USB port on the computer panel.
  - Turn on the USB hard drive. Then turn on the instrument.
  - After the instrument completes the boot sequence and starts running the data acquisition program, hit the **ESC** key to terminate the program and return to the DOS prompt for the **A:** drive.
  - Follow the sequence outlined in Subsection 7.2.4: type **D: <cr>**, respond to the bogus error message by typing "**A**" for "**Abort**", and the DOS prompt for the **D:** drive (i.e. the USB drive) will appear.
  - Copy the data files from **C:/DATA** onto the **D:** drive using DOS commands as described in Subsection 7.2.4.

20 New England Business Center Andover, MA 01810-1077 *t* 978.689.0003 *f* 978.689.3232
www.psicorp.com

  - When the copying is complete, turn everything off, disconnect the USB drive, the video monitor and the keyboard, and replace the computer panel cover.
- Post-flight data analysis:
  - Connect the portable USB drive to an external PC computer equipped with the PSI data analysis software.
  - Copy the data file(s) to the external computer.
  - Run the "**BATCH**" code as described in Subsection 7.2.3.
  - Inspect the housekeeping and photometric data for anomalies, examine the pressure data for altitude variations and the ΔP data for flow rates, and compare the dual-channel and single-channel ozone results for consistency.
  - Perform data scrubbing and averaging as desired.
  - Save the archival data and print plots as desired.
  - The output files can be read into a spreadsheet program such as Excel for further processing, plotting, and comparisons to other data sets.

20 New England Business Center Andover, MA 01810-1077 *t* 978.689.0003 *f* 978.689.3232
www.psicorp.com

20 New England Business Center Andover, MA 01810-1077 *t* 978.689.0003 *f* 978.689.3232
www.psicorp.com